# THE DEGRADATION OF GEL-SPUN POLY(β-HYDROXYBUTYRATE) FIBROUS MATRIX.

## VOLUME II.

LESLIE JOHN RAY FOSTER

Doctor of Philosophy

THE UNIVERSITY OF ASTON IN BIRMINGHAM

August 1992

## LIST OF CONTENTS.

# Volume 2.

# Chapter Six.

## The Degradation Of PHB(FM) In The Physiological Degradation Model.

## 6.0 General Introduction.

This chapter deals with the degradation of the blended and unblended PHB(FM) in the physiological degradation model. Degradation was monitored using gravimetric analysis and the partially degraded samples investigated. Thus, the nature of the degradation under physiological conditions of pH 7.4 and temperature 37.5°C. was determined and then related to the degradation of the same samples in the accelerated degradation model. These comparisons would then provide indications as to the suitability of utilizing the accelerated degradation model as an indication to the possible degradation of samples under physiological conditions and as implantation devices.

## 6.1. The Degradation Of PHB(FM)IP In The Physiological Degradation Model.

### 6.1.0. Introduction.

Samples of PHB(FM)IP weighing approximately 305mg. ±1.6%, were degraded in the physiological degradation model. The undegraded fraction of the samples was determined using gravimetric analysis at periodic time intervals and then examined using phase contrast and scanning electron microscopy (SEM), differential scanning calorimetry (DSC) and FTIR photoacoustic spectroscopy (PAS). The results obtained were then compared with those from the accelerated degradation model.

### 6.1.1. The Degradation Profiles Of PHB(FM)IP.

6.1.1.1. Degradation Profile In The Physiological Degradation Model.

Graph 6.1. illustrates the degradation profile of the PHB(FM)IP monitored by gravimetric analysis, an induction period from day 1 to approximately day 56 was observed with a change in degradation from approximately 0.2 to 1.7%. These values were within a 5% error range and as such little or no change in degradation was concluded. This initial induction period was probably due to a gradual removal of the solvent residue, the fracturing and fragmentation of some of the weaker fibres and the degradation of the relatively small amounts of particulate matter.

During this induction period (stage 0) the buffer gradually penetrated the fibres and began to degrade the primary amorphous regions, this then led to the collapse of the weakened fibres, such that between days 56 and 125 the degradation rate gradually increased. At day 125, 95% of the sample still remained, after this the degradation proceeded (stage I) with a linear rate of approximately 0.11%dy.$^{-1}$ until day 324, where 73% of the sample remained undegraded. This stage I was due to the gradual collapse of the matrix and continued fragmentation of the fibres and fibre fragments.

Thus, after an initial induction period lasting approximately 50-60 days the matrix gradually collapsed and degraded.

6.1.1.2. Comparison With The Accelerated Degradation Model Profile.

A comparison of the PHB(FM)IP degradation profiles from the physiological and accelerated degradation models (Fig. 6.1.) shows that the physiological profile possessed

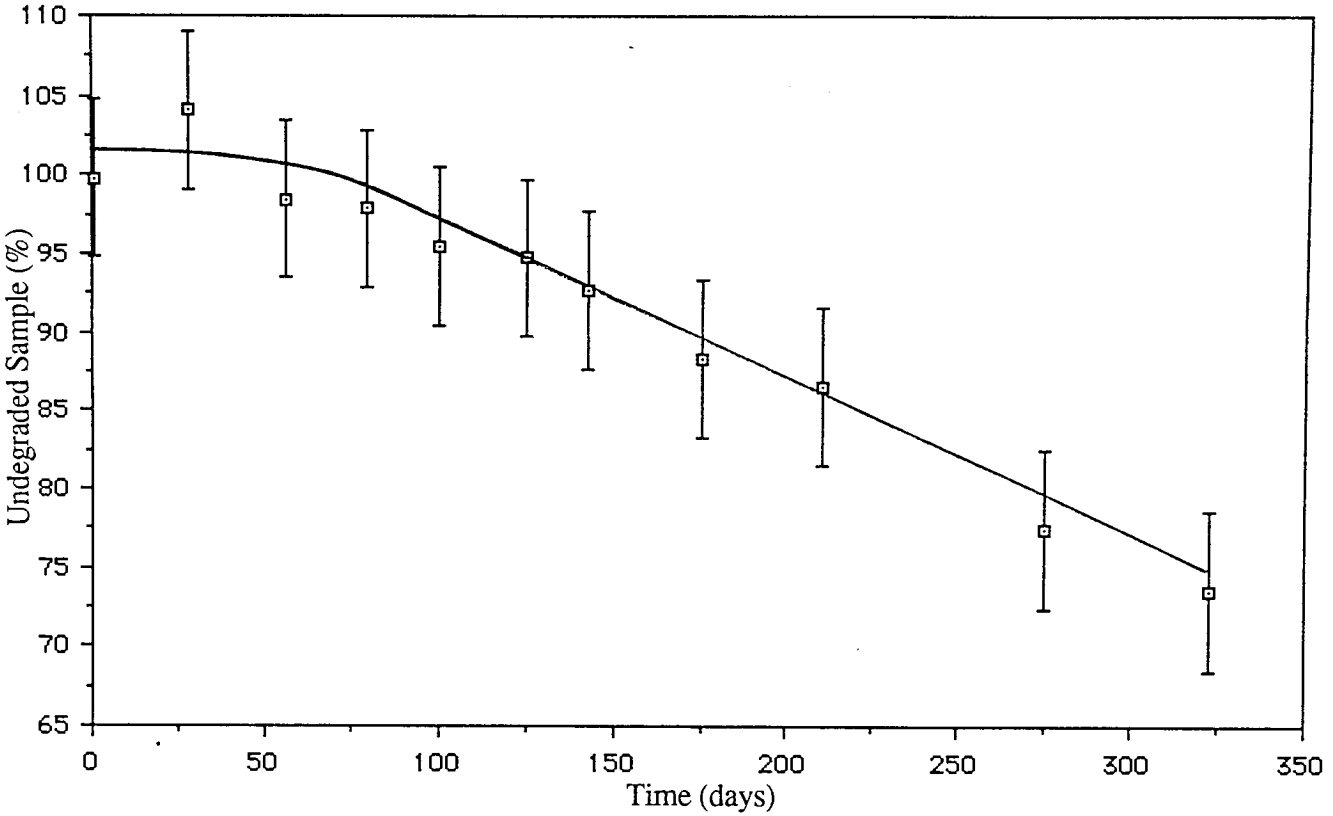


**Graph 6.1.**

**Degradation Profile Of PHB(FM)IP,In The Physiological Model, Monitored By Dry Weight Loss.**

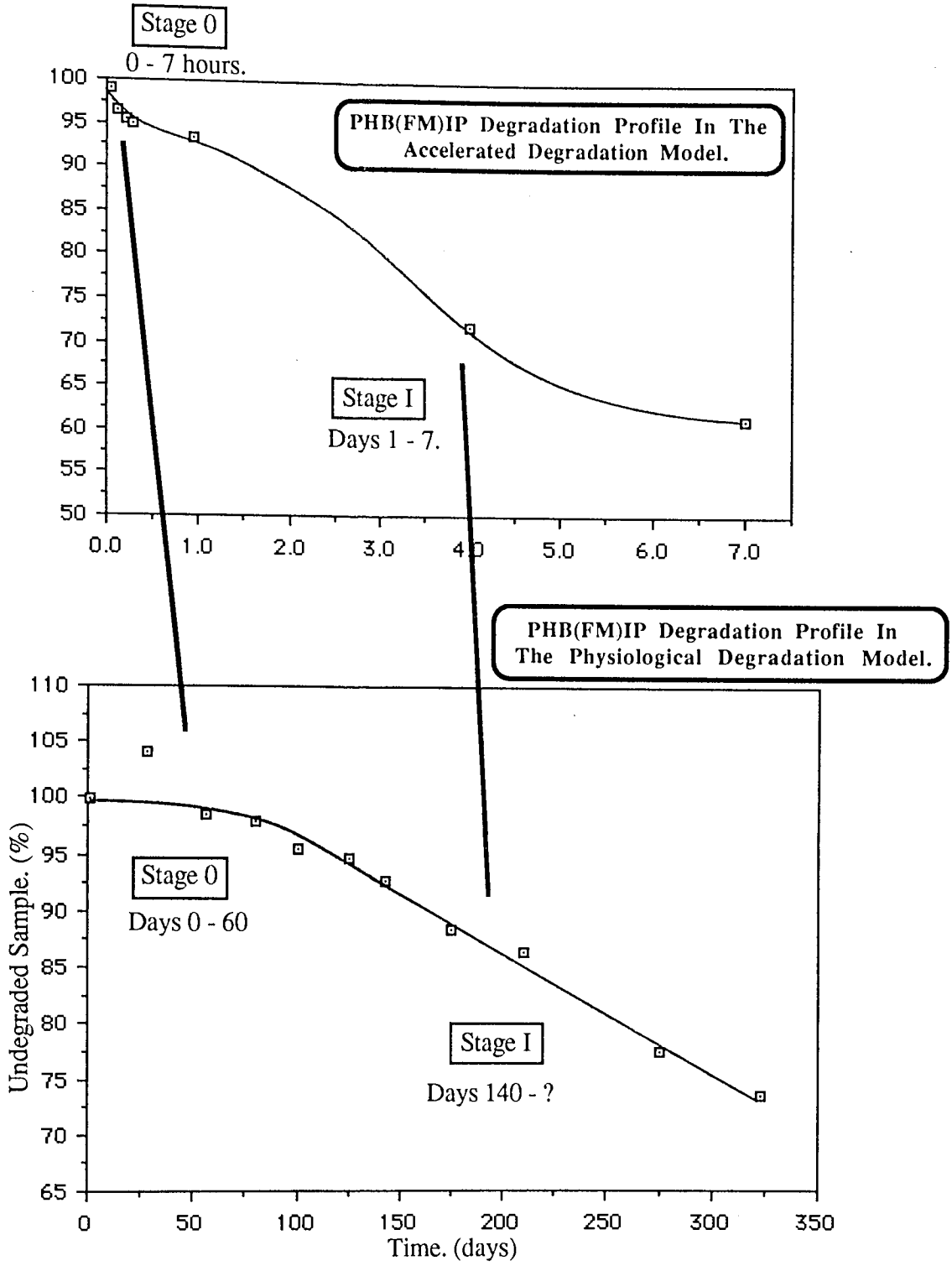


**Figure 6.1.**

**Comparison Of PHB(FM)IP Degradation Profiles From Different Degradation Models.**

more pronounced degradation stages than the accelerated profile.

The induction stage 0 for the physiological degradation model profile revealed little degradation between days 1 and 56, approximately. The induction period was less noticeable in the accelerated degradation model profile and was observed until around 7 hours degradation. After the induction stage the degradation rate in both profiles increased, this was observed to occur more gradually for the physiological model profile compared to the accelerated. The stage I degradation rate was linear in both cases with rates of approximately 0.11%$dy.^{-1}$ and 0.65%$dy.^{-1}$ for the profiles from the physiological and accelerated degradation models respectively.

The initial matrix collapse and degradation in the accelerated model occurred with a proportionately greater degradation rate than in the physiological degradation model, but after this the difference in the degradation rates between the two models was not as great. Therefore, it was concluded that fibre fragment settlement and compaction had more influence on the PHB(FM)IP degradation in the accelerated model than in the physiological and this was reflected in their degradation profiles.

### 6.1.2. Observations Of The Partially Degraded Samples.

Observations of the partially degraded fibres using phase contrast microscopy revealed little change in the matrix structure during the initial induction stage 0, the matrix still retained its integrity and relatively few fibres were fragmented. The fragmentation gradually increased in the degradation stage I after approximately day 50, (Plate 6.1).

Examination of the fibre samples at higher magnifications utilizing SEM also illustrated little degradation in the induction stage, (Plate 6.2). A small amount of fragmentation was still observed by day 56 as illustrated in plate 6.4., which shows a large proportion of the fibres were still readily flexible, including the small 'fine' fibres. This indicated that the relatively small amount of fragmentation observed was most likely due to the SEM handling and mounting procedures, nevertheless, these fibres were most probably weakened as part of the degradation process. It was observed that at day 120 a substantial proportion of the fibres had fragmented, such that the matrix formed a partially collapsed fibre fragment mass at the phial base. Undegraded particulate matter was also observed, trapped by the matrix, (Plates 6.5 & 6.6).

The degradation observations were similar to those noticed for the partially degraded samples from the accelerated degradation model, with the initial induction stage samples retaining matrix integrity but possessing weakened fibres. Thus, the observations from samples after 28 and 56 days degradation were comparable with the accelerated model samples from 1 to 5 hours degradation, whilst the observations from day 120 in the physiological degradation model where comparable with those from approximately days 3 to 4 for samples in the accelerated degradation model.

Using SEM the changes in fibre diameters during the degradation were determined for a number of samples. Graphs 6.2. to 6.7. illustrate the fibre diameter distributions for the partially degraded samples after 1, 28, 56, 120, 175 and 275 days degradation respectively.

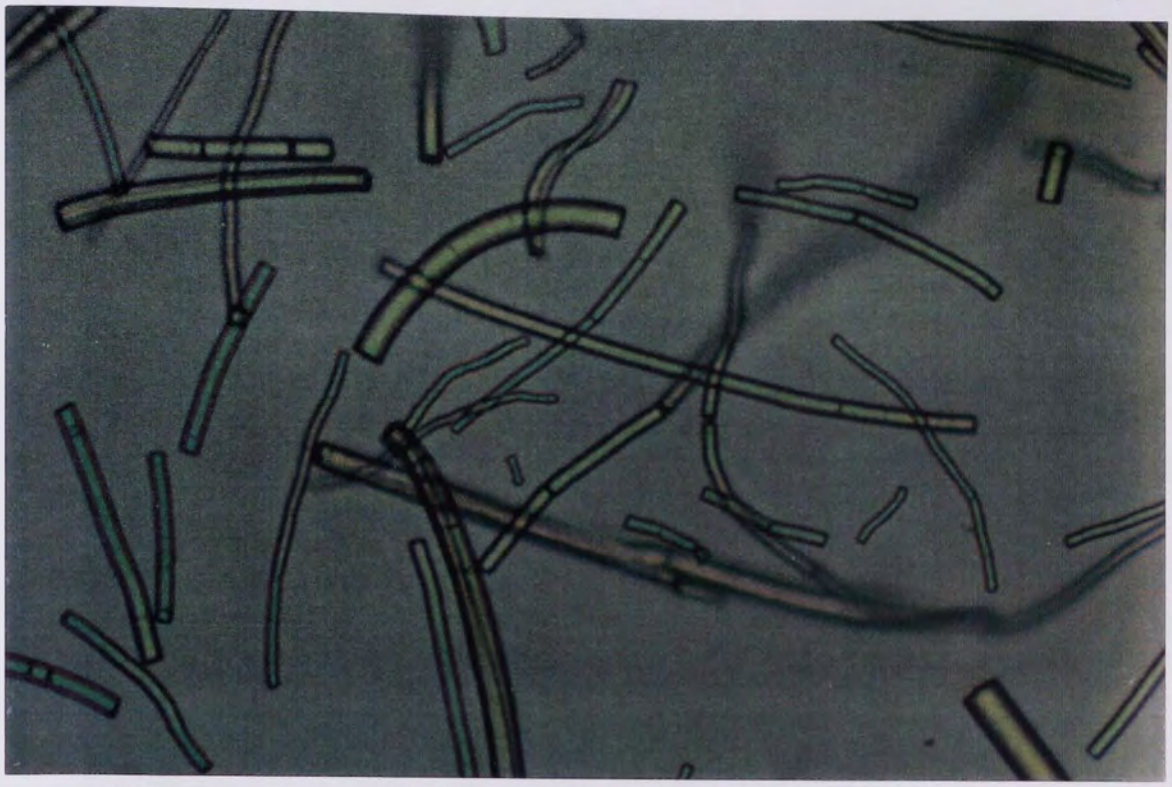

**Plate 6.1.** (x25) 50 Days Degradation.
**PHB(FM)IP; Small Degree Of Fragmentation Most Probably Due To The Filtering And Drying Procedures.**

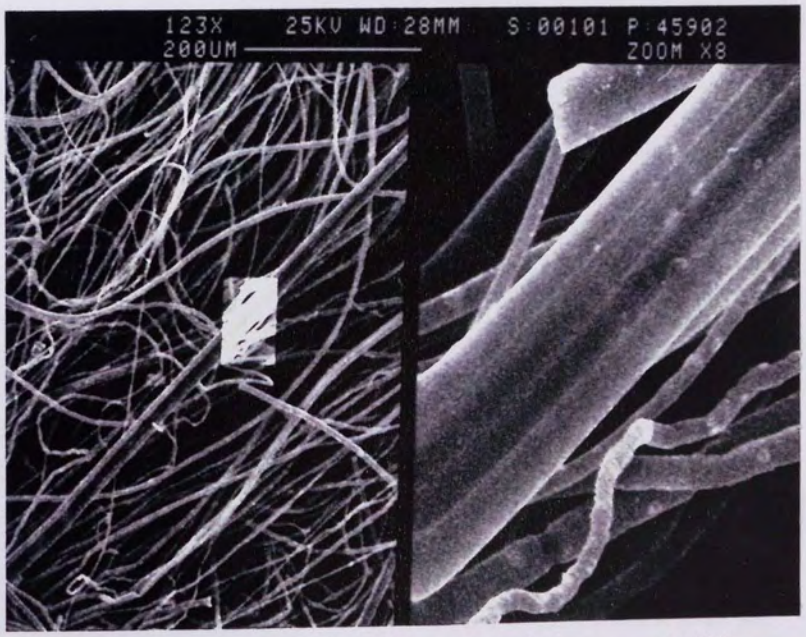


**Plate 6.2.** (x123) 28 Days Degradation. (x984)
**PHB(FM)IP; Matrix Integrity Still Present After 28 Days In The Physiological Degradation Model Also Illustrating A Group Of Agglutinated Fibres.**

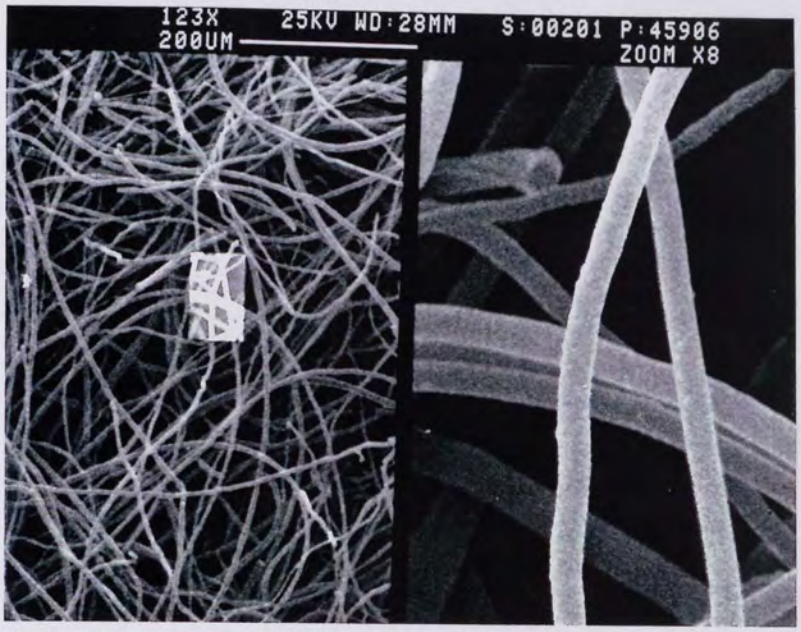


**Plate 6.3.** (x123) 56 Days Degradation. (x984)
**PHB(FM)IP; Matrix Integrity Still Present After 56 Days Degradation.**

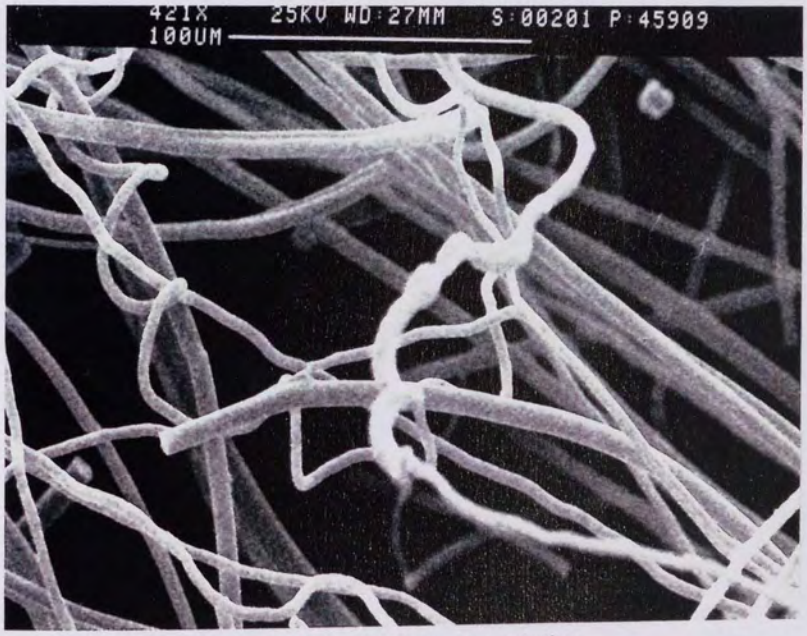


**Plate 6.4.** (x421) 56 Days Degradation.
**PHB(FM)IP; Integrity Of The Small 'Fine' Fibres.**

**Plate 6.5.** (x121) 80 Days Degradation. (x968)
**PHB(FM)IP; Fragmentation Of The Small 'Fine' Fibres To Particulate Matter Trapped By The Remaining Matrix.**

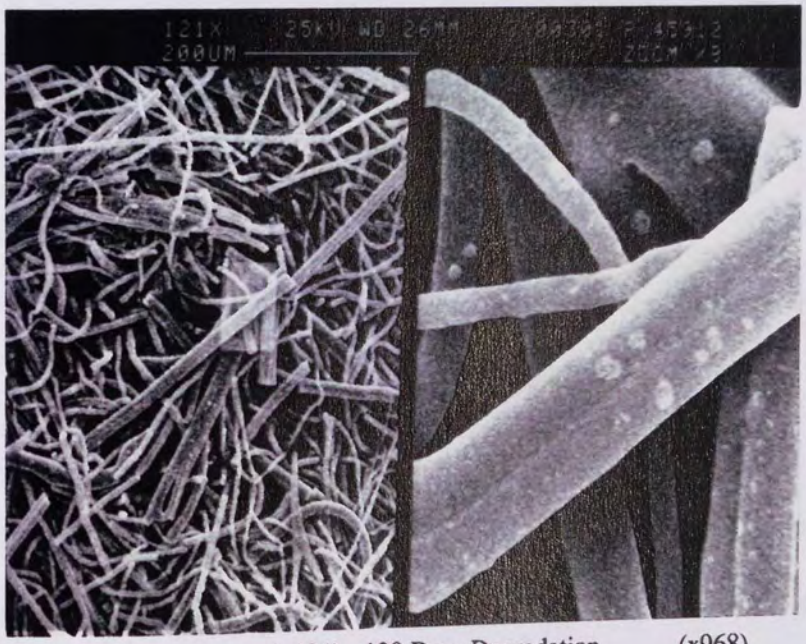


**Plate 6.6.** (x121) 120 Days Degradation. (x968)
**PHB(FM)IP; Collapse Of The Matrix And The Presence Of Small Particulate Matter.**

The fibre diameter distribution for the day 1 sample was similar to that of the undegraded with the main diameters being 1-2 and 4-5um. and possessing frequencies of 20% each. The distributions remained approximately the same after 28 days degradation, however, after 56 days it became more even in the medium sized diameter range (6-15um.), whilst the main peaks of 1-2 and 4-5um. were still observed.

At day 120, fibres were observed at all the diameters. The 1-2um. peak had decreased in frequency from 20% to 14% but the 4-5um. peak had increased to 24%. Similarly, the very small fibres with 0-1um. diameter had increased to approximately 12%. This 'fine' fibre peak at 0-1um. drastically decreased to 4% by day 175 as did the distributions from 1 to 3 microns. However, the frequency at the 3-4um. range increased from around 2% at day 120 to approximately 16%.

After 275 days degradation the fibre diameter distributions in the small diameter range of <6um. were drastically reduced with no fibres observed at 0-1 and 2-3um. However, the frequencies for fibres in the 3 to 8 micron ranges had increased so that the two narrow distribution peaks of 1-2 and 4-5um. observed in the previous samples were replaced by a relatively broad peak around the 5-6um. range. Thus, the main distribution of fibres appeared to shift towards the higher diameter ranges.

Considering the distributions as small, medium and large diameters for <6, 6-15 and >15um. respectively, provided a clearer picture when represented against the degradation time, (Graph 6.8). As can be observed from graph 6.8, the small diameter fibre frequency increased from 64% at day 1 to a peak at day 28 with 72%, this was due to the

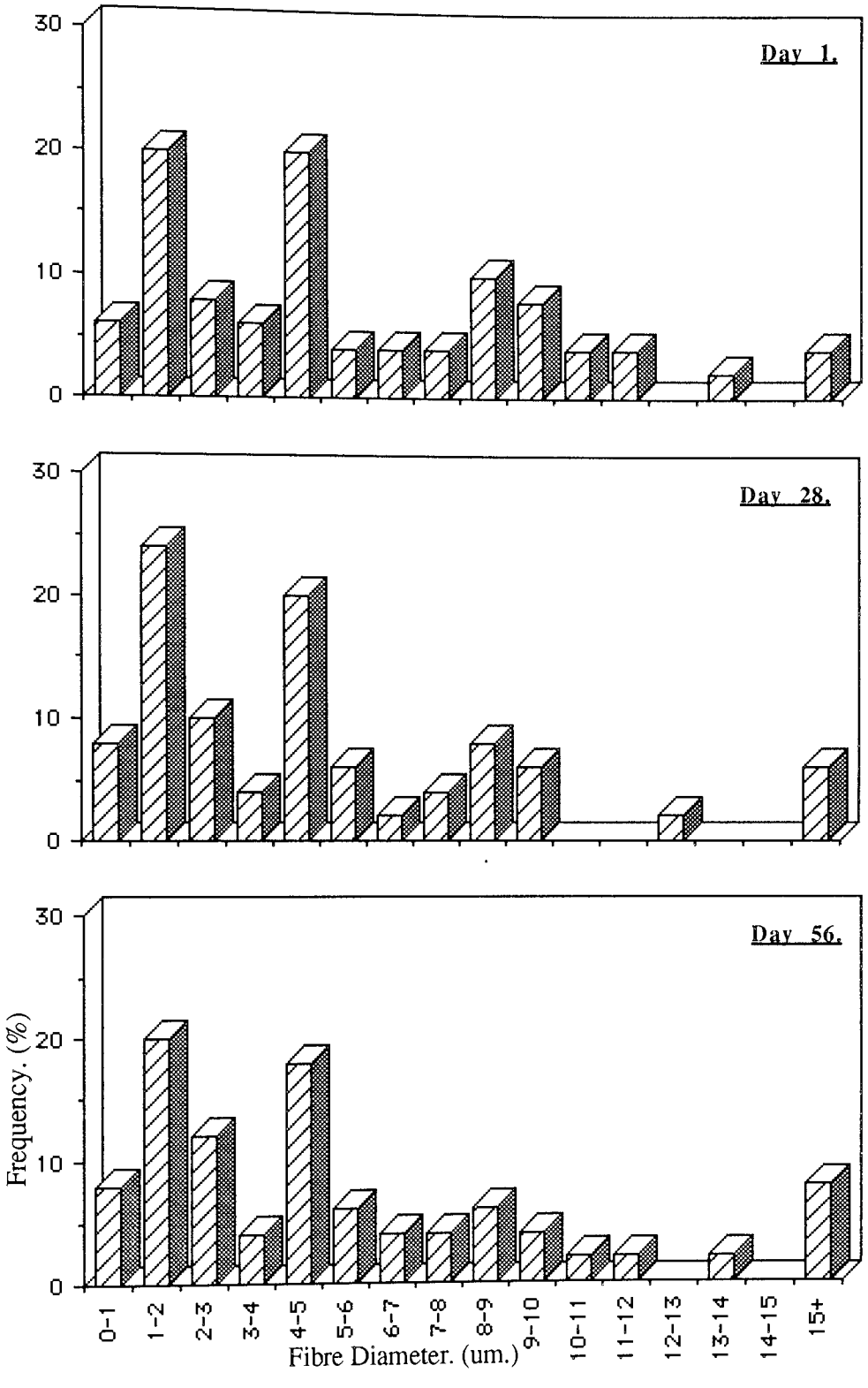


**Graphs 6.2. to 6.4.**

**Change In Fibre Diameter Distribution For PHB(FM)IP During Degradation In The Physiological Degradation Model.**

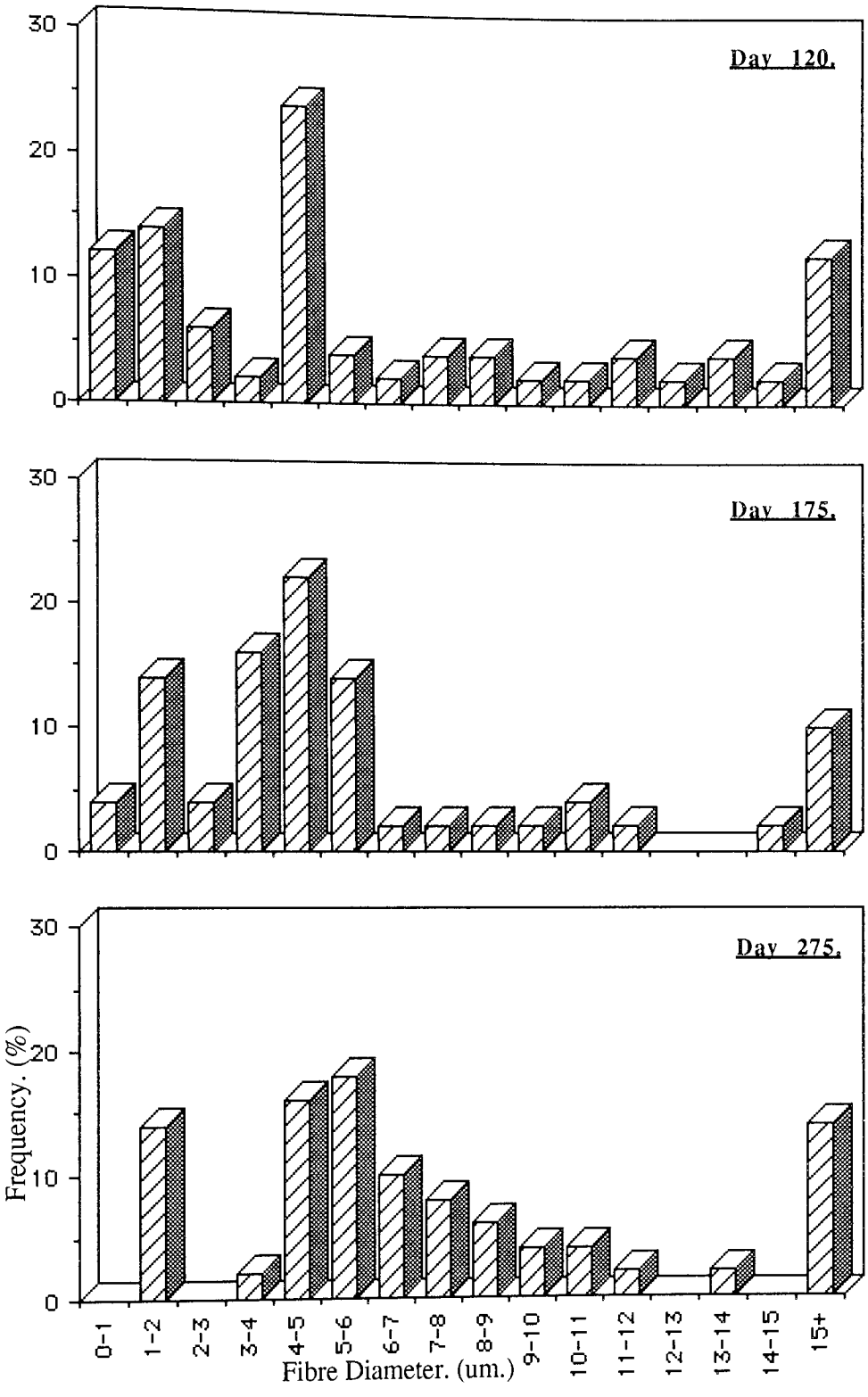


Graphs 6.5. to 6.7.

Changes In Fibre Diameter Distribution For PHB(FM)IP During Degradation In The Physiological Degradation Model.

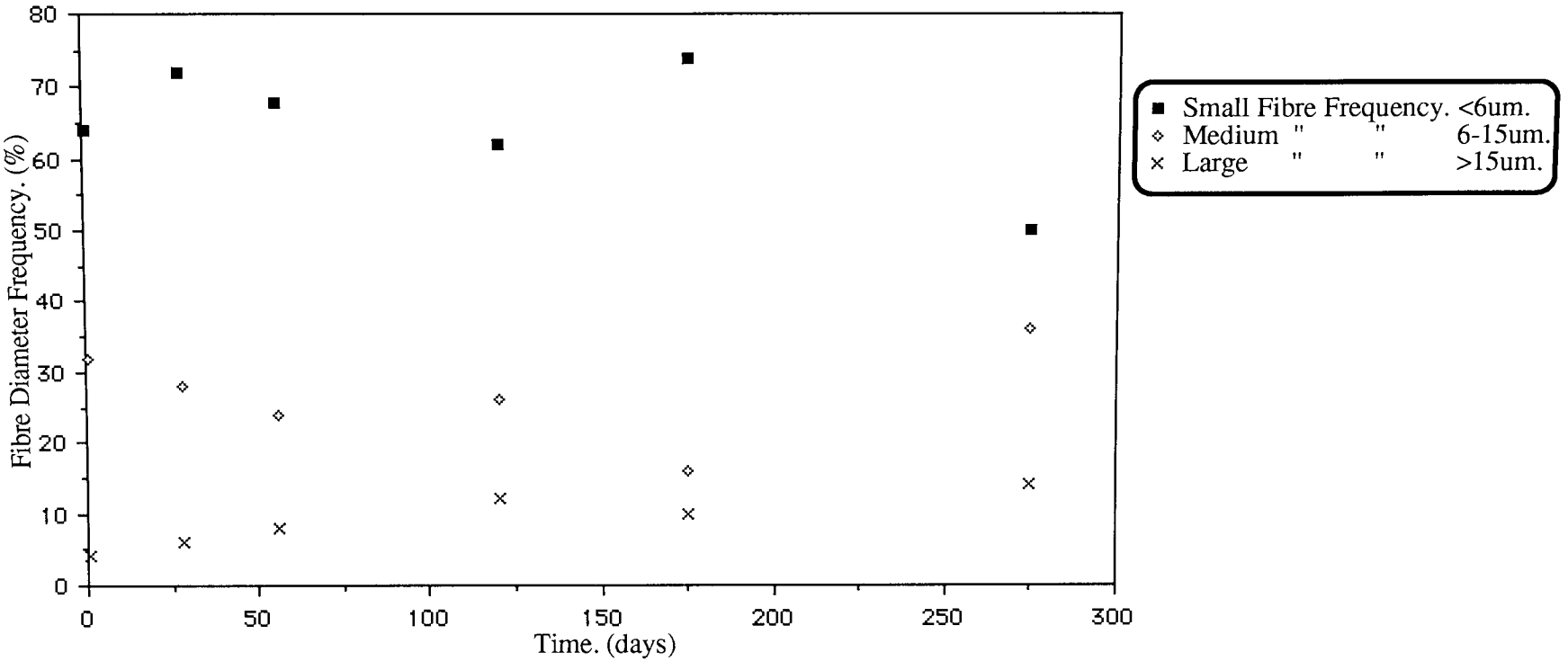


**Graph 6.8.**

**General Fibre Diameter Distribution For PHB(FM)IP During Degradation In The Physiological Degradation Model.**

fragmentation of a proportion of these fibres. As a result of this, the medium sized fibre frequency was reduced, so that a corresponding 'dip' was observed. After day 28 some of the medium sized fibres gradually fragmented until day 120, similarly, the number of large diameter fibres also gradually increased from day 1 to day 275 due to fragmentation. Thus, the medium and large fibre frequencies increased slightly, this then caused a corresponding decrease in the small diameter frequency due to the counting procedure.

At day 175 the small diameter frequency increased again to 74% from 62% at day 120, this caused a corresponding decrease in the medium sized fibres, which readily fragmented by day 275 and caused a decrease in the number of small diameter fibres counted.

Thus, it was concluded that fragmentation of the small diameter fibres occurred initially until around day 28, after which the gradual fragmentation of the large diameter and a relatively small proportion of the medium sized fibres occurred. Further fragmentation of the small and medium sized fibres occurred at day 175, although this was more noticeable with the small diameter fibres. These small fibres then readily degraded to particulate matter and the large number of medium sized fibre fragments became apparent.

### 6.1.3. Characterization Of The Partially Degraded PHB(FM)IP.

#### 6.1.3.0. Introduction.

The partially degraded samples from the physiological degradation model were examined using DSC and the melting points (mp.), fusion enthalpies ($\Delta$Hm.) and glass transition temperatures (Tg.) were determined. The samples were also examined using FTIR-PAS.

The results from these experiments helped to determine the nature of the PHB(FM)IP degradation in the physiological model and its relation to that of the IP sample in the accelerated model.

6.1.3.1. Differential Scanning Calorimetry (DSC) Studies.

Graph 6.9 illustrates the change in the melting point of the partially degraded samples during degradation, whilst graph 6.10 shows the change in the fusion enthalpy.

There was initially little change in the melting point of the partially degraded PHB(FM)IP, which remained at approximately 175°C. for about 100 days, (Graph 6.9). This tended to indicate that during the initial induction period, where only a small amount of degradation was observed, there was no change in the stability of the remaining PHB fibres. However, graph 6.10 revealed a gradual increase in the fusion enthalpy from approximately 72Jg.$^{-1}$ at day 1 to a peak of approximately 98 Jg.$^{-1}$ around day 145. This trend was also similar to that of the percentage crystallinity and thus, the crystallinity increased from approximately 70% at day 1 to about 94% at day 145. These results indicated that the amorphous regions of the matrix were gradually degraded in the induction stage.

After day 100 the melting point gradually decreased until approximately 166°C. at day 323. Similarly, the fusion enthalpy also decreased after day 145, so that a peak was observed, (graph 6.10). A similar enthalpy peak was also observed for the partially degraded IP samples from the accelerated degradation model, (Graph 4.28). The accelerated model enthalpy peak was at day 4 and this indicated that the degradation at day

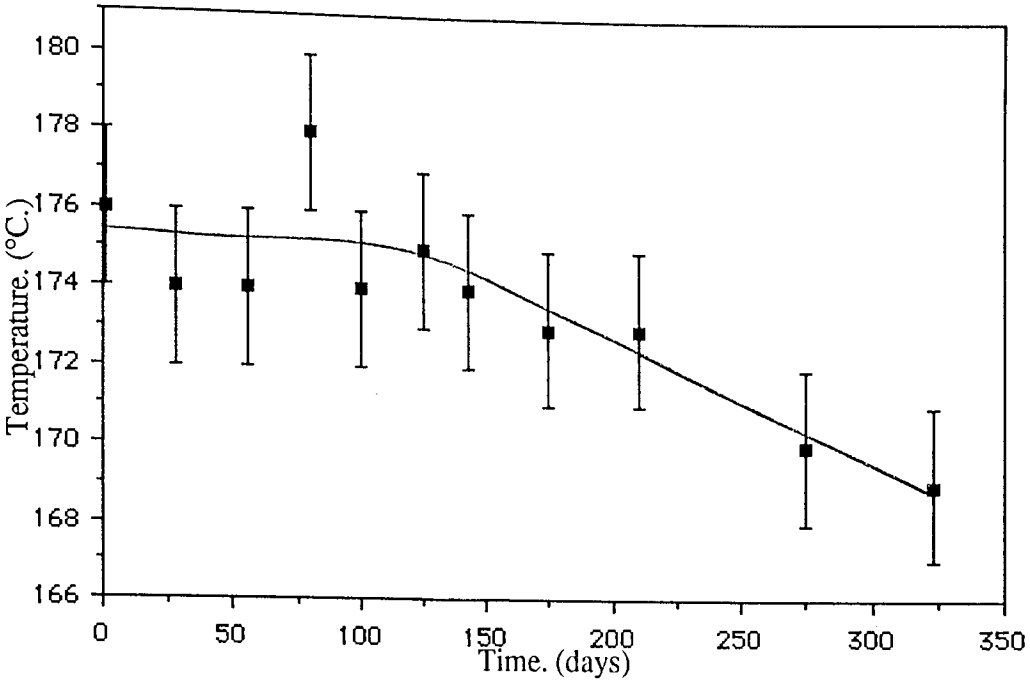


**Graph 6.9.**

**Change In Melting Point Of PHB(FM)IP, During Degradation In The Physiological Degradation Model.**

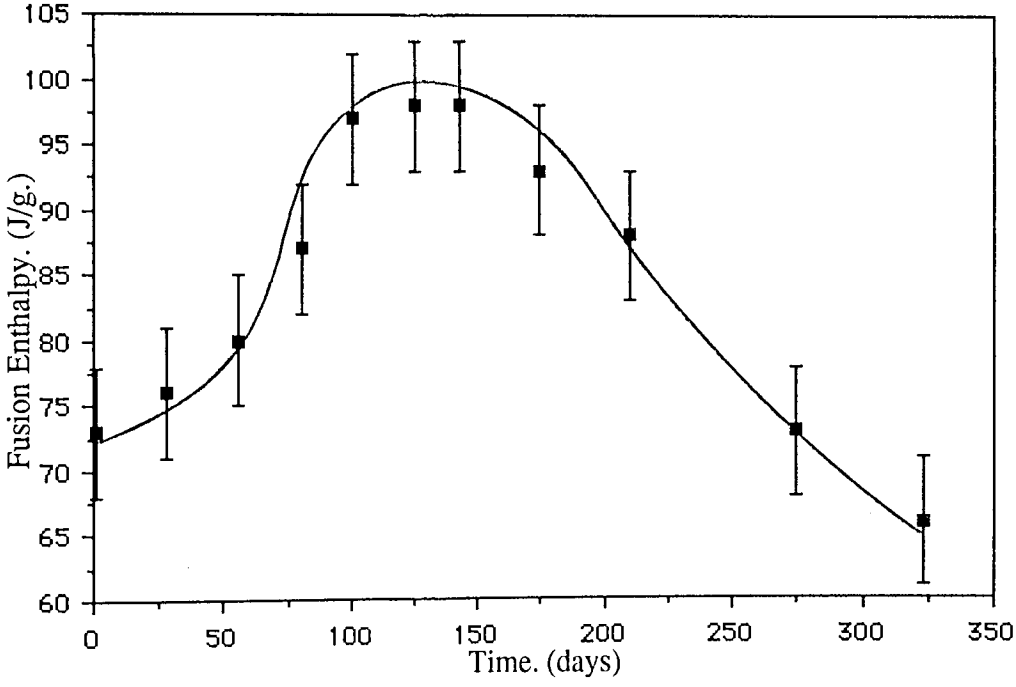


**Graph 6.10.**

**Change In Fusion Enthalpy Of PHB(FM)IP, During Degradation In The Physiological Degradation Model.**

4 in the accelerated degradation model was comparable to that of day 130 in the physiological degradation model. This conclusion was also substantiated by the similarity in the observations of the partially degraded samples from the two degradation models. (Sec. 6.1.2.).

No glass transition temperatures were determined for samples from 1 to 175 days degradation, even utilizing the first order derivative, this indicated the high crystalline nature of the samples. However, after day 175 some of the samples had noticeable Tg.'s. At day 325 the Tg. was approximately -19°C.

6.1.3.2. Photoacoustic Spectroscopy (PAS) Studies.

The PAS traces obtained from the partially degraded samples revealed little difference from those of the undegraded, whilst subtracting the traces revealed similar differences as those obtained from the accelerated degradation model samples. A carbonyl shift and carboxylate ion peak were observed at the 1768 and 1718cm.$^{-1}$ wavebands respectively. This confirmed that the PHB degradation occurred by cleavage of the ester bonds as was determined from the samples in the accelerated degradation model.

### 6.1.4. Conclusions.

It was concluded that the degradation of the PHB(FM)IP was more prolonged in the physiological degradation model than the accelerated, such that the degradation stages were comparatively more pronounced. There was an initial induction period of approximately 50-60 days which revealed little change in the matrix structure but a gradual weakening of the polymer chains and fibres. These weakened fibres then gradually

collapsed and the degradation proceeded more quickly. During the initial induction period and the matrix collapse the amorphous regions were gradually degraded, so that a maximum crystallinity of approximately 94% was observed around day 145 and this was the beginning of the stage I degradation.

## 6.2. Degradation Of The Co-blended PHB(FM)IP In The Physiological Degradation Model.

### 6.2.0. Introduction.

Co-blended PHB(FM)IP samples were degraded in the physiological degradation model and the degradation monitored by gravimetric analysis. The degradation profiles were then compared to that obtained for the PHB(FM)IP. The partially degraded samples were examined utilizing phase contrast and scanning electron microscopy (SEM), differential scanning calorimetry (DSC) and FTIR-photoacoustic spectroscopy (PAS).

### 6.2.1. Degradation Profiles Of The Co-blended Samples.

Graphs 6.11. to 6.13. illustrate the degradation profiles for the following co-blended samples in the physiological degradation model:

| | | |
|---|---|---|
| 1) | L.Pec.9. | 9% Pectin. |
| 2) | L.Pec.15. | 15% Pectin. |
| 3) | L.Pec.25.S. | 25% Pectin, (Start of the manufacturing run). |
| 4) | L.Pec.25.E. | " " (End " " " " ). |

In contrast to the PHB(FM)IP degradation profile, samples L.Pec.9., L.Pec.15. and L.Pec.25.E. did not show any initial induction periods but revealed initial weight losses. These losses were due to the pectin, which degraded comparatively faster than the PHB. For samples L.Pec.9. and L.Pec.15. these weight losses were similar to their initial ideal pectin loadings of 9 and 15% respectively, however, sample L.Pec.25.E. showed a loss of approximately 19%, whilst sample L.Pec.25.S. did not exhibit any initial weight loss and possessed a profile more similar to that of the PHB(FM)IP. These results indicated that the blending at the comparatively high percentage loadings was inefficient.

As a result of the pectin degradation there was an increase in the available surface area to volume ratio of the remaining matrix and this facilitated in the PHB degradation. Similarly, the pectin degradation also introduced structural weaknesses in a proportion of the fibres which facilitated in the fibre and matrix collapse, this also further increased the surface area to volume ratio. The degradation of the PHB then proceeded more rapidly.

The pectin ensured that the matrix degradation was considerably greater than that of the IP sample. The degradation at day 325 for the co-blends was approximately the same for L.Pec.9., L.Pec.15. and L.Pec.25.E. with 48, 51 and 55% degradation respectively, whilst sample L.Pec.25.S. had 38% degradation. These values contrasted with the IP sample which exhibited approximately 27% degradation at day 325.

Thus, taking the pectin loading into consideration, it was concluded that blending the PHB(FM)IP with pectin increased the degradation of PHB in the physiological model by a further 13%, approximately, above the degradation of the unblended PHB(FM)IP at day

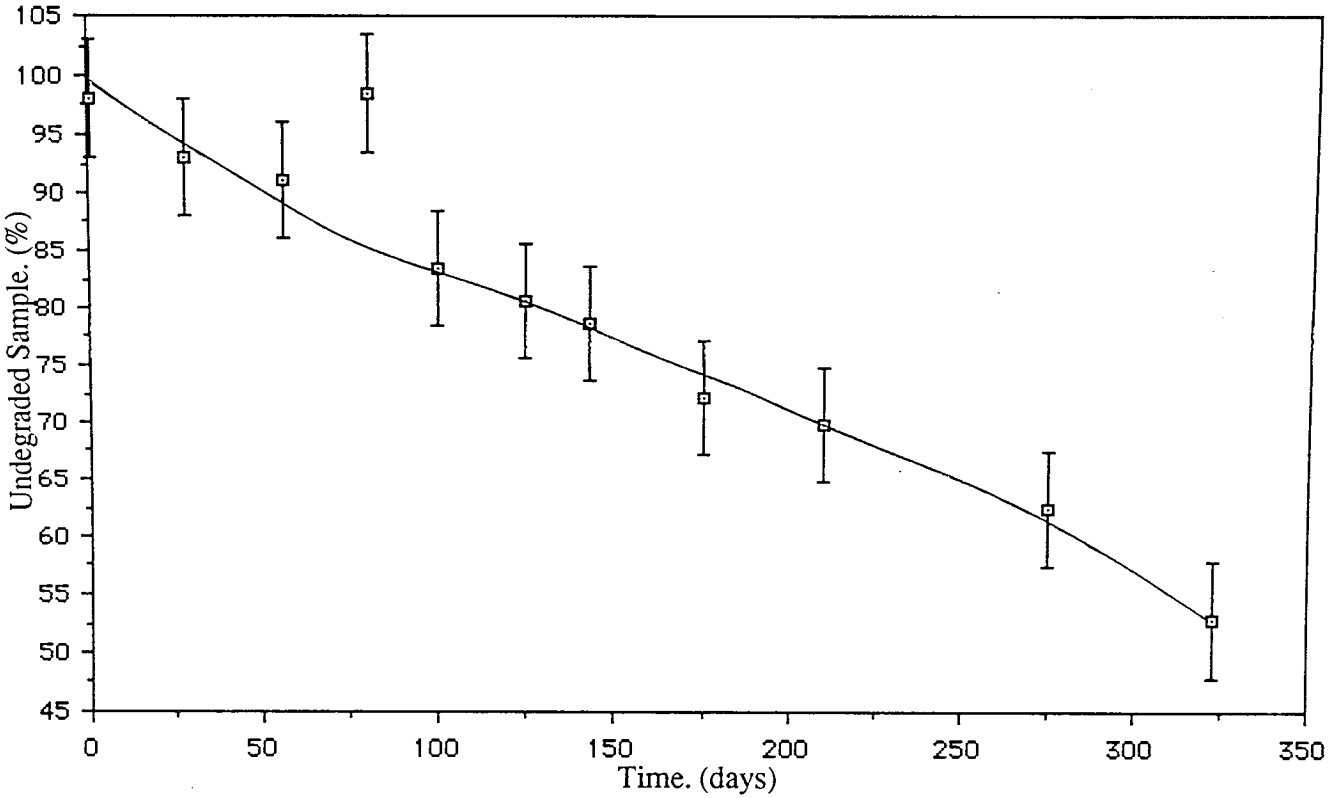


**Graph 6.11.**

**Degradation Profile Of L.Pec.9. In The Physiological Model. Monitored By Dry Weight Loss.**

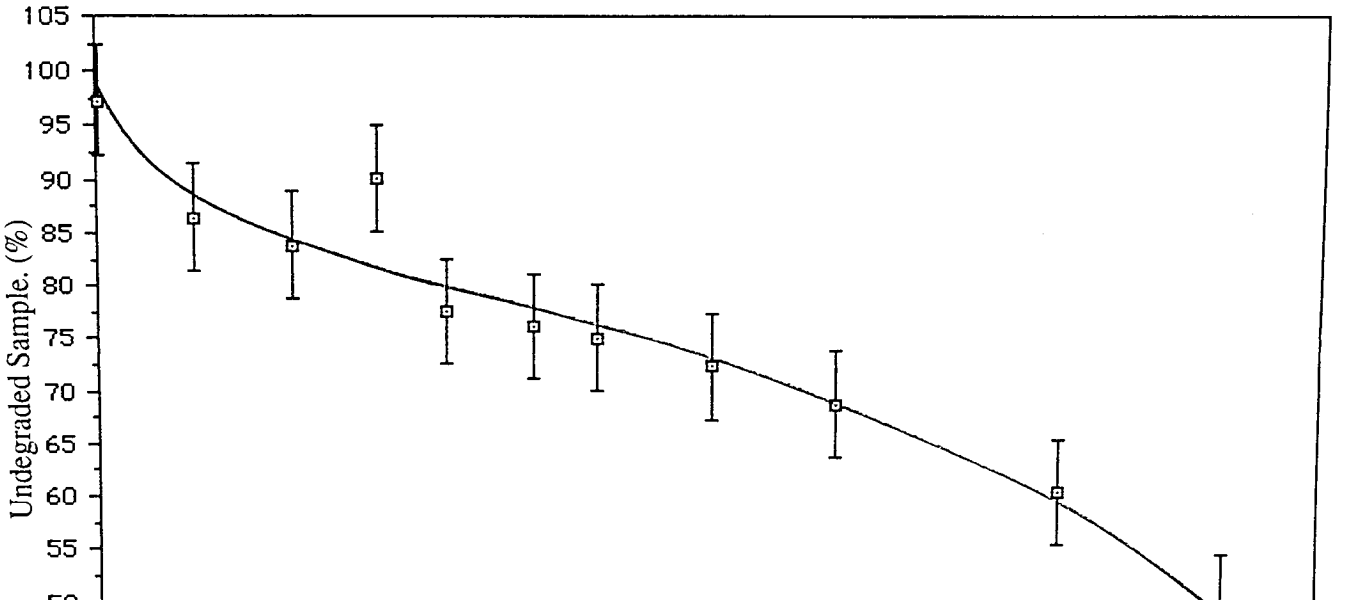


**Graph 6.12.**

**Degradation Profile Of L.Pec.15. In The Physiological Model. Monitored By Dry Weight Loss.**

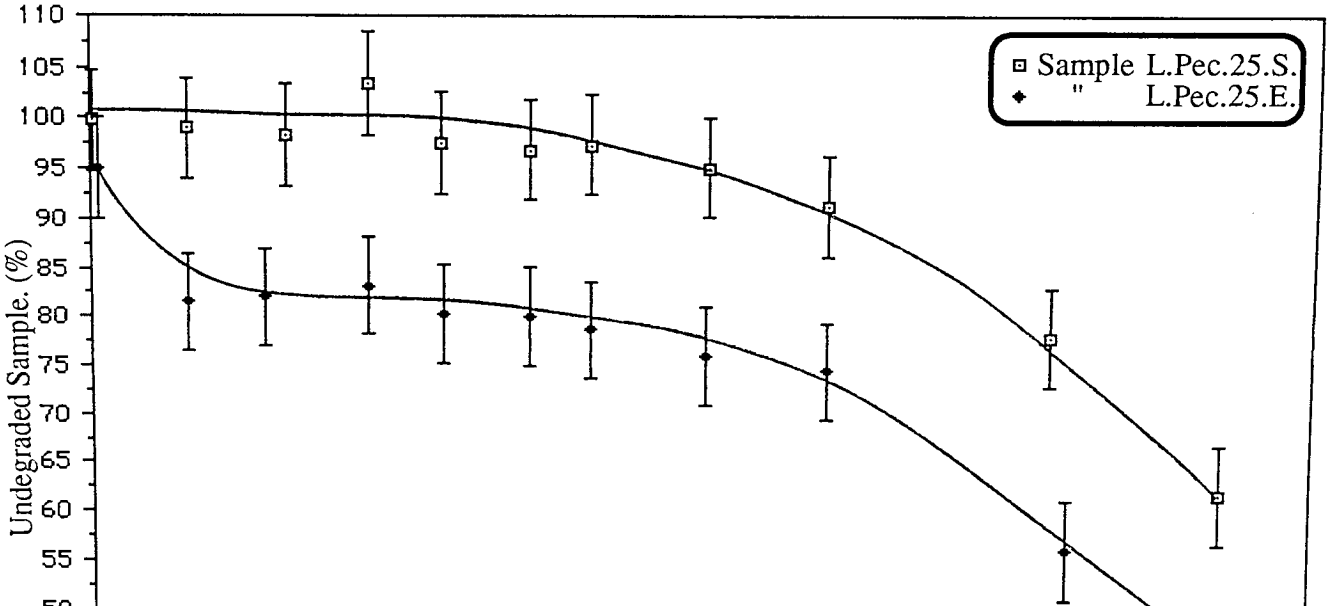


**Graph 6.13.**

**Degradation Profiles Of L.Pec.25.S. And L.Pec.25.E. In The Physiological Degradation Model, Monitored By Dry Weight Loss.**

325, irrespective of the pectin loading. Increasing the pectin loading above 15% reduced the blending efficiency, such that the loadings failed to match the initial ideal.

### 6.2.2. Observations Of The Partially Degraded Samples.

The observations of the partially degraded co-blends (Plates 6.7-6.15) using phase contrast and SEM were similar to those examined from the accelerated degradation model and were consistent with the conclusions from the physiological degradation profiles.

Samples L.Pec.9., L.Pec.15. and L.Pec.25.E. possessed noticeable pectin cavities by day 28 and a relatively large amount of fragmentation compared to the IP sample from the same time was also observed, (Plates 6.8, 6.9 & 6.13). This fragmentation was also facilitated by the handling and mounting techniques. However, substantial proportions of the matrices still maintained integrity, (Plates 6.13 & 6.15). There was little difference in the degradation of the samples by day 80, which exhibited a similar amount of fragmentation to those observed at day 28, (Plate 6.9). By day 143 fragmentation had increased and fracturing in the remaining fibre fragments was also noticed, (Plate 6.10).

Sample L.Pec.25.S. did not exhibit any noticeable pectin cavities, this tended to confirm the absence of pectin, which was also indicated in the degradation profile. However, fracturing and fragmentation of the fibres were observed by day 80, but to a comparatively lesser extent than the other co-blended samples, (Plate 6.11).

Thus, the degradation of the co-blends was characterized by the initial pectin degradation and the formation of the pectin cavities which led to an initial matrix collapse to fibre

**Plate 6.7.** (x15) 28 Days Degradation.
**L.Pec.15.; Fibre Fragmentatation Readily Observed In The Small And Large Diameter Fibres, Also Illustrating The Pectin Cavities.**

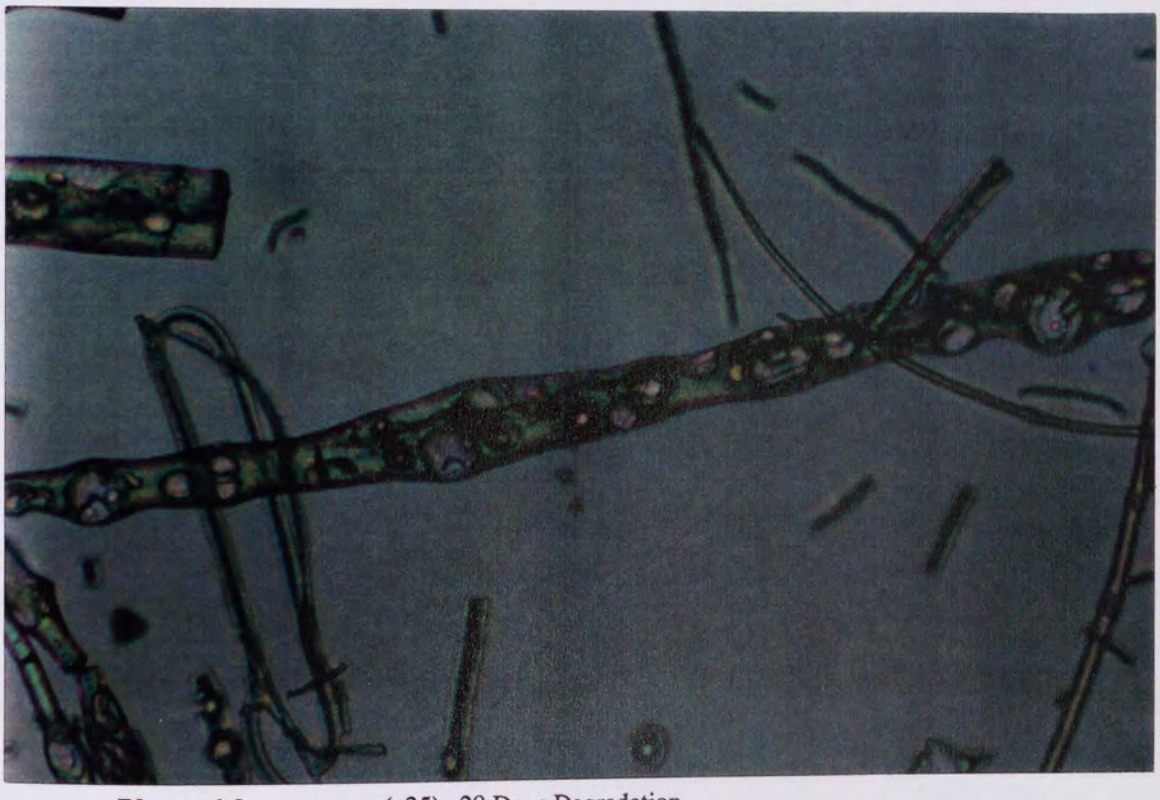

**Plate 6.8.** (x25) 28 Days Degradation.
**L.Pec.15.; Readily Noticeable Pectin Cavities In A Large Diameter Fibre, Increases The Available Surface Area To Volume Ratio And Facilitates Degradation.**

**Plate 6.9.** (x15) 80 Days Degradation.
**L.Pec.15.; Greater Degree Of Fragmentation Than In Plate 6.7.**

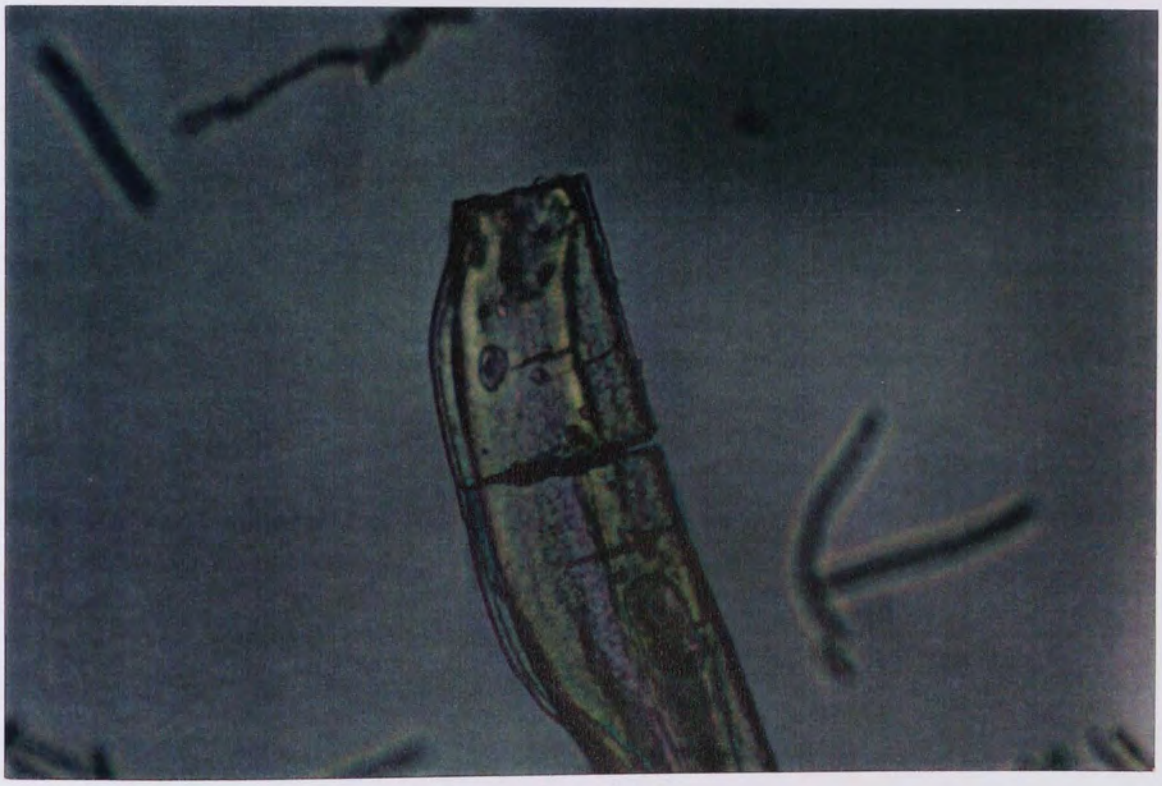

**Plate 6.10.** (x25) 28 Days Degradation.
**L.Pec.15.; Pectin Cavities And Fracturing In A Large Diameter Fibre.**

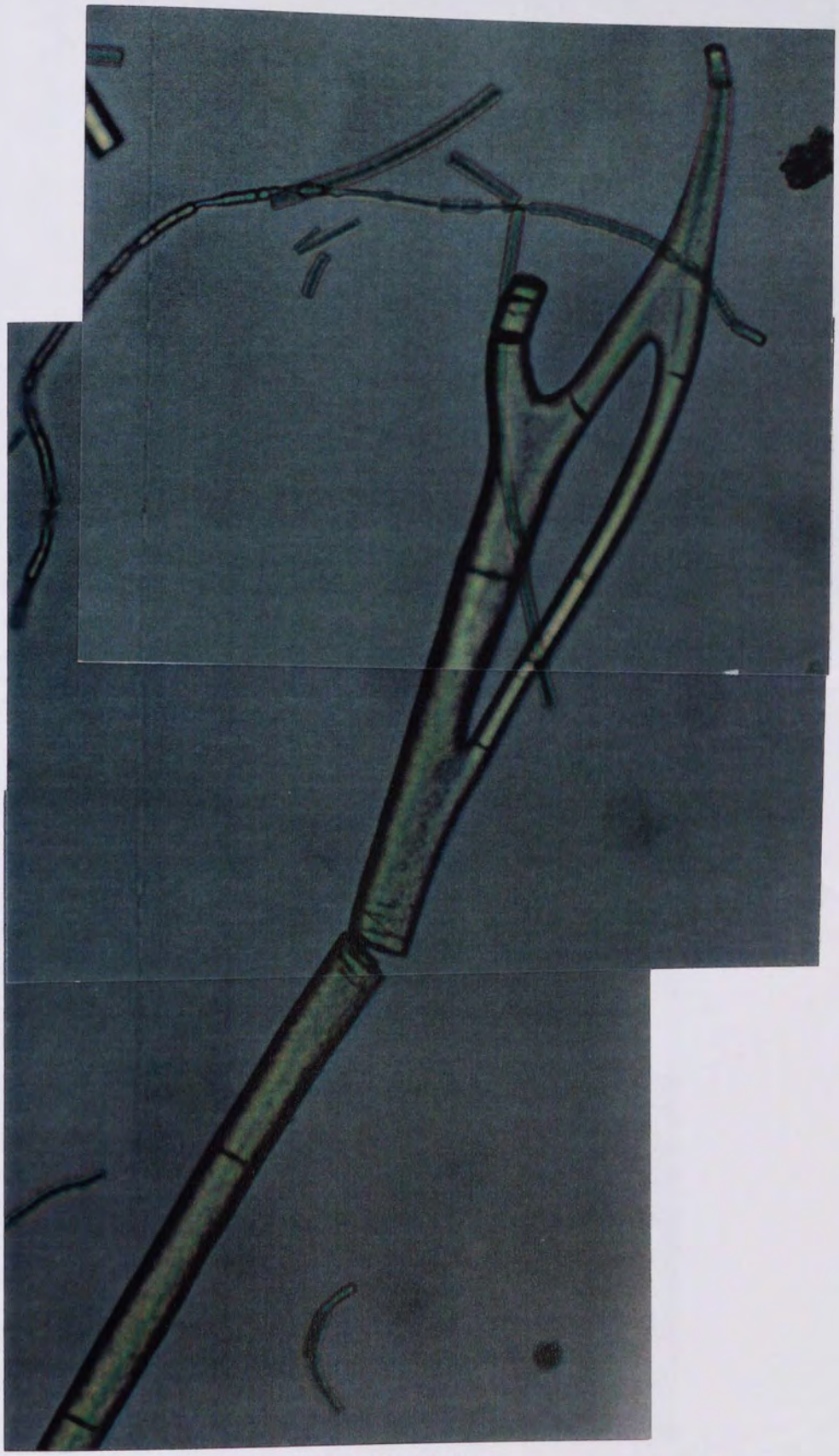

**Plate 6.11.** (x25) 80 Days Degradation.
**L.Pec.25.S.; Large Diameter Fibre With Fracturing Due to Filtering And Drying, Also Illustrating The Apparent Lack Of Pectin Loading Compared To L.Pec.15. In Plates 6.7-6.8.**

**Plate 6.12.** (x25) 28 Days Degradation.
**L.Pec.25.E.; Heavily Pectin Loaded Large Diameter Fibre, Compared To Its Counterpart L.Pec.25.S. In Plate 6.11.**

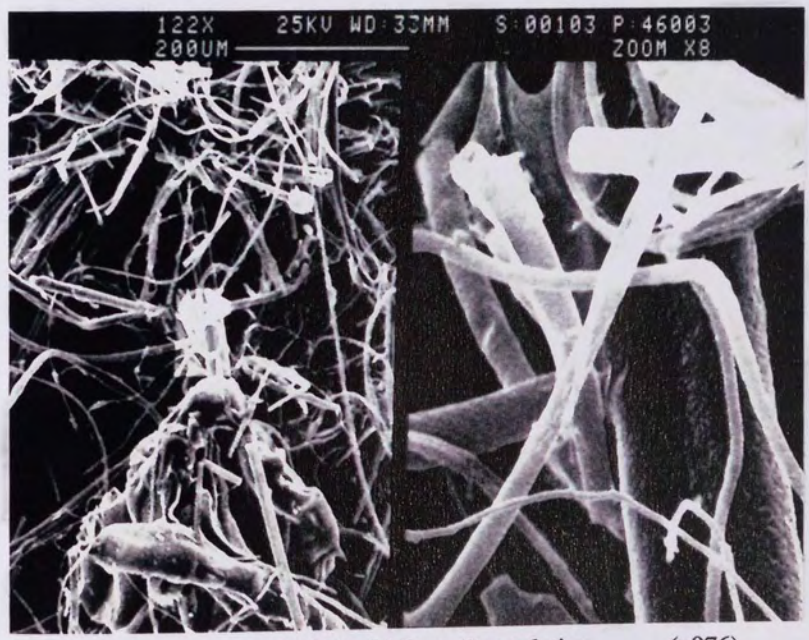


**Plate 6.13.** (x122) 56 Days Degradation. (x976)
**L.Pec.9.; Fibre Fragmentation In A Proportion Of The Small 'Fine' Fibres And Some Of The Larger Diameter Fibres.**


**Plate 6.14.** (x245) 56 Days Degradation.
**L.Pec.15.; Gradual Increase In The Degree Of Fibre Fragmentation After 56 Days In The Physiological Degradation Model.**


**Plate 6.15.** (x4.76K) 56 Days Degradation.
**L.Pec.15.; Irregular Surfaces Of Small Diameter Fibres.**

fragments by day 28. These fibre fragments then remained relatively stable until around day 80 before further fragmentation occurred. These observations at days 28 and 80 were comparable with those from the accelerated degradation model around 7 hours degradation, whilst the later observations around day 143 in the physiological degradation model were similar to the day 1 degradation in the accelerated model.

Thus, the method of degradation for the co-blended samples in the physiological degradation model was the same as that for samples from the accelerated degradation model. However, similar to the IP sample (Sec. 6.1.), the degradation stages were more pronounced.

Graphs 6.14 to 6.19 illustrate the changes in the fibre diameter distributions for the L.Pec.9. fibres during degradation in the physiological degradation model. The partially degraded L.Pec.15. fibre diameter distributions are illustrated in graphs 6.20 to 6.25 and the distributions for the L.Pec.25.S. and L.Pec.25.E. samples are illustrated in graphs 6.26 to 6.31.

The L.Pec.9. fibre diameter distributions were characterized by an initial frequency increase of the 0-2 micron diameter range until day 56, this was accompanied by a gradual increase in the variation of the fibre diameters. After day 56, the number of fibres possessing diameters in the 0 to 2 micron range gradually decreased and at day 275 no fibres were observed at 0-1um. and only 4% possessed diameters in the 1-2um. range. The variation of fibre diameters continued to increase after day 56 with frequencies observed at all the diameter ranges except the 11-12um. at day 175 and the 0-1um. at day

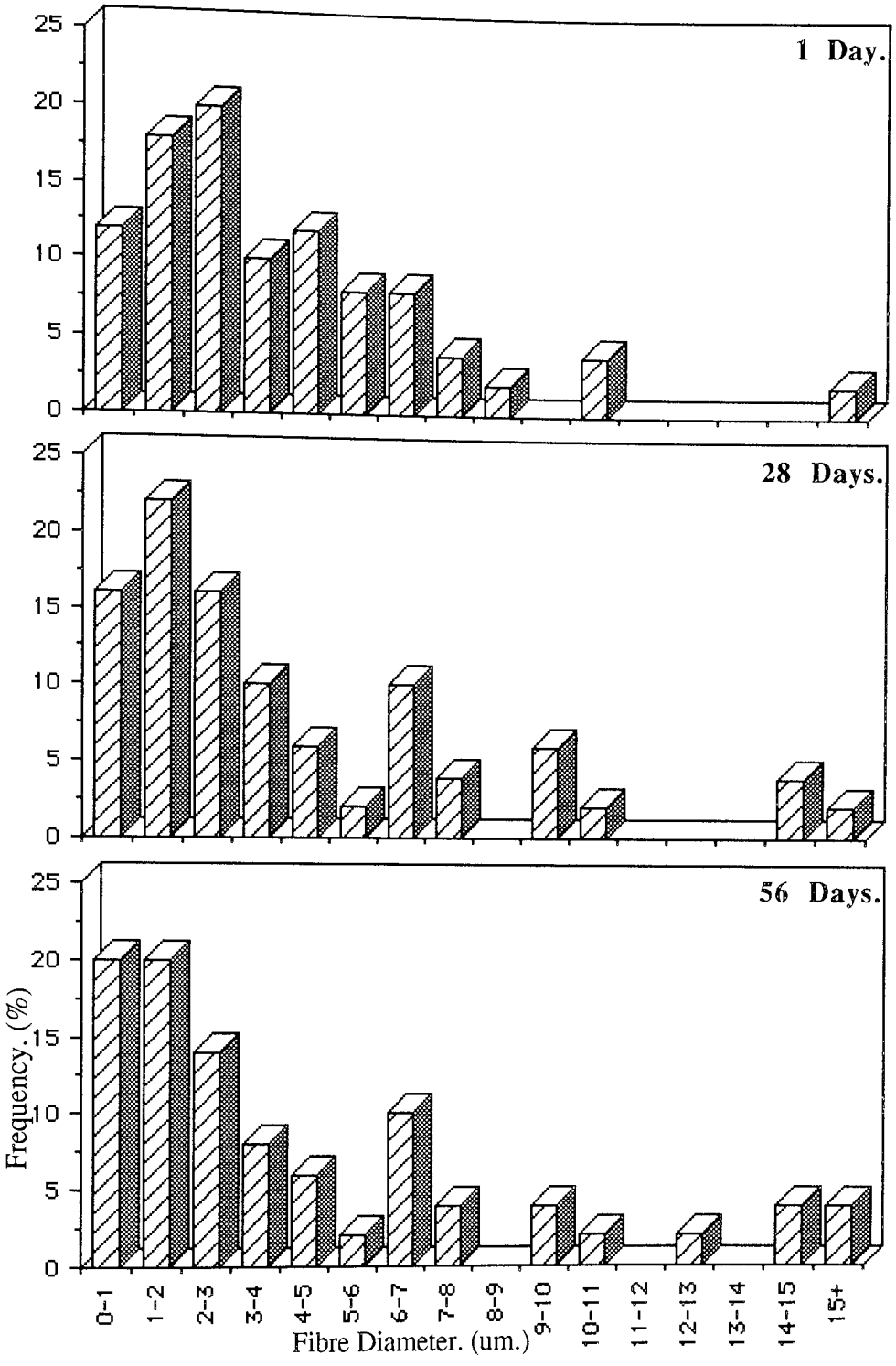


**Graphs 6.14 To 6.16.**

**Fibre Diameter Distributions For L.Pec.9. During Degradation In The Physiological Degradation Model.**

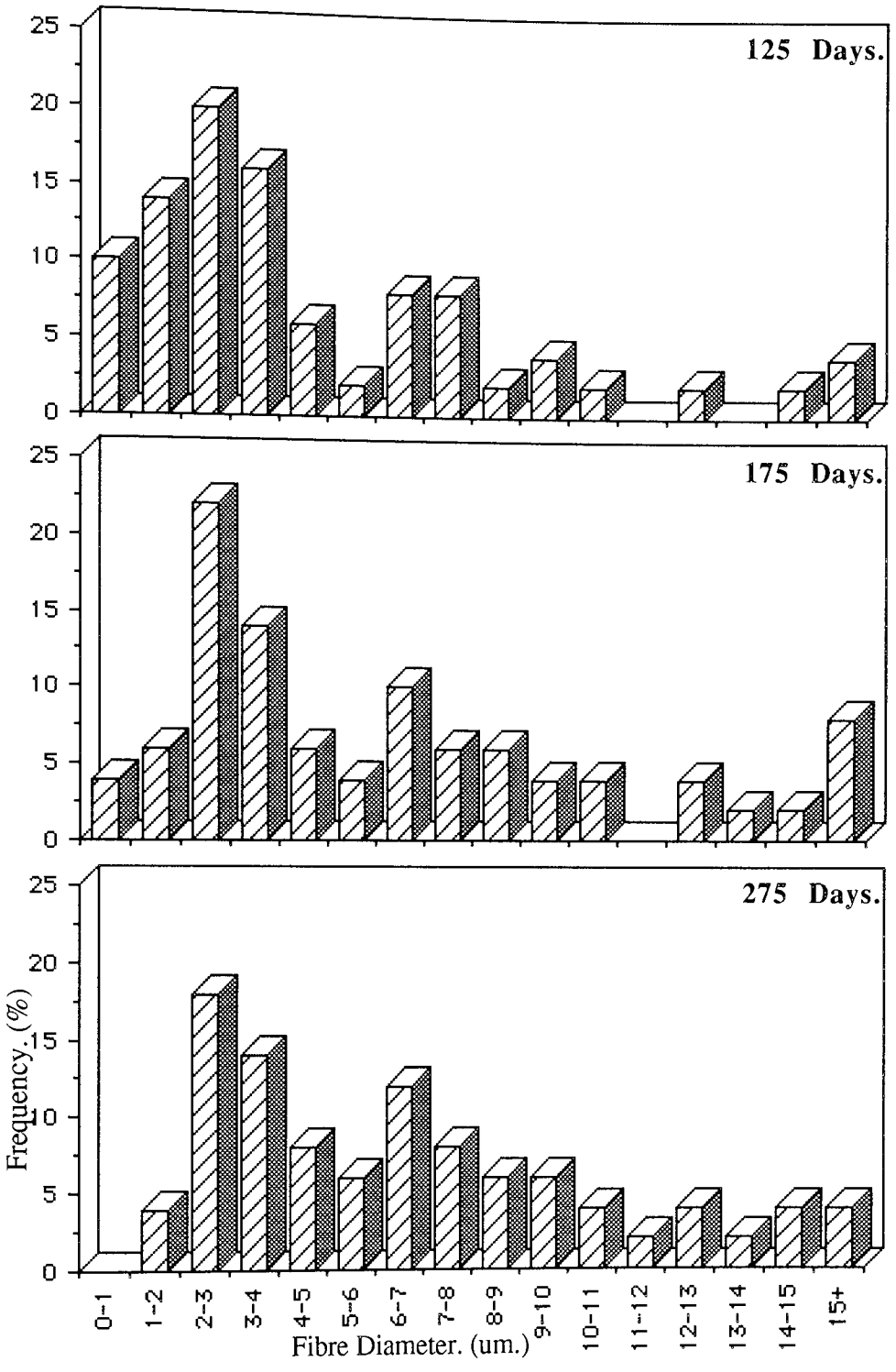


**Graphs 6.17 To 6.19.**

**Fibre Diameter Distributions For L.Pec.9. During Degradation In The Physiological Degradation Model.**

275. These trends were similar to those exhibited by the PHB(FM)IP fibre diameter distributions, however, the homopolymer fibres at the 0-1 and 1-2um. diameters appeared more stable and showed similar frequencies during degradation until after day 56 when they gradually decreased. These comparisons tended to indicate that the blending initially increased the number of fibres with small diameters between 0 and 2 microns and that these fibres were weaker than their homopolymer counterparts, as a result of this, they gradually fragmented until around day 56.

Similar to the L.Pec.9. fibre diameter distributions, the distribution of the L.Pec.15. diameters also exhibited an initial increase in the 0 to 2 micron range, with a noticeable increase in the 1-2um. frequency from 18% at day 1 to 26% at day 56. After day 56 the 0 to 2um. range frequencies gradually decreased, however, the 1-2um. diameter fibres were comparatively more stable than their L.Pec.9. counterparts and their frequency did not decrease as substantially, (Graphs 6.20-6.25).

In contrast to the L.Pec.9. distributions, there was a gradual decrease in the variation of the L.Pec.15. fibre diameters until day 275, where no frequencies observed at 0-1um. and between the 9 to 15 micron ranges. The fibre diameter distributions were characterized by a gradual frequency increase of the large diameters at the 15+ micron range from approximately 8% at day 1 to around 18% at day 275. These results indicated that increasing the pectin loading from 9 to 15% increased the initial number of large diameter fibres and that these fibres were comparatively heavily loaded with pectin, which upon dissolution facilitated in their fragmentation.

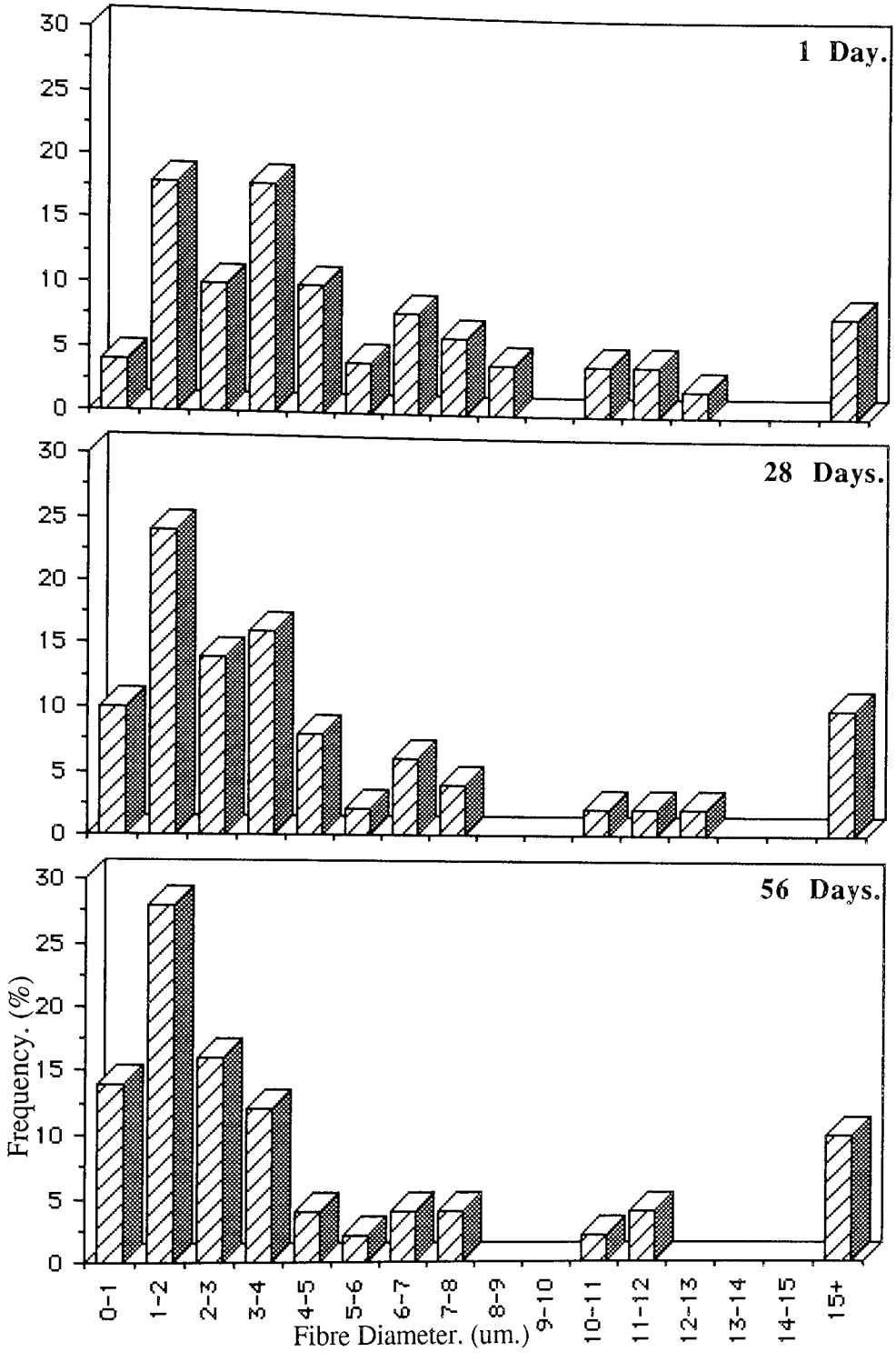


**Graphs 6.20 To 6.22.**

**Fibre Diameter Distributions For L.Pec.15. During Degradation In The Physiological Degradation Model.**

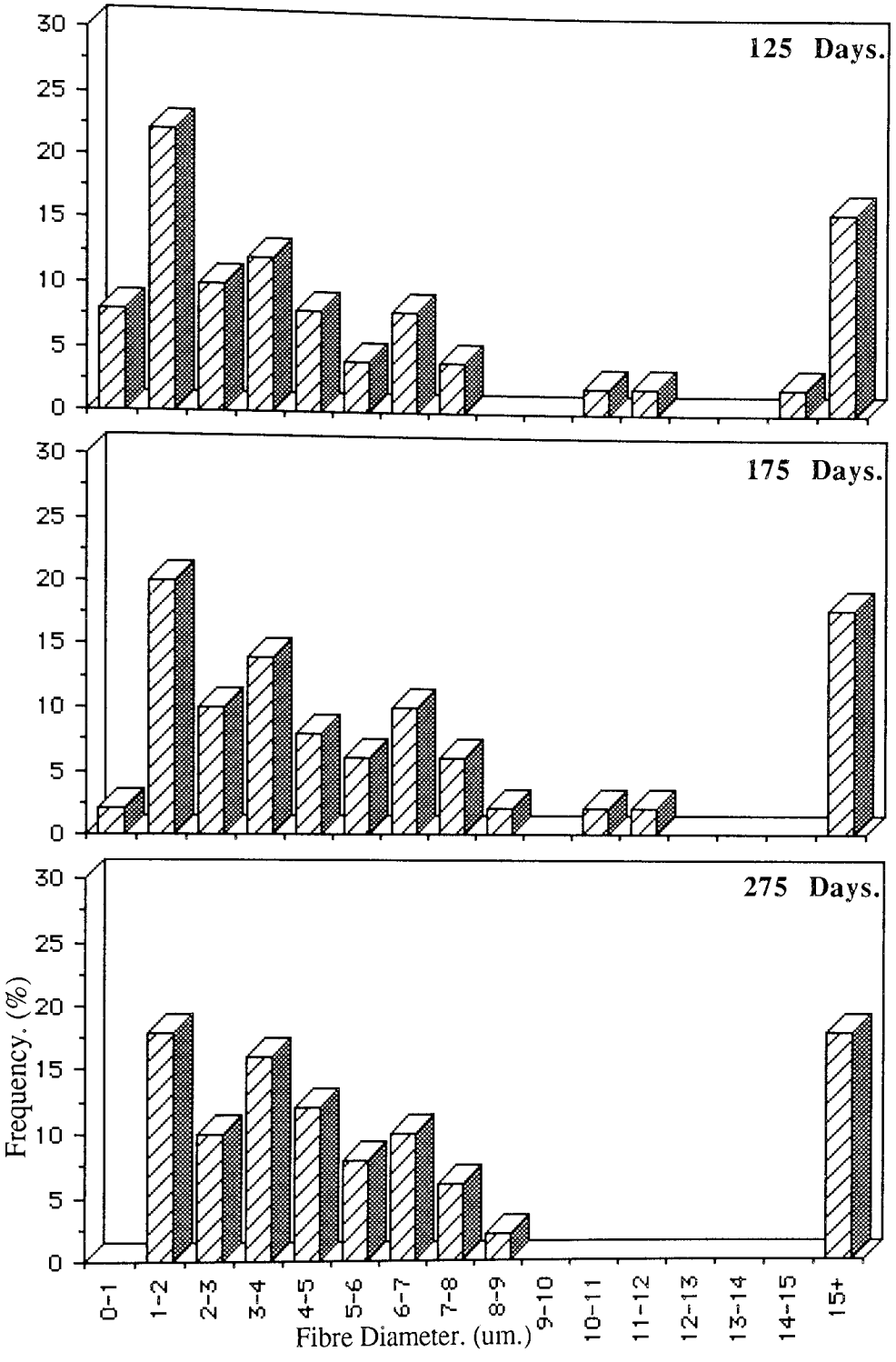


**Graph 6.23 To 6.25.**

**Fibre Diameter Distributions For L.Pec.15. During Degradation In The Physiological Degradation Model.**

The fibre diameter distributions of the L.Pec.25.E. sample illustrated in graphs 6.26 to 6.31 exhibited a gradual increase in the frequency of the large diameter fibres (15+um.) from 8% at day 1 to approximately 20% at day 56, before gradually decreasing to around 10% at day 275. This trend was due to the gradual dissolution of the pectin by day 28 and the subsequent fragmentation of the weakened large diameter fibres by day 56. In contrast, the large diameter fibres from sample L.Pec.25.S. (Graphs 6.26-6.31) possessed only a 2% frequency at day 1 and this remained similar throughout the degradation experiment. No L.Pec.25.E. fibres were counted at the 0-1um. range whilst the main distribution peak shifted to 4-5um. from the 1-2um. peak observed in the L.Pec.9. sample. The fibres at this 4-5um. peak were relatively stable and as a result of this, their frequency gradually decreased from 32% at day 1 to 16% at day 175, due to the fragmentation of the other fibres and the counting procedure. After day 175, these fibres fragmented and their frequency increased to approximately 26%. This fragmentation coincided with the increase in degradation around day 200 observed in the degradation profile, graph 6.13.

The fibre diameter distributions of the L.Pec.25.S. sample exhibited similar trends to those discussed for the L.Pec.9. sample. There was a gradual increase in the frequencies of the fibres possessing diameters between 0 and 3 microns until around day 56, after which the 0-1um. range frequency gradually decreased, whilst the frequencies of those fibres with diameters between 1 and 3 microns continued to increase until around day 175. Similarly, the distribution variation for L.Pec.25.S. also increased until day 125 and then decreased at day 175 with no frequencies observed between 10 and 15 microns, in contrast, the L.Pec.25.E. distributions exhibited frequencies at all the diameter ranges

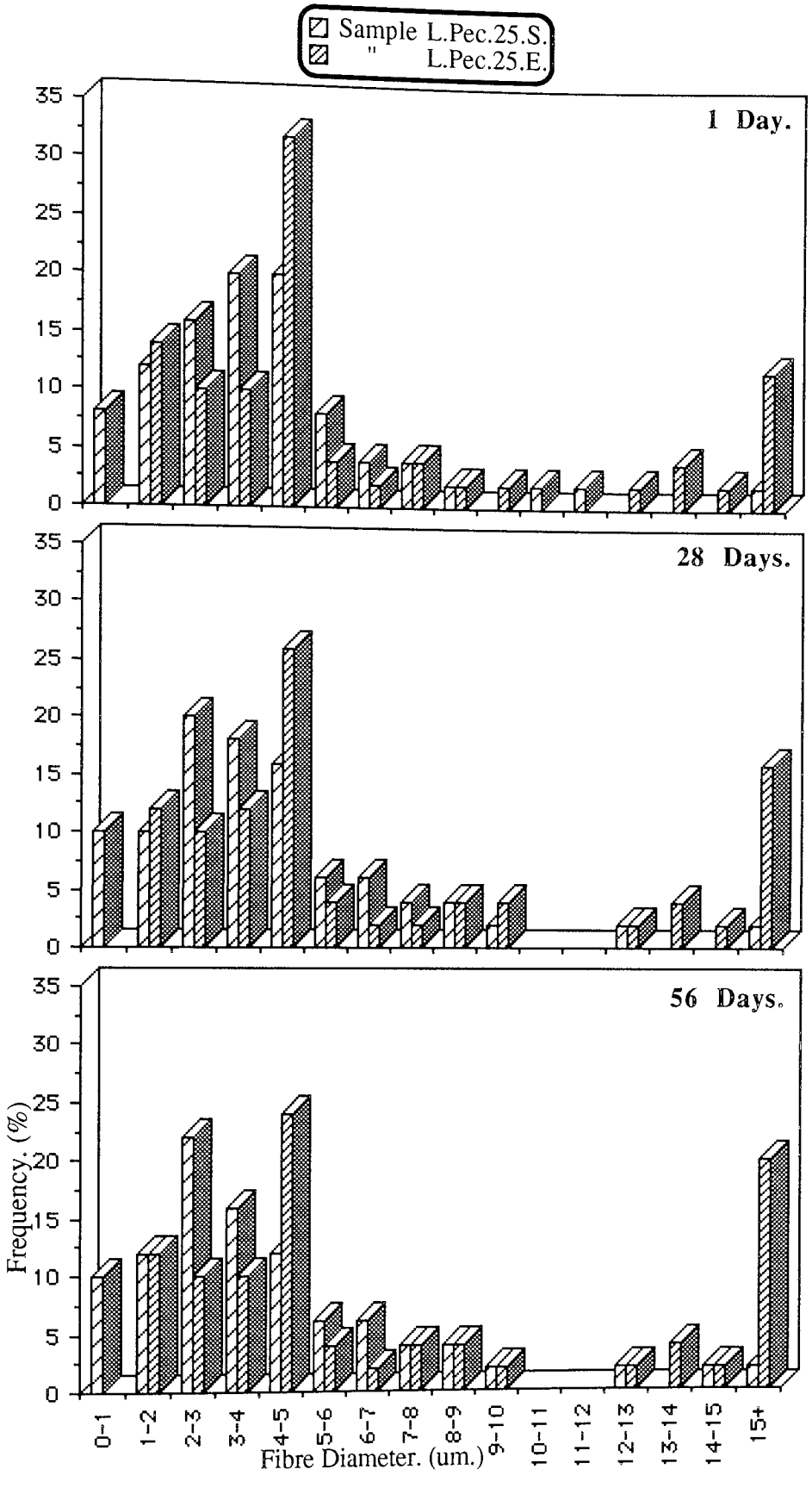


**Graphs 6.26 To 6.28.**

**Fibre Diameter Distributions For L.Pec.25.S. And L.Pec.25.E. During Degradation In The Physiological Degradation Model.**

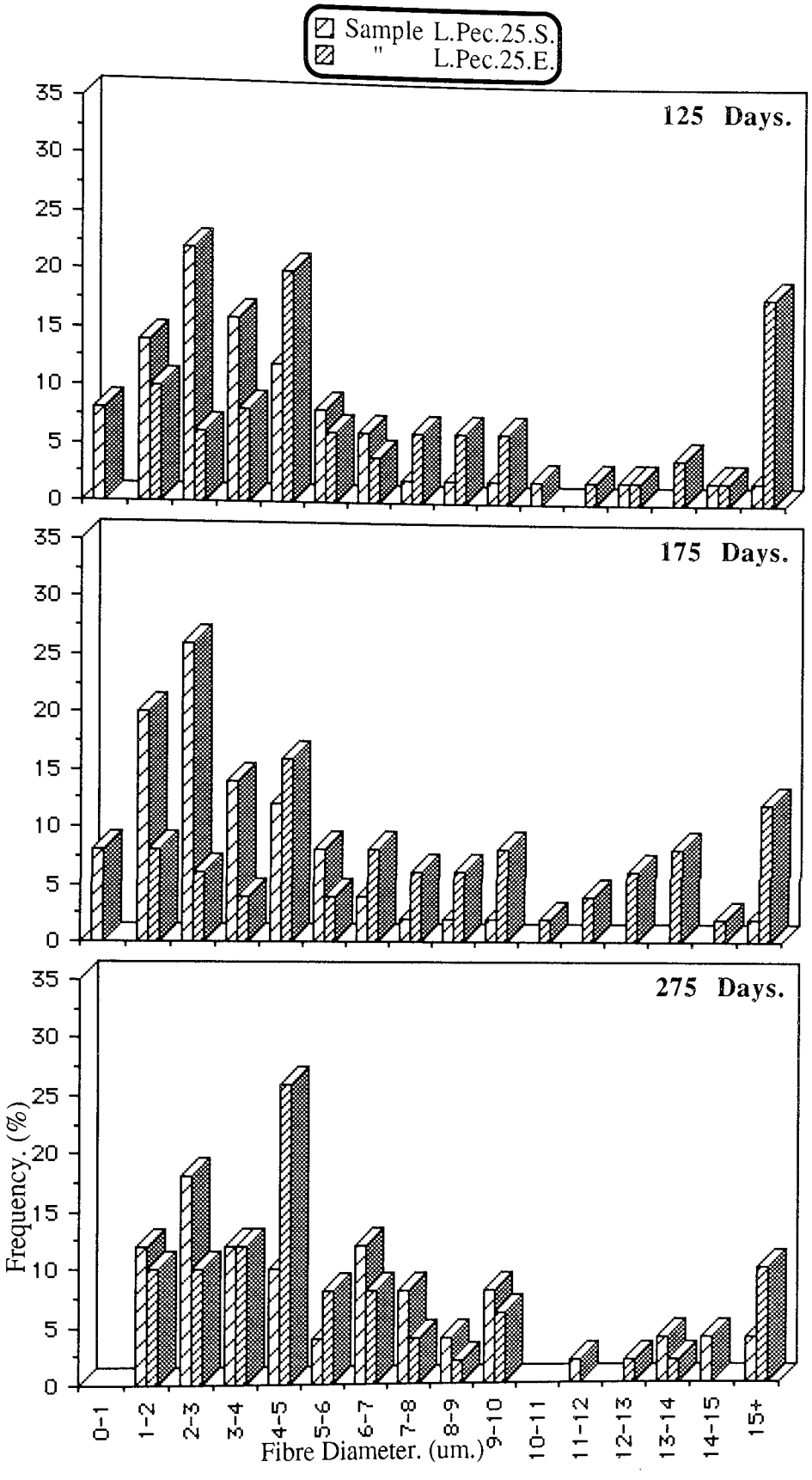


**Graphs 6.26 To 6.28.**

**Fibre Diameter Distributions For L.Pec.25.S. And L.Pec.25.E. During Degradation In The Physiological Degradation Model.**

except the 0-1um. range.

Graphs 6.32 to 6.35 illustrate the general fibre diameter distributions of the co-blends according to the groups; small, medium and large, for diameters <6, 6-15 and >15um. respectively. As can be observed from graph 6.32 there was a gradual decrease in the small diameter frequency of the L.Pec.9. sample with a corresponding increase in the medium and large sized fibres. This contrasted with the general fibre diameter distribution from the accelerated degradation model (Graph 5.33) which showed an initial increase in the small diameter frequency and then a sharp decrease after approximately 7 hours degradation, with a corresponding frequency decrease and then increase in the medium sized fibres.

The general fibre diameter distributions of the L.Pec.15. sample (Graph 6.33) were similar to those determined from the accelerated degradation model, (Graph 5.39.). In the accelerated degradation model the number of small fibres from L.Pec.15. increased until 7 hours degradation before decreasing, however, in the distribution from the physiological degradation model this initial small fibre increase was observed until around day 56 and the decrease at day 125. Similarly, the general fibre diameter distribution for the L.Pec.25.E. sample, (Graph 6.34), was comparable to that obtained for the sample in the accelerated degradation model. However, in this instance, there was a gradual decrease in the L.Pec.25.E. small diameter frequency until 6 hours degradation and then an increase, whilst in the physiological degradation model, the small diameter frequency decreased until around day 175 and then increased. The distribution trends for the medium and large diameter groups from the two degradation models were also comparable.

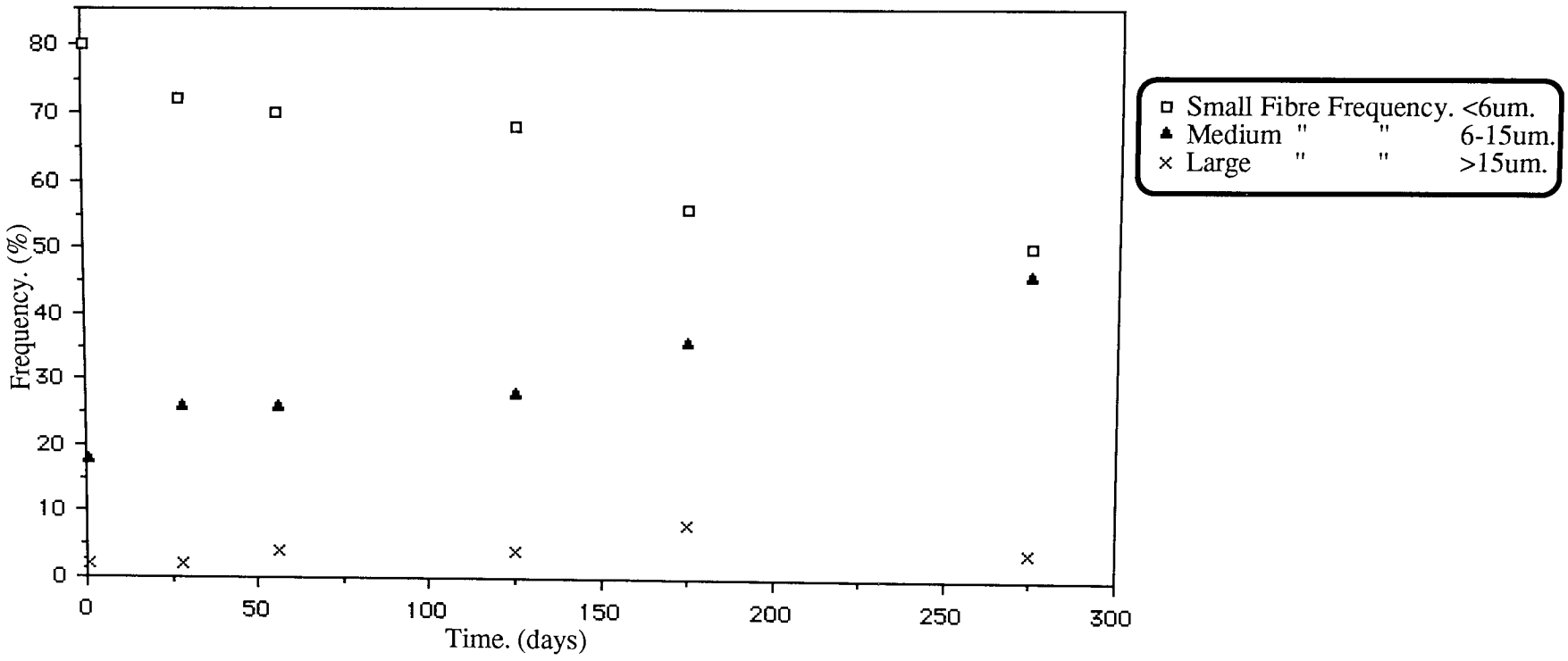


**Graph 6.32.**

**General Fibre Diameter Distributions Of L.Pec.9. During Degradation In The Physiological Degradation Model.**

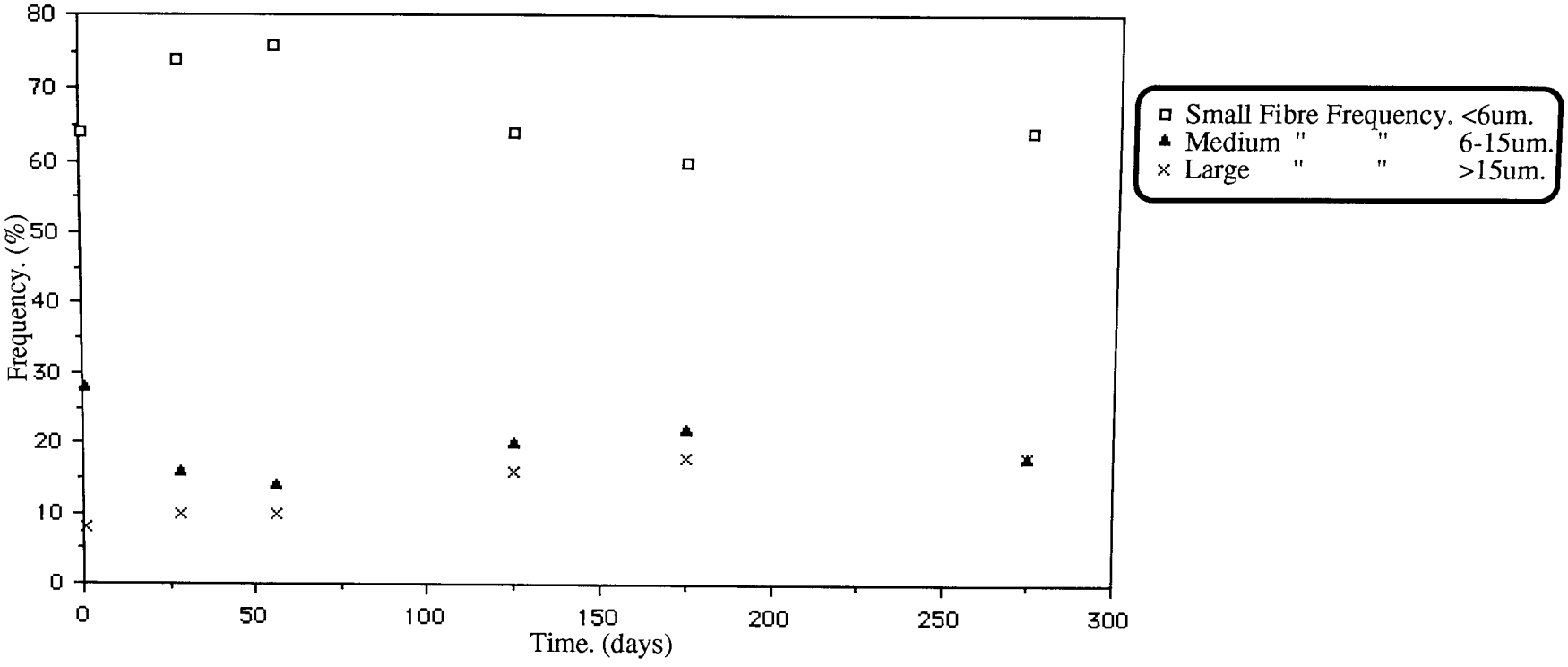


**Graph 6.33.**

**General Fibre Diameter Distributions Of L.Pec.15. During Degradation In The Physiological Degradation Model.**

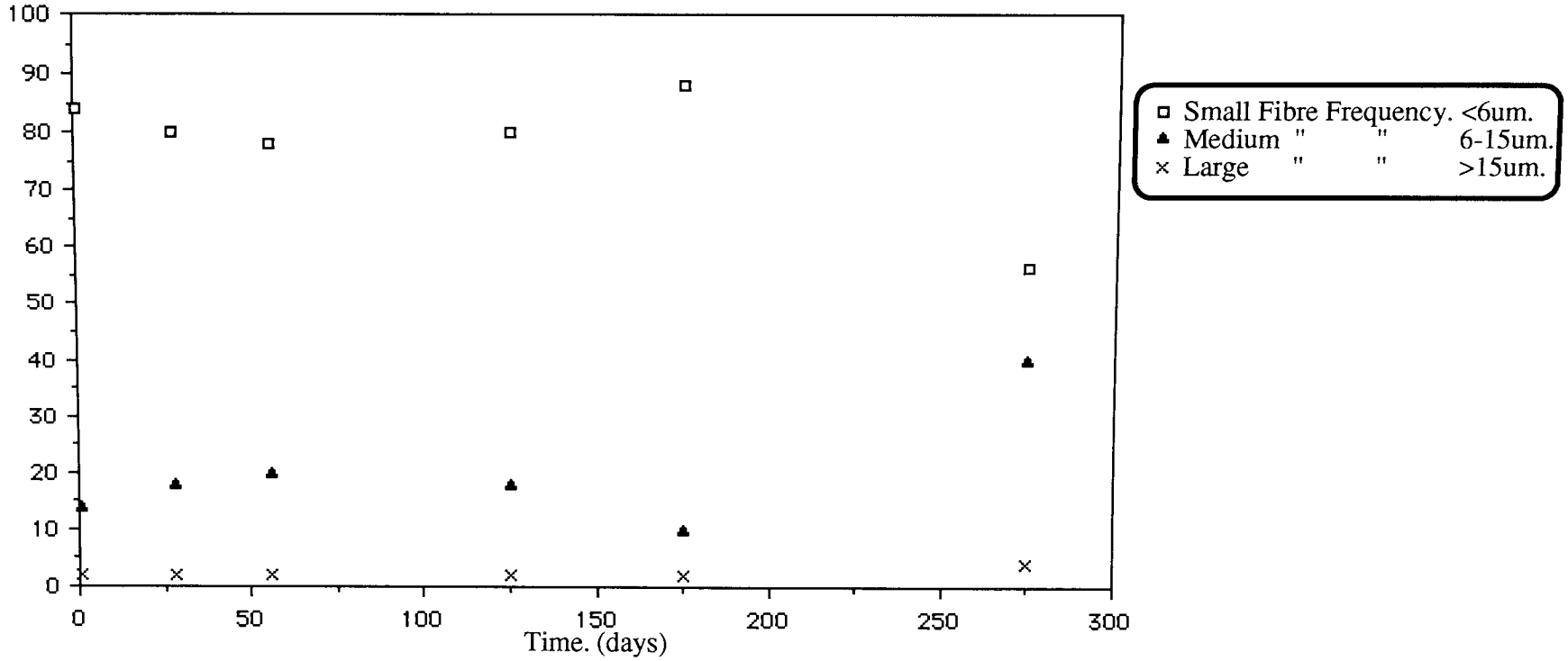


**Graph 6.34.**

**General Fibre Diameter Distribution For L.Pec.25.S. During Degradation In The Physiological Degradation Model.**

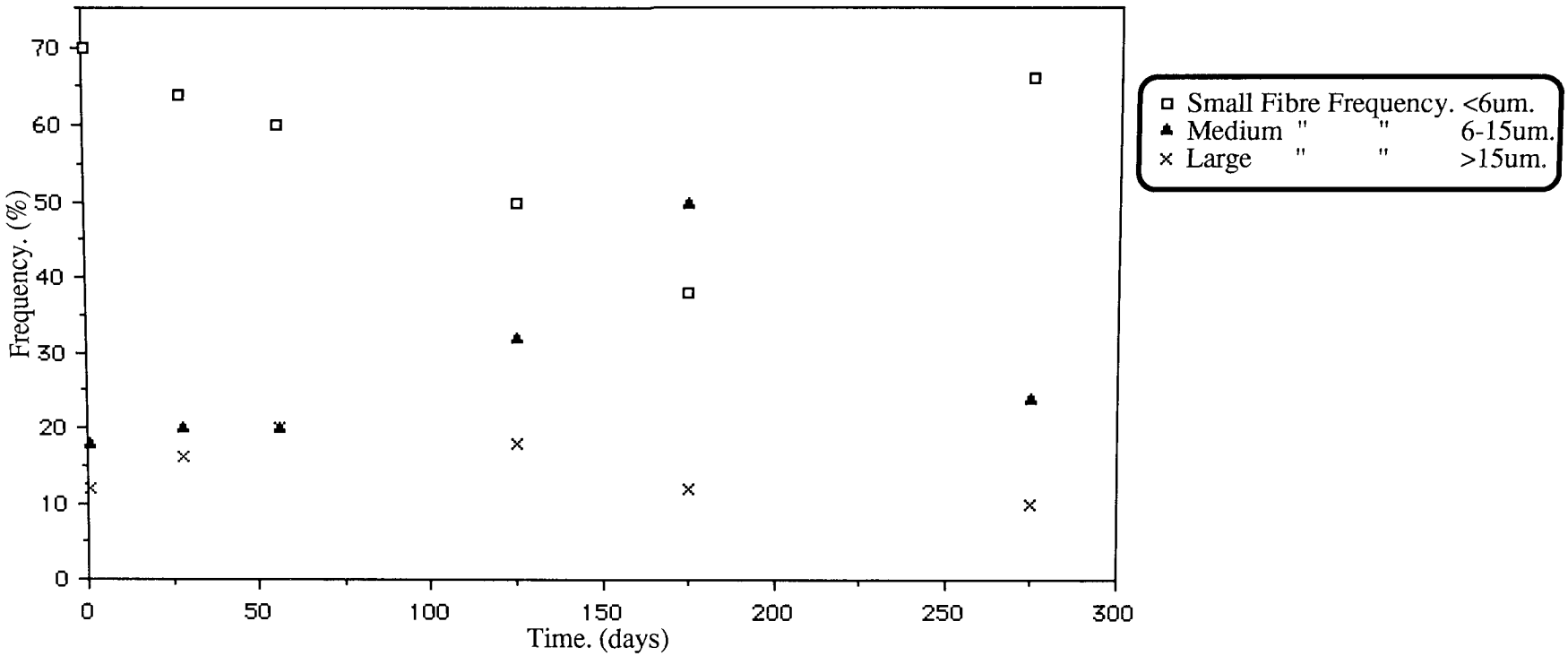


**Graph 6.35.**

**General Fibre Diameter Distribution For L.Pec.25.E. During Degradation In The Physiological Degradation Model.**

Graph 6.34 illustrates the general fibre diameter distribution for the L.Pec.25.S. sample which showed little change in the diameter group frequencies for the first 125 days degradation, this was comparable to the first 3 hours degradation for the sample in the accelerated degradation model. After day 125 there was a slight increase in the small diameter frequency from around 80 to 88% at day 175 with a corresponding decrease in the medium sized fibres from 18 to approximately 10%. After day 175 the medium sized fibres fragmented and their frequency increased to approximately 40% at day 275, with a decrease in the small diameter frequency to 58%. The large diameter fibres maintained a similar frequency during the experiment. This apparent lack of frequency change in the first 175 days for the L.Pec.25.S. diameter groups coincided with the comparatively little weight loss observed in the degradation profile, graph 6.13.

Therefore, it was concluded that blending the PHB(FM)IP with pectin increased the initial number of small diameter fibres at the 0-2um. range and weakened these fibres so that fragmentation readily occurred. Increasing the pectin loading increased the initial number of large diameter fibres (>15um.) and these were also relatively weak compared to their homopolymer counterparts, so that fragmentation occurred after the pectin dissolution.

### 6.2.3. Characterization Of The Partially Degraded Co-blends.

The partially degraded co-blend samples were examined utilizing DSC and the melting points, fusion enthalpies and glass transition temperatures determined. The samples were also examined using FTIR-PAS. As can be observed from graphs 6.33 to 6.40, the changes in the melting point and fusion enthalpy during the degradation followed similar trends for all the co-blended samples. These trends were also similar to those determined

for the PHB(FM)IP.

The melting point graphs were characterized by an initial induction period where there was little change until around days 50 to 75. After this period the melting point gradually decreased, so that at day 325 there was an overall change in the co-blends of approximately -12 ±2°C. This contrasted with the melting point change for the IP sample which decreased by approximately 6 ±2°C.

The change in the fusion enthalpies of the co-blended samples were characterized by a gradual increase to a peak before gradually decreasing. This peak corresponded to a point of maximum crystallinity, after which the remaining PHB matrix readily degraded. This enthalpy increase was approximately 17 ±5$Jg.^{-1}$, which was similar to that determined for the IP sample; 25 ±5$Jg.^{-1}$ However, it was observed that increasing the pectin loading increased the time period before this enthalpy/crystallinity peak was attained, (Table 6.1.).

| Sample: | Actual Pectin Loading: | Time To Reach Crystallinity Peak: |
|---|---|---|
| L.Pec.9. | 9% | 90 days. |
| L.Pec.25.S. | 0% (approx.) | 130 " |
| PHB(FM)IP | 0% | 145 " |
| L.Pec.15. | 15% | 170 " |
| L.Pec.25.E. | 19% | 225 " |

**Table 6.1.**

**Time To Attain Maximum Enthalpy/Crystallinity For Co-blends In The Physiological Degradation Model.**

The samples with relatively low pectin loadings, L.Pec.9. and L.Pec.25.S., reduced the

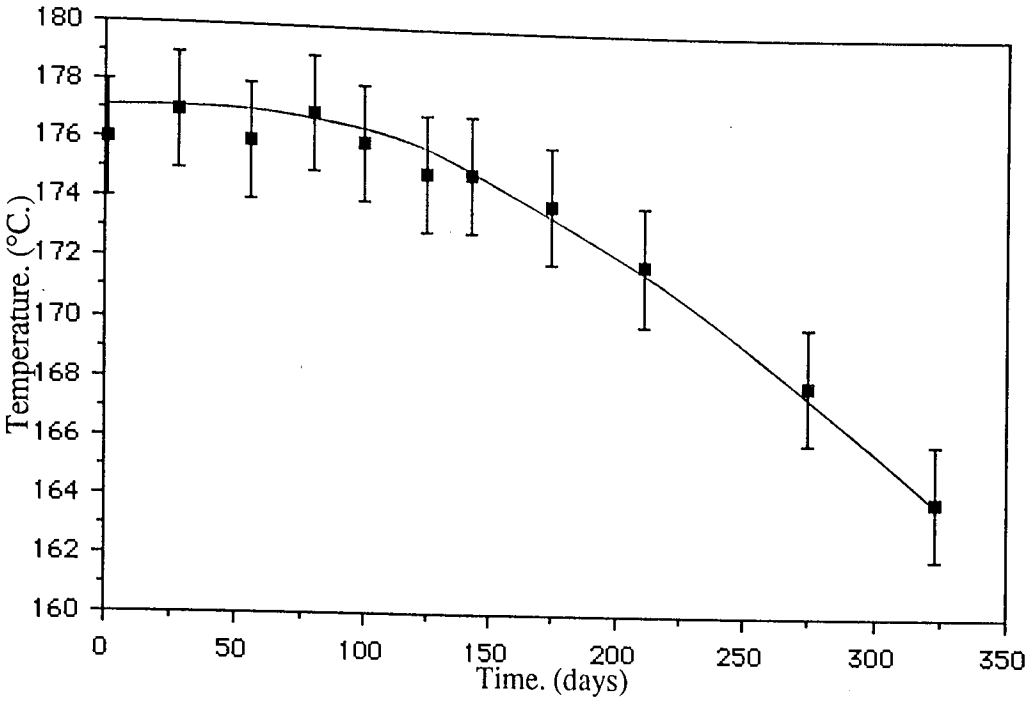


**Graph 6.36.**

**Change In Melting Point Of L.Pec.9. During Degradation In The Physiological Degradation Model.**

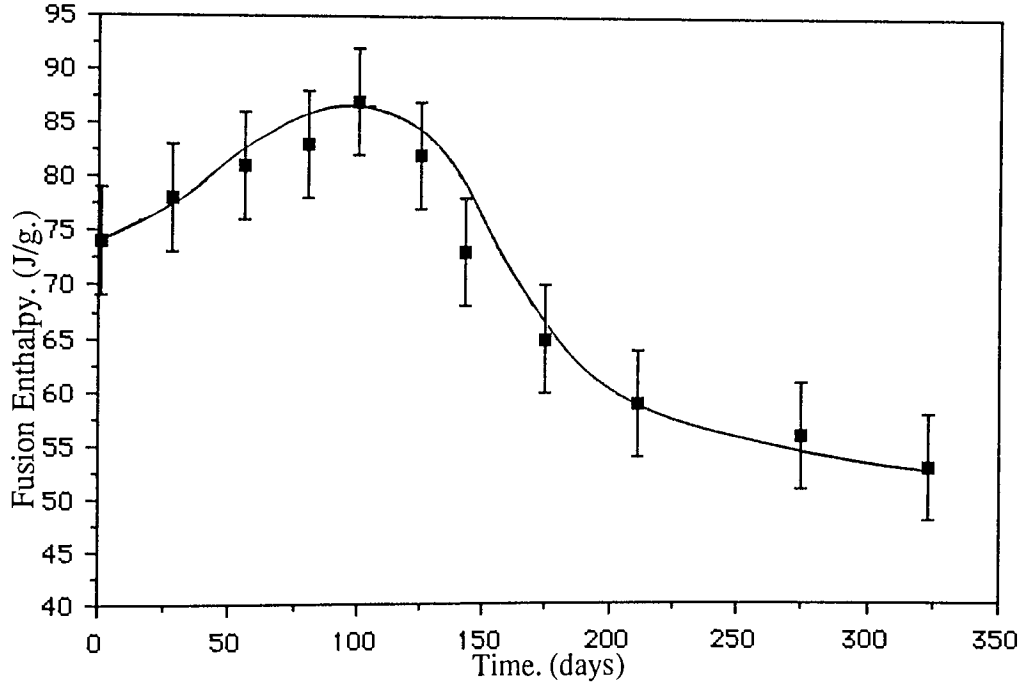


**Graph 6.37.**

**Change In Fusion Enthalpy Of L.Pec.9. During Degradation In The Physiological Degradation Model.**

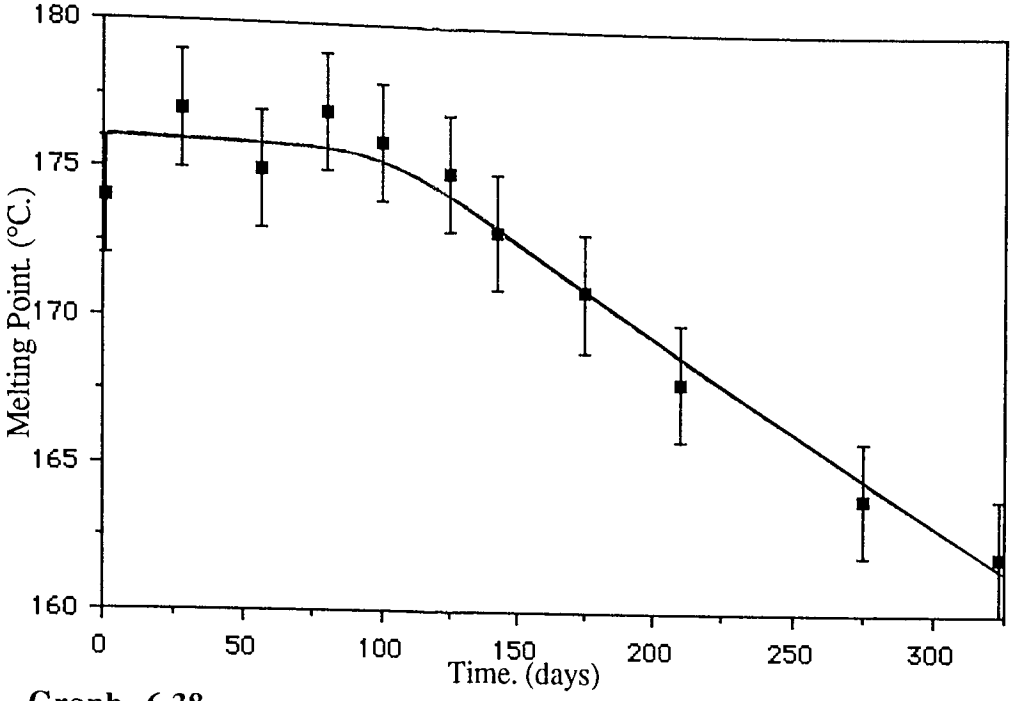


**Graph 6.38.**

**Change In Melting Point Of L.Pec.15. During Degradation In The Physiological Degradation Model.**

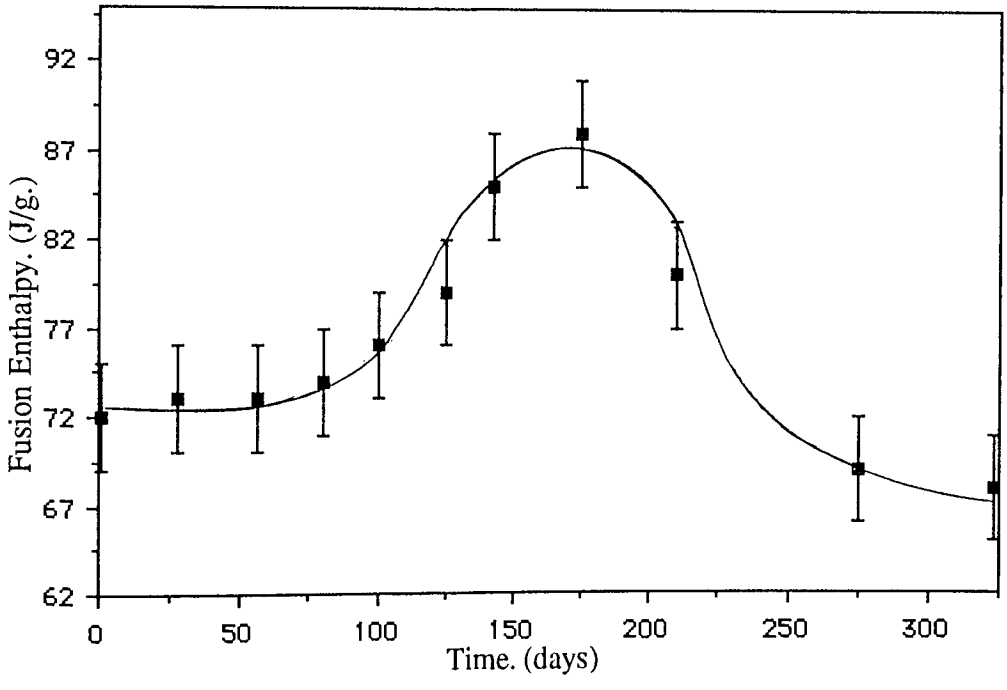


**Graph 6.39.**

**Changes In Fusion Enthalpy Of L.Pec.15. During Degradation In The Physiological Degradation Model.**

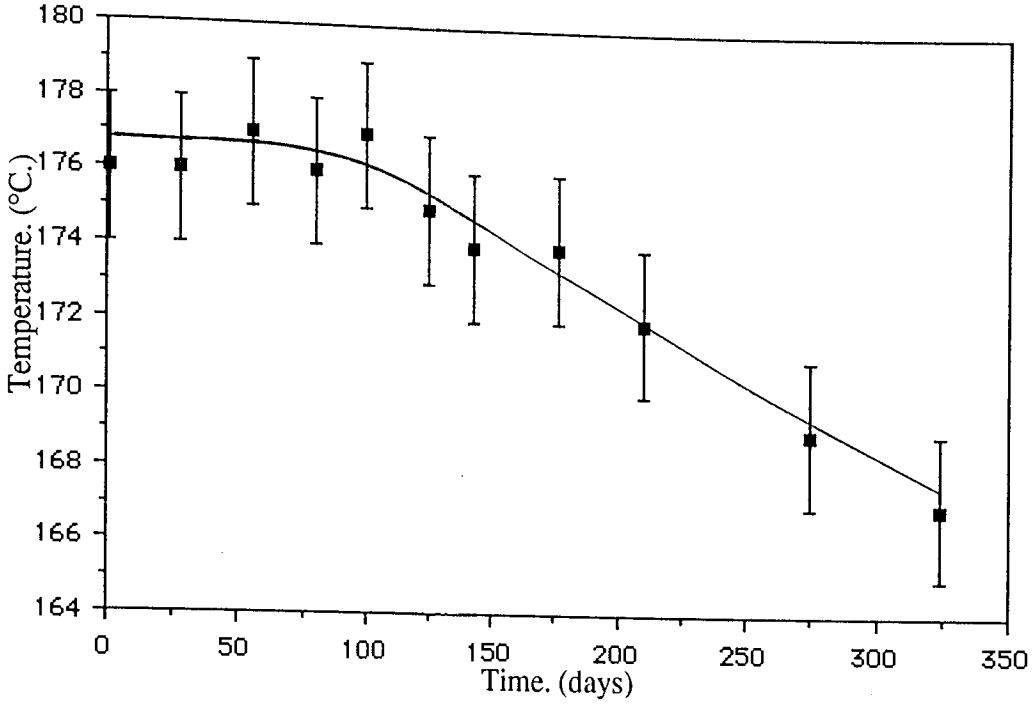


Graph 6.40.

Change In Melting Point Of L.Pec.25.S. During Degradation In The Physiological Degradation Model.

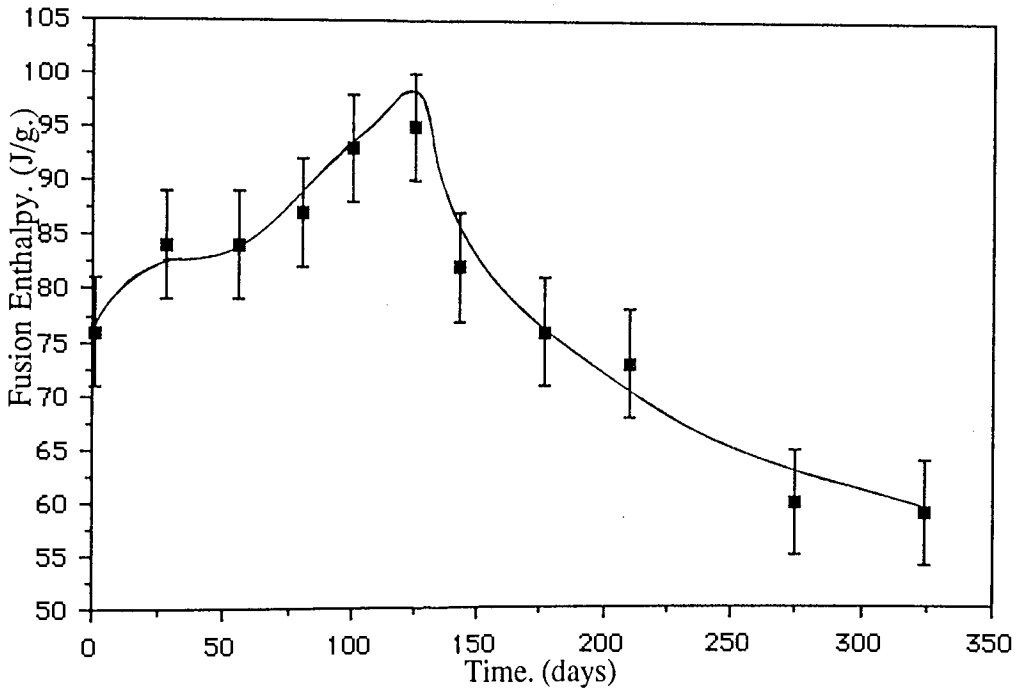


Graph 6.41.

Change In Fusion Enthalpy Of L.Pec.25.S. During Degradation In The Physiological Degradation Model.

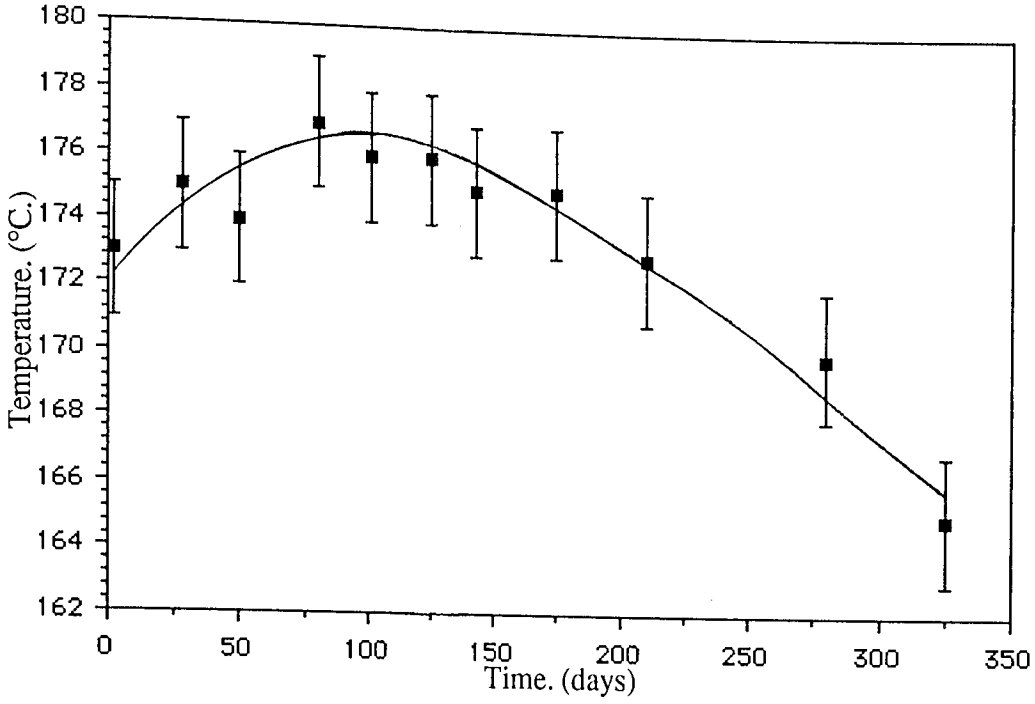


Graph 6.42.

Change In The Melting Point Of L.Pec.25.E. During Degradation In The Physiological Degradation Model.

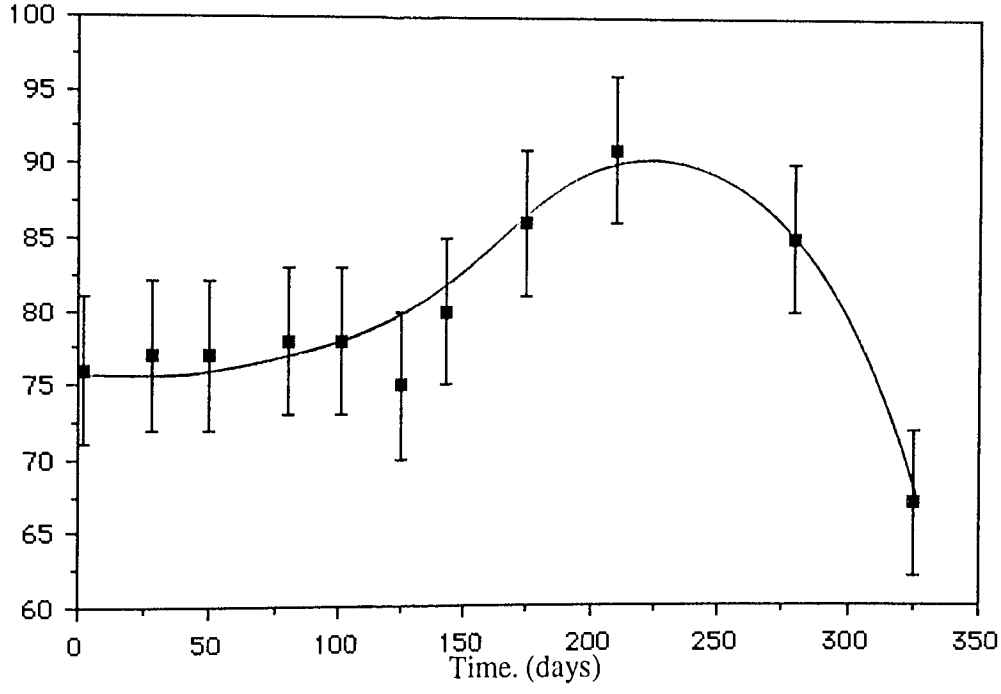


Graph 6.43.

Change In The Fusion Enthalpy Of L.Pec.25.E. During Degradation In The Physiological Degradation Model.

time period necessary to attain maximum crystallinity when compared to the IP sample. These peak shifts were observed for the samples from the accelerated degradation model, but were not as conclusive.

In contrast to the PHB(FM)IP sample, the glass transition temperatures (Tg.) were quite noticeable for most of the samples during the degradation. In some instances the use of the first order derivative was necessary, whilst in others no discernible Tg. was measured. Graphs 6.41 to 6.44 illustrate the changes in the Tg. during the degradation for the co-blended samples. As can be observed the changes in the Tg. were similar. The partially degraded L.Pec.9. showed a gradual decrease in the Tg. from 2 ±3°C. at day 1 to approximately -10 ±3°C. at day 175, before levelling out around -13 ±3°C. until day 323.

Sample L.Pec.15. initially showed little change in the Tg. which varied from 2 ±3°C. at day 28 to -3 ±3°C. at day 125. After this, the Tg. suddenly decreased to -11 ±3°C. at day 143 and maintained a similar value until the end of the experiment. A similar trend was observed for sample L.Pec.25.E. which had a comparatively sudden decrease from 0 ±3°C. at day 143 to -8 ±3°C. at day 175. In contrast, sample L.Pec.25.S. exhibited a gradual decrease in the Tg. from 2 ±3°C. at day 1 to approximately -8 ±3°C. at day 325.

Thus, it was concluded that those samples with a comparatively low pectin loading; L.Pec.9. and L.Pec.25.S., showed a more gradual decrease in the Tg., whilst the comparatively higher loadings of samples L.Pec.15. and L.Pec.25.E., exhibited little change initially but then a sudden decrease. There was an average decrease of -14 ±3°C. for all the samples.

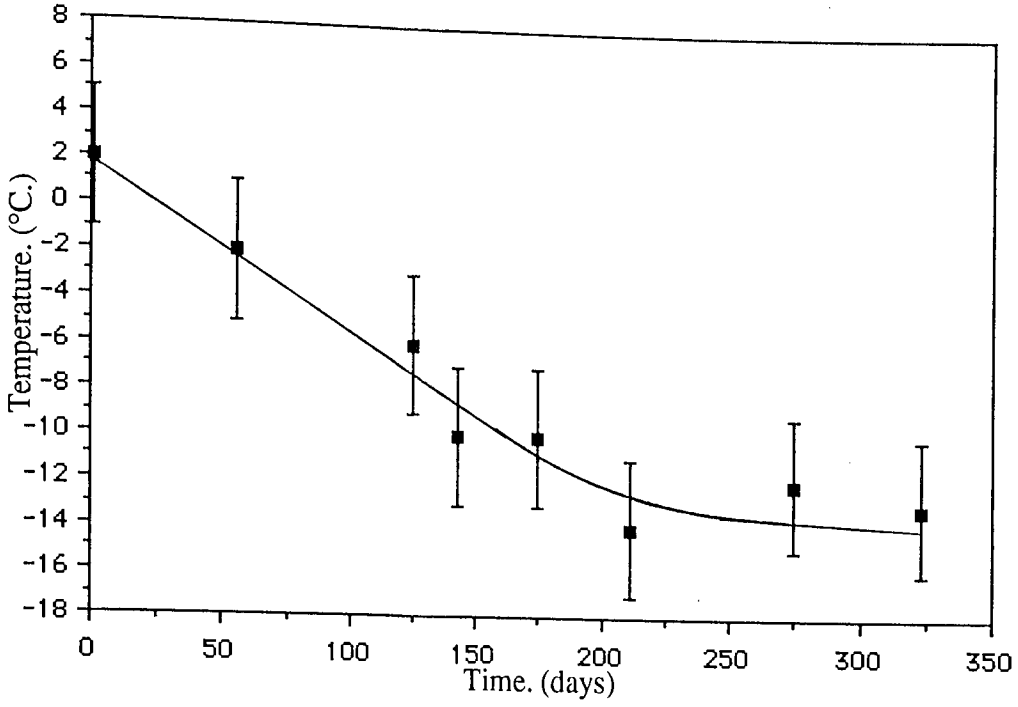


Graph 6.44.

Change In The Glass Transition Temperature Of L.Pec.9. During Degradation In The Physiological Degradation Model.

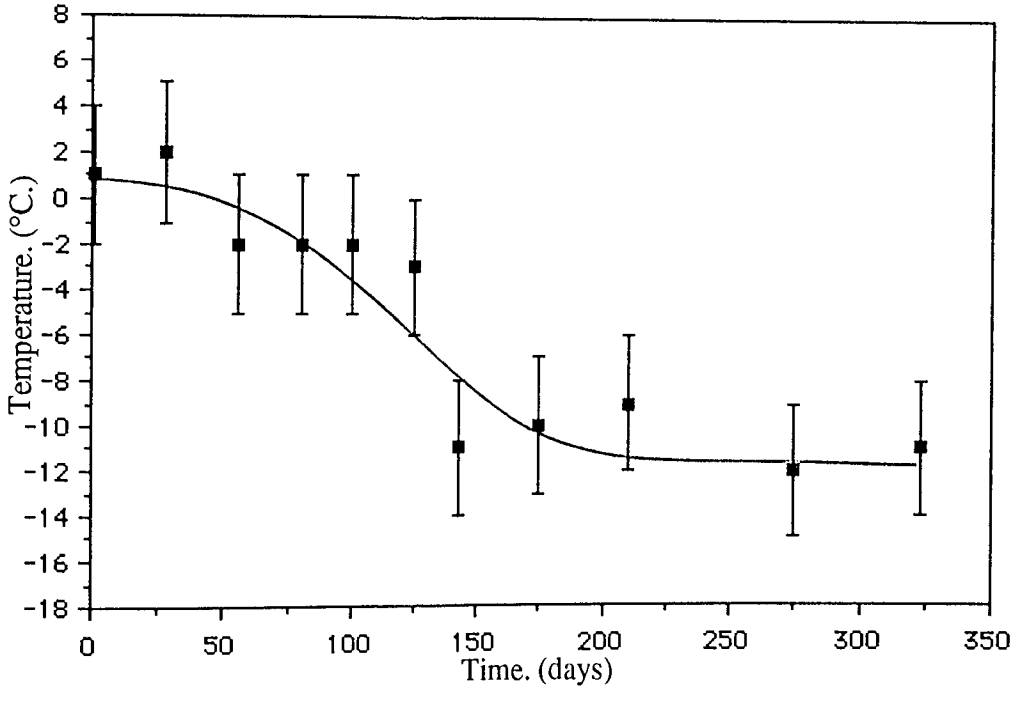


Graph 6.45.

Change In The Glass Transition Temperature Of L.Pec.15. During Degradation In The Physiological Degradation Model.

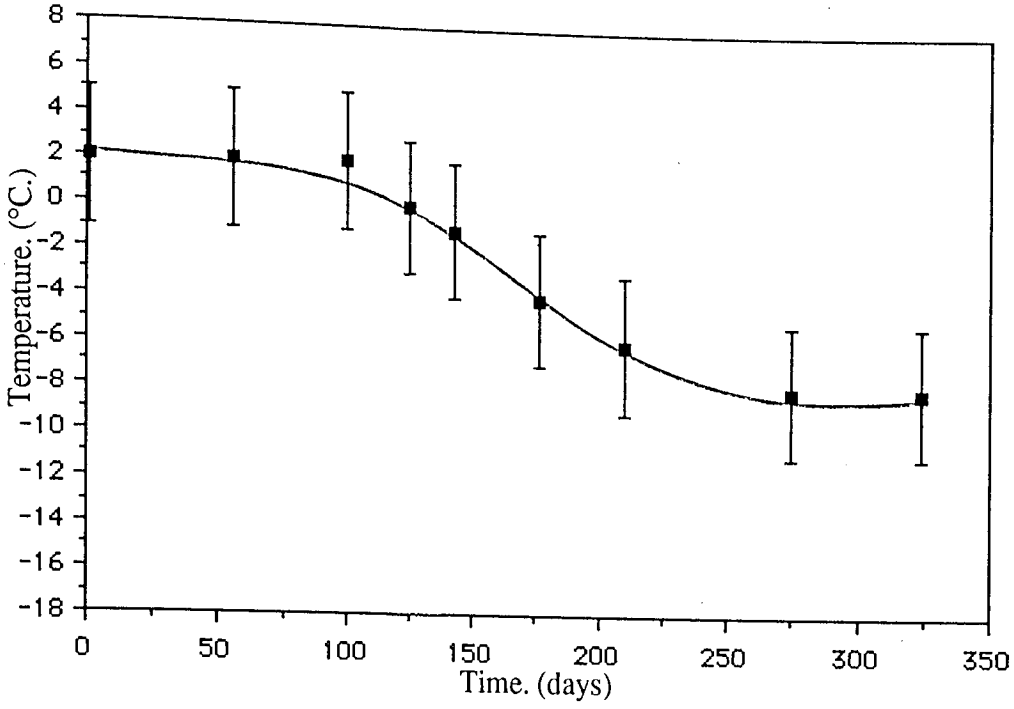


Graph 6.46.

Change In Glass Transition Temperature Of L.Pec.25.S. During Degradation In The Physiological Degradation Model.

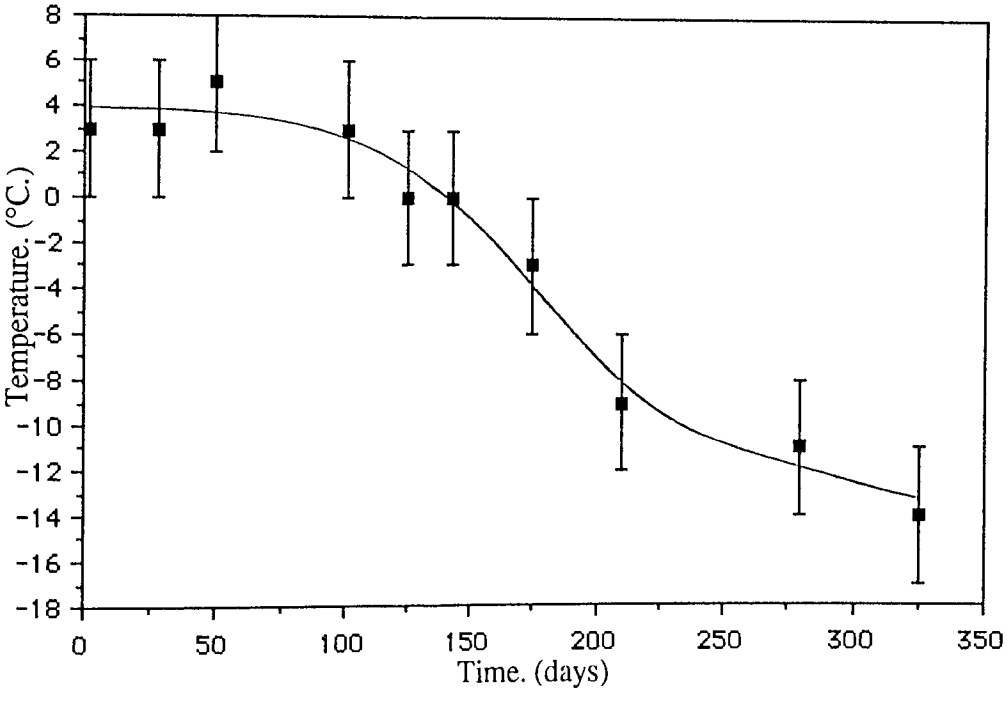


Graph 6.47.

Change In Glass Transition Temperature Of L.Pec.25.E. During Degradation In The Physiological Degradation Model.

### 6.2.4. Conclusions.

It was concluded therefore that, similar to the PHB(FM)IP degradation, the degradation nature of the co-blended samples in the physiological degradation model was more prolonged than that of the co-blends in the accelerated degradation model.

There was an initial pectin loss by day 28 which facilitated the partial collapse of the matrix and increased the available surface area to volume ratio, so that the degradation of the PHB proceeded comparatively more quickly than in the unblended PHB(FM)IP.

The time taken to attain the maximum crystallinity for the partially degraded samples were reduced compared to the IP sample, for those samples with low pectin loadings. Increasing the loading above 9-15% increased the necessary time and reduced the blending efficiency.

## 6.3. General Conclusions.

It was concluded that the degradation of the blended and unblended PHB(FM)IP in the physiological degradation model was similar to the degradation in the accelerated model, however, the degradation stages were more prolonged and pronounced. There was a noticeable induction stage 0 lasting until around days 50 to 60 for the PHB(FM)IP degradation, during this time the buffer gradually penetrated the fibres and began to degrade the primary amorphous regions. This then led to the collapse of the weakened fibres, stage I. At stage I there was a gradual increase in the degradation rate until around

day 125 where a linear rate of approximately 0.11%dy.$^{-1}$ was determined. Similarly, the stage I in the accelerated degradation model exhibited a linear degradation rate of approximately 0.65%dy.$^{-1}$. Thus, the degradation profiles were comparable, (See Fig. 6.1).The degradation profiles for the co-blends were similar to that determined for the homopolymer. However, in these cases, initial weight losses followed by less noticeable induction stages were observed, this was due to the gradual degradation of the pectin.

The relatively more noticeable stages in the physiological degradation profiles helped to clarify the nature of the PHB(FM) degradation. The limiting factor of settlement and compaction apparently exhibited more influence on the sample degradation in the accelerated degradation model than in the physiological and these were reflected in the degradation profiles obtained.

The phase contrast and scanning electron microscopy observations were consistent with the degradation process as determined from the accelerated degradation model and from the conclusions drawn from the degradation profiles in this chapter. Similarly, the fibre diameter distributions also confirmed those conclusions from the accelerated degradation studies, with fragmentation first occurring in the small diameter fibres and the diameter distribution gradually shifting to the larger diameter ranges. Blending the PHB(FM)IP also shifted this distribution initially in the undegraded samples and increased the number of large diameter fibres, which were comparatively heavily loaded with pectin and as a result readily fragmented.

There was little change in the melting points of the partially degraded samples during an

induction period lasting until around days 50 to 75. After day 75, a gradual decrease was observed, so that at day 324, when the experiment was terminated, the PHB(FM)IP exhibited an overall decrease of approximately 6 ±2°C., compared to a decrease of around 12 ±2°C. for the co-blends. In contrast, the fusion enthalpy changes showed no induction stage but gradually increased to a single peak. This peak was attained more quickly for those samples with comparatively low pectin loadings, L.Pec.9. and L.Pec.25.S. and was delayed for those samples with relatively higher loadings, L.Pec.15. and L.Pec.25.E. Thus, the amorphous regions of the sample were initially degraded.

Therefore, it was concluded that the degradation of the fibrous matrix samples in the accelerated degradation model provided an accurate indication as to the degradation of the same samples in the physiological degradation model and thus, a clearer picture as to their biodegradation within the body system.

# Chapter Seven.

## The Degradation Of Melt Processed Biopol Samples Compared To Gel-spun PHB(FM)IP.

## 7.0. General Introduction.

The structure and degradation of the fibrous matrix samples and the effects of blending with various polysaccharides, copolymerizing with PHV and altering the production process on the degradation has been investigated and discussed in previous chapters. In this chapter the degradation profiles for a number of melt processed PHB based samples, possessing various PHV and carbohydrate loadings and different sample shapes, are determined utilizing the same accelerated and physiological degradation models used to determine the fibrous matrix degradation. The comparison of the degradation profiles of these samples and that of the PHB(FM)IP, gives an indication as to the suitability of these samples for use as medical implantation devices.

The degradation of the melt processed samples in the physiological degradation model was then compared to their degradation in the physiological model used by Yasin.[99] This provides a basis to which the degradation of the fibrous matrix samples could be compared to a wider range of melt processed samples investigated by Yasin.

## 7.1. The Degradation Of Melt Processed Samples Compared To PHB(FM)IP In The Accelerated Degradation Model.

### 7.1.0 Introduction.

A number of melt processed discs and stepped plaques with varying percentage loadings, made according to the processing methods of Dr. Yasin,[99] with the same standard initial

weight of 305mg. (±1.6%) were degraded in the accelerated degradation model. The samples are listed below:

| Sample. | Ratio PHB:PHV | Blending Agent And Loading. | | Sample Shape. |
|---|---|---|---|---|
| 12V-10SA. | 88:12 | Sodium Alginate | 10% | HD |
| 12V-30SA. | 88:12 | Sodium Alginate | 30 | SP |
| 20V-10BT. | 80:20 | Bran and Talc | 10 | SP |
| 20V-30Amy. | 80:20 | Amylose | 30 | HD |
| 12V-10Dex. | 88:12 | Dextran | 10 | HD |
| 20V-30Dex. | 80:20 | Dextran | 30 | HD |

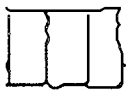

Stepped Plaque. SP

Half A Circular Disc. HD

The discs and plaques were altered to the standard weight, this generally entailed halving the initial samples so that half circular discs and stepped plaques of equivalent masses were produced, (Plate. 7.1). These were then degraded in the same experimental system as the PHB(FM)IP, previously discussed in chapter 4. The degradation of the samples was measured by gravimetric analysis, whilst the degradation of sample 12V-10SA. was also investigated utilizing monomer and particulate analysis. The degradation profiles were then compared to that of PHB(FM)IP.

These experiments were performed in order to provide a comparison of the degradation profiles for the melt processed samples with the fibrous form. This was important, since the melt processed samples had possible uses as other forms of medical implantation devices.

### 7.1.1. The Degradation Of Sample 12V-10SA. Compared To PHB(FM)IP.

Graph 7.1 illustrates the degradation of the PHB component to the monomer for sample 12V-10SA. expressed as a percentage of the initial PHB weight, and compares it to that of PHB(FM)IP. Similarly, graph 7.2 illustrates the degradation profiles for the two samples according to monomer and particulate analysis, whilst graph 7.3 illustrates the sample degradation as monitored by gravimetric analysis.

The comparisons of graphs 7.1 to 7.3 build up a comprehensive picture of the degradation process of sample 12V-10SA. in which the characteristics are an initial induction period with relatively little degradation until around day 8, followed by a gradual increase in degradation until a practically linear degradation rate of approximately 2.9%$dy.^{-1}$ around day 19. The initial induction period was due to the penetration of the injection moulded sample by the degrading medium and the gradual dissolution of the sodium alginate. This corresponded to a gradual increase in the surface area to volume ratio of the P(HB-HV) copolymer component which then readily degraded. The gravimetric analysis was also characterized by a short term increase in the sample wet weight due to an increase in the porosity as the sodium alginate dissolved out of the sample. As degradation progressed, both the wet and dry weights began to decrease, until the sample fragmentation and porosity decrease reduced their difference, so that around day 37 no significant difference between the wet and dry weights was determined.

In contrast to the 12V-10SA. degradation, the fibrous matrix degradation profiles were characterized by an initial rapid degradation due to the matrix collapse and corresponding

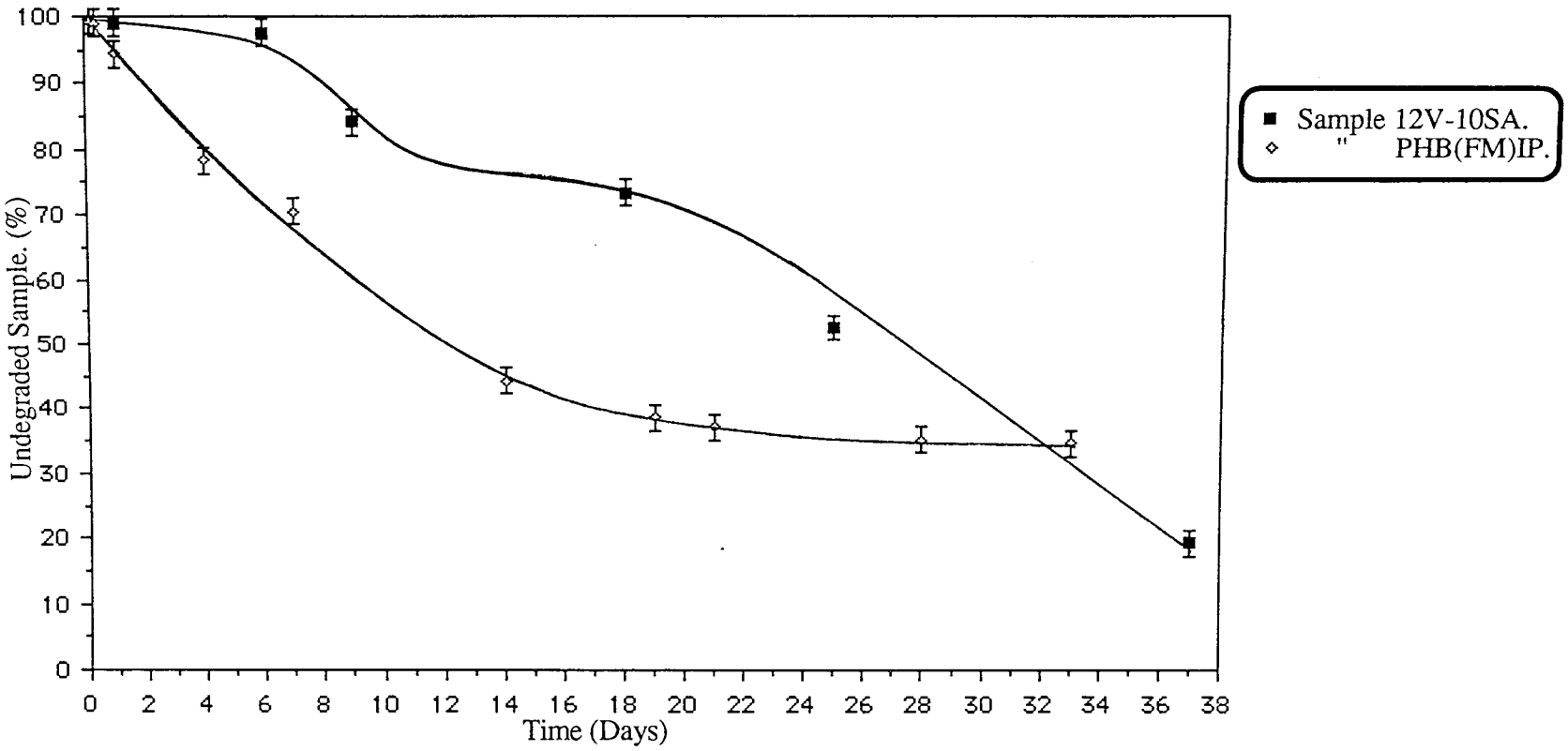


Graph 7.1.

The Degradation Of The PHB Component For Sample 12V-10SA. In The Accelerated Degradation Model, Determined By Monomer Analysis, Compared To PHB(FM)IP.

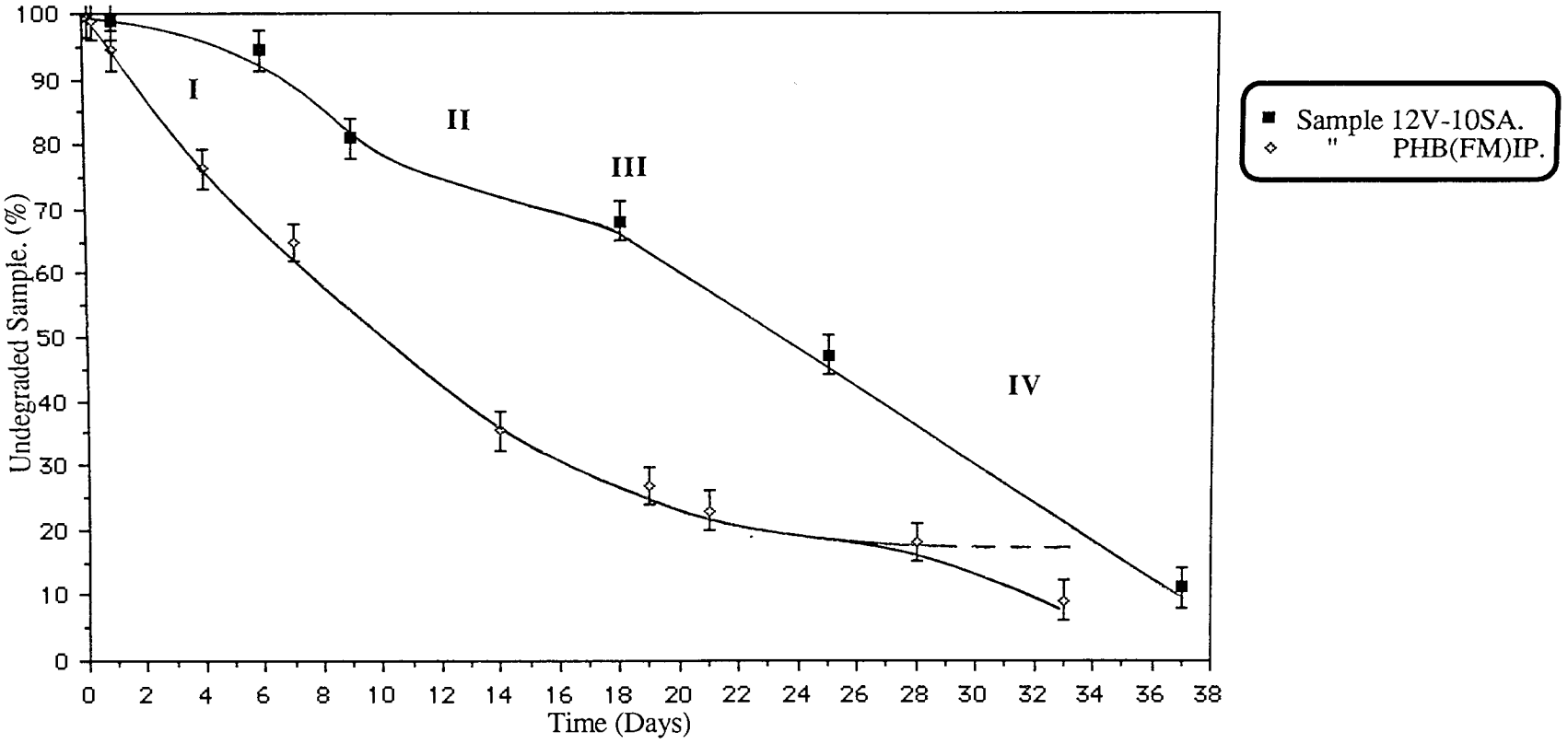


**Graph 7.2.**

**The Degradation Of Sample 12V-10SA, In The Accelerated Degradation Model, Determined By Monomer And Particulate Analysis, Compared To PHB(FM)IP.**

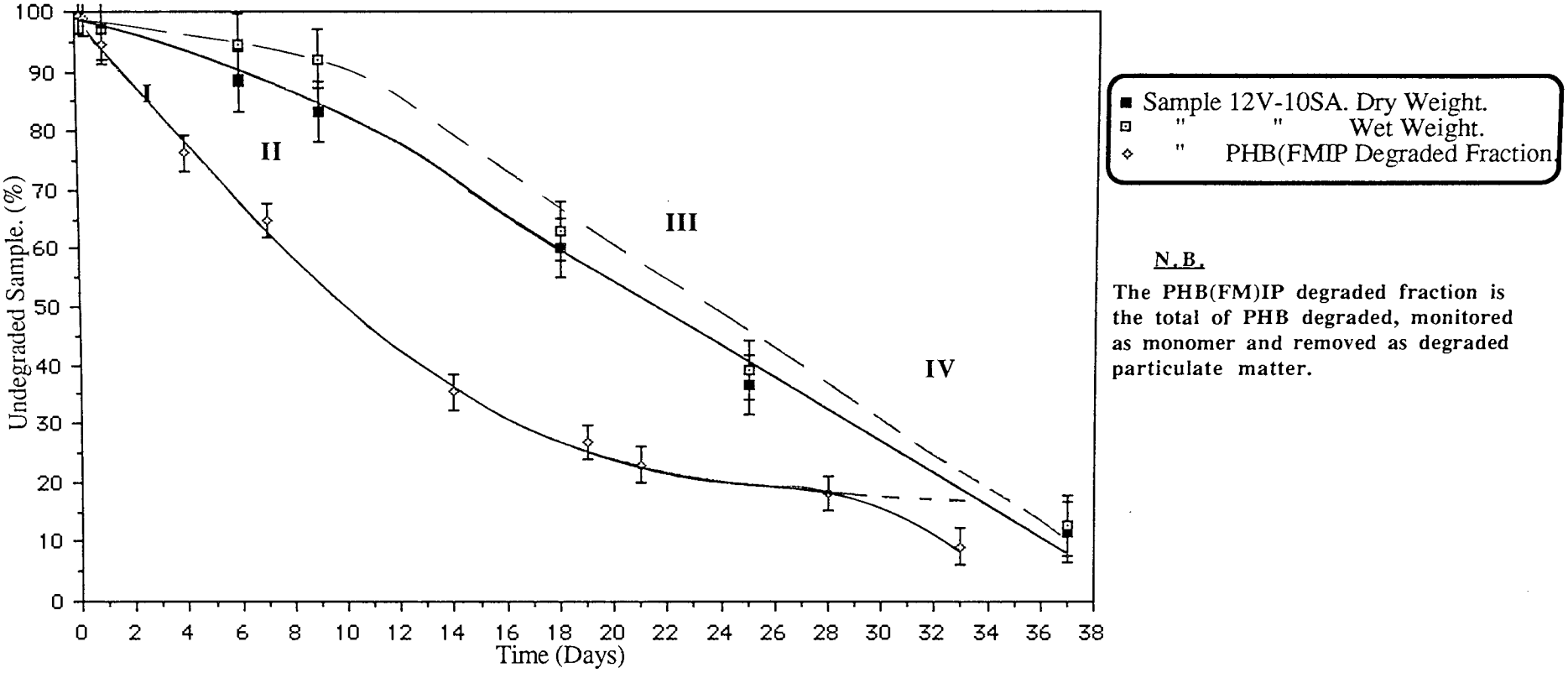


N.B.

The PHB(FM)IP degraded fraction is the total of PHB degraded, monitored as monomer and removed as degraded particulate matter.

Graph 7.3.

The Degradation Of Sample 12V-10SA. In The Accelerated Degradation Model. Determined By Gravimetric Analysis. Compared To PHB(FM)IP.

increase in the surface area to volume ratio, (Graphs 7.1-7.3). During degradation stages I to III the PHB(FM)IP degradation exceeded that of the 12V-10SA. sample, despite the fact that the melt processed sample possessed a lower initial PHB weight, which facilitated its degradation, as discussed in chapter 4. At degradation stage IV the limiting factors of matter compaction and residual 'degradation resistant' matter (See chapter 4) had a greater influence on the PHB(FM)IP than on 12V-10SA., so that the degradation of both samples was approximately equal at 81% around day 33. At day 19, at the beginning of the step stage IV for PHB(FM)IP, there was approximately 63 and 31% degradation for samples PHB(FM)IP and 12V-10SA. respectively, with the overall linear degradation rates of approximately 3.3 and 1.6%$dy.^{-1}$ respectively.

Thus, the 12V-10SA. degradation profile is one of an induction period followed by a practically linear degradation in comparison to the much more rapid initial degradation followed by a plateauing effect exhibited by the PHB(FM)IP degradation. Although considerably less PHB was initially present for sample 12V-10SA., the sample surface area to volume ratio delayed and reduced the PHB degradation so that the fibrous matrix, by virtue of its comparatively larger surface area to volume ratio, degraded more quickly.

### 7.1.2. Comparisons Between The Degradation Of The Melt Processed Samples And PHB(FM)IP.

Graph 7.4 illustrates the degradation profile of sample 12V-30SA. monitored by dry weight loss and compares it to that obtained for PHB(FM)IP. The greater degradation of the 12V-30SA. sample compared to the 12V-10SA. was due to the increased surface area to volume ratio of the stepped plaque compared to the half circular disc and to the greater

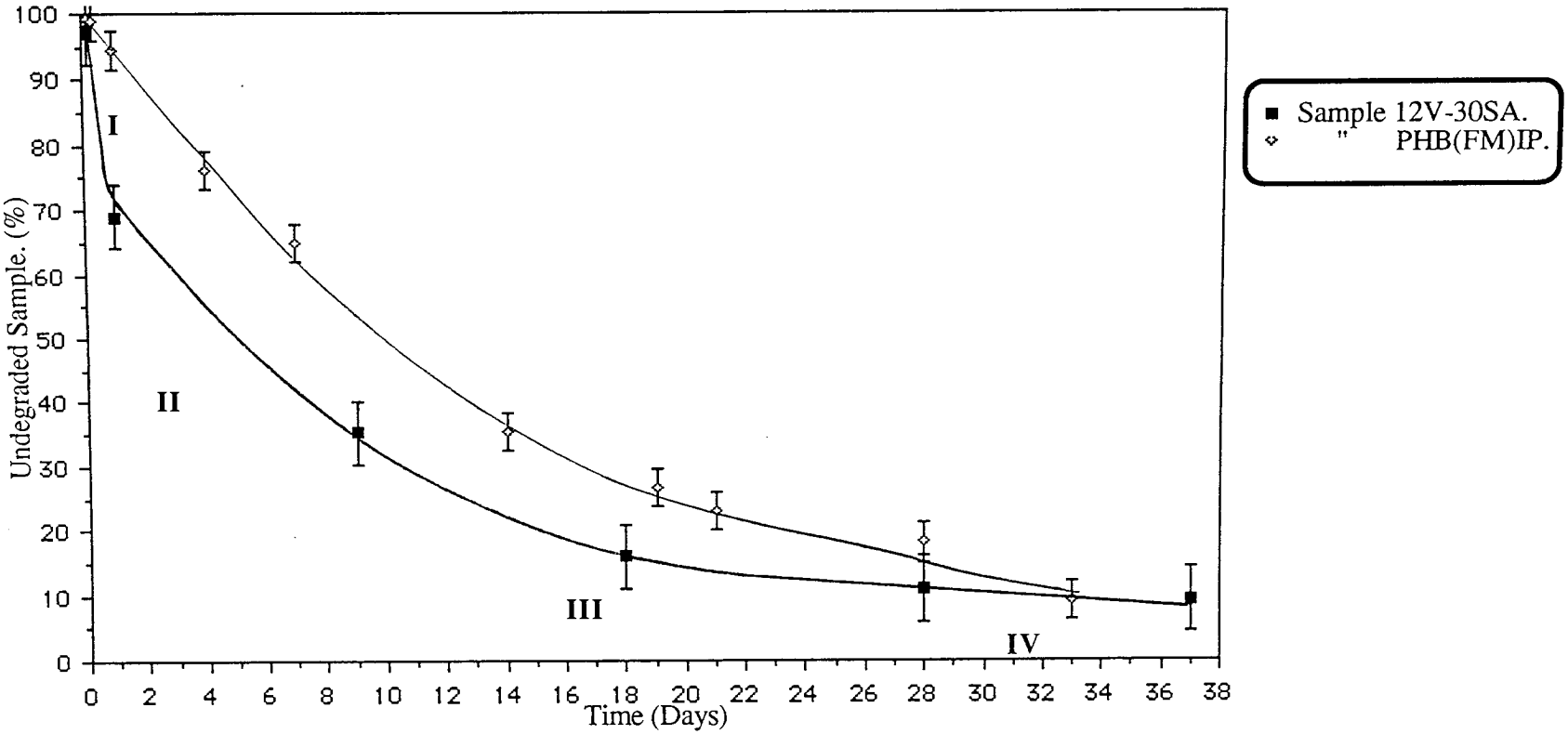


**Graph 7.4.**

**Degradation Profile For Sample 12V-30SA. In The Accelerated Degradation Model. Determined By Dry Weight Loss Analysis. Compared To PHB(FM)IP.**

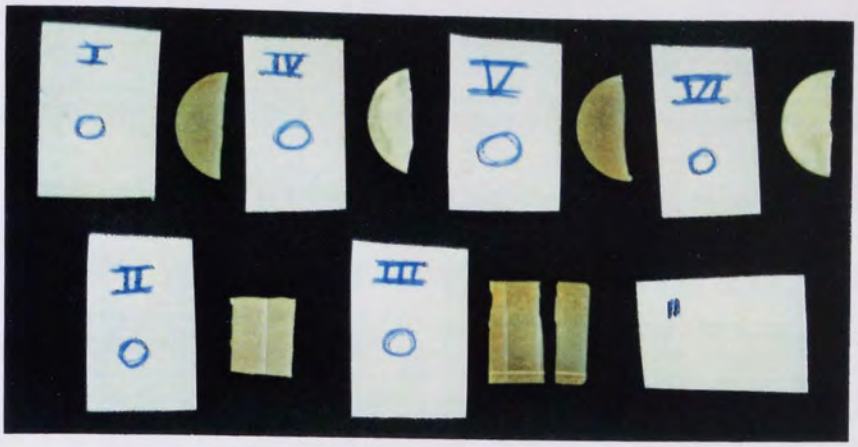


I 12V-10SA.
II 12V-30SA.
III 20V-10BT.
IV 20V-30Amy.
V 12V-10Dex.
VI 20V-30Dex.

Plate 7.1.

Undegraded

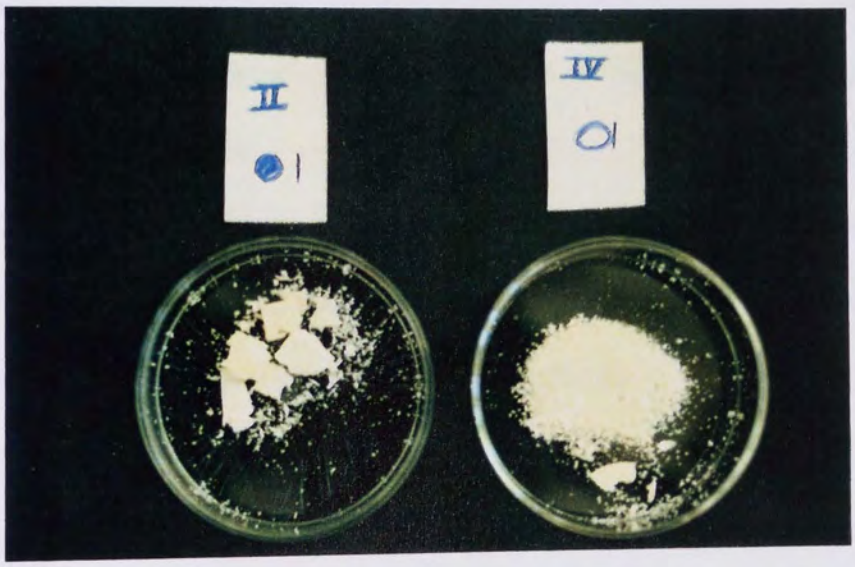


Plate 7.2.

Day 1
Degradation.

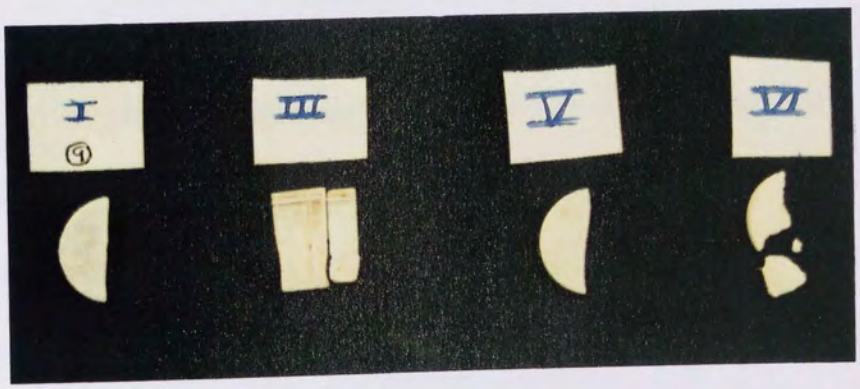


Plate 7.3.

Day 9
Degradation.

Plates 7.1 To 7.3.
Undegraded And Partially Degraded Melt Processed PHB Based Samples, Degraded In The Accelerated Degradation Model.

sodium alginate loading. This increase in the loading facilitated the degradation not only by simple sample weight loss, because of its relatively rapid degradation compared to PHB, but also due to the further increase in the surface area to volume ratio of the partially degraded plaque, (Plate 7.3).

The sodium alginate degraded by day 2 with a 31% weight loss. This facilitated the sample fragmentation and PHB degradation. The degradation rate then gradually decreased due to the limiting factors discussed in chapter 4. After day 2 the 12V-30SA. degradation profile trend was similar to that of the PHB(FM)IP. However, the stage IV was slightly greater for the IP sample, so that at day 19 the 12V-30SA sample exhibited 72% degradation and an overall linear degradation rate of approximately 3.8%dy.$^{-1}$, compared to 63% and 3.3%dy.$^{-1}$ for the PHB(FM)IP.

Therefore the potential for further degradation was greater for PHB(FM)IP than 12V-30SA. This was confirmed by the slight increase in the IP degraded particulate matter at day 33 due to agitation, illustrated in graph 7.4, and the photographic record of Plates 7.1 to 7.3, where sample 12V-30SA. collapsed within two days but sample 12V-10SA. retained integrity until after day 9. Similar to 12V-30SA., sample 20V-10BT. was also a stepped plaque but collapse was not as great or rapid as with sample 12V-30SA. This was due to the lower loading of 10% bran and talc. Similarly, the increased PHV component did not facilitate the degradation.

The degradation profile of sample 20V-10BT. was practically linear with a degradation rate of approximately 3%dy.$^{-1}$ until day 18, (Graph 7.5), when a gradual decrease was

observed due to the limiting factors. Similar to 12V-30SA., there was an undegraded fraction at termination of the experiment of approximately 7.4%, however the 12V-30SA. degradation profile exhibited little degradation at stage IV whilst no such plateauing effect was observed for sample 20V-10BT.

Sample 20V-30Amy. possessed 30% amylose and a 20% PHV component of the P(HB-HV) in half a circular disc. This was similar to sample 20V-30Dex., but as can be observed from graphs 7.6 and 7.7, the degradation profiles were quite different. In 20V-30Amy the 30% amylose rapidly degraded within the first day and this was observed as the large degradation rate at stage I, (Plate 7.2). However, due to the PHV component and the sample shape, the degradation of the remaining P(HB-HV) was comparatively reduced and the degradation rate gradually decreased to the terminal step stage IV beginning around day 19, with 63% degradation.

Thus, it was concluded that for sample 20V-30Amy., the stage I of the degradation profile was due to the amylose degradation, stages II and III due to the PHB and stage IV due to the PHV degradation. These accounted for approximately 29, 55 and 16% respectively, these values matched the alleged initial loadings of 30, 56 and 14% respectively. This indicated the accuracy of the loadings, a lack of blending between the biopol and the amylose and the comparatively greater resistance to degradation of the PHV component.

Therefore, the degradation of 20V-30Amy. was originally greater than that of PHB(FM)IP until approximately day 13, after which the degradation profiles were similar. At stage IV the primary limiting factor for 20V-30Amy. was the degradation

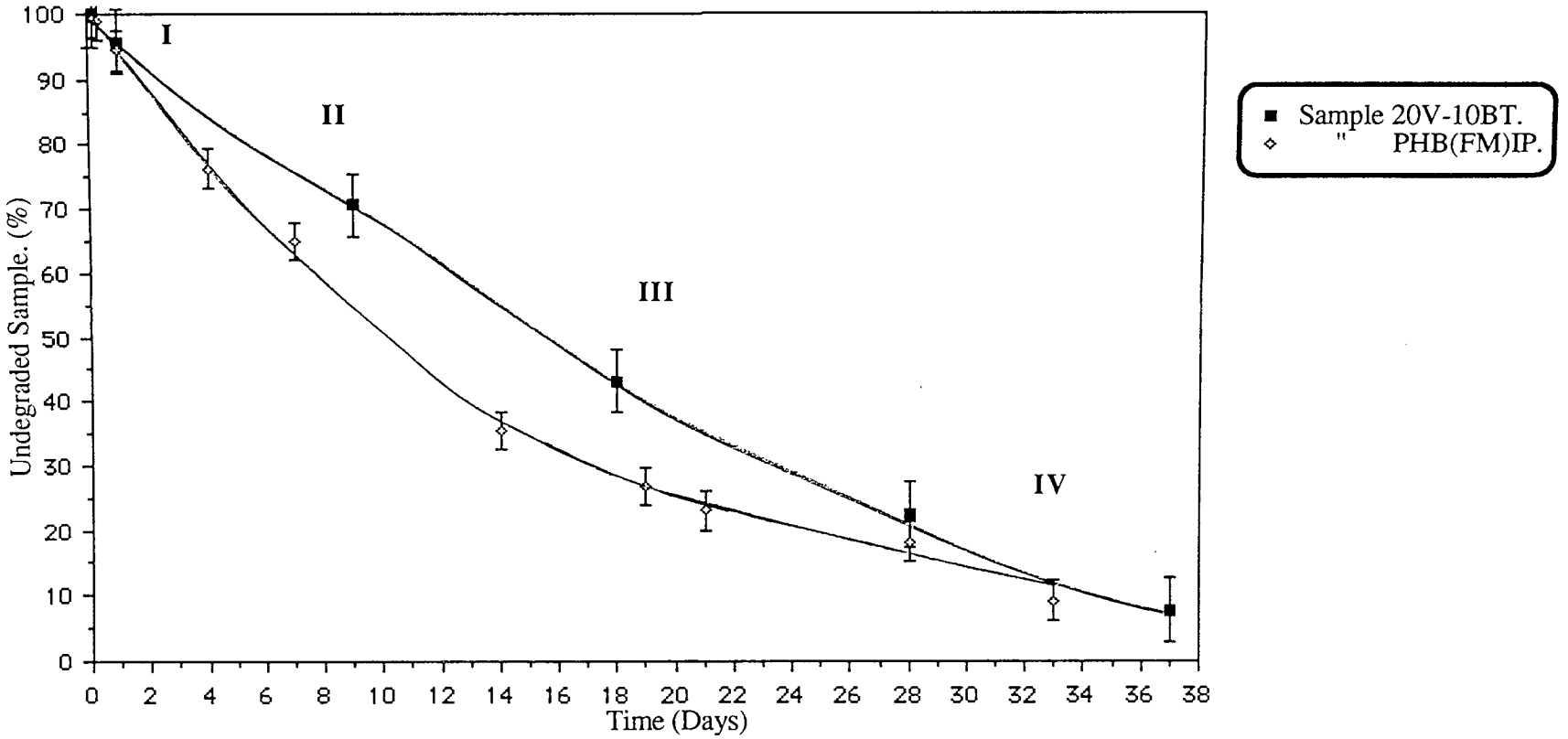


**Graph 7.5.**

**Degradation Profile For Sample 20V-10BT. In The Accelerated Degradation Model. Determined By Dry Weight Loss Analysis. Compared to PHB(FM)IP.**

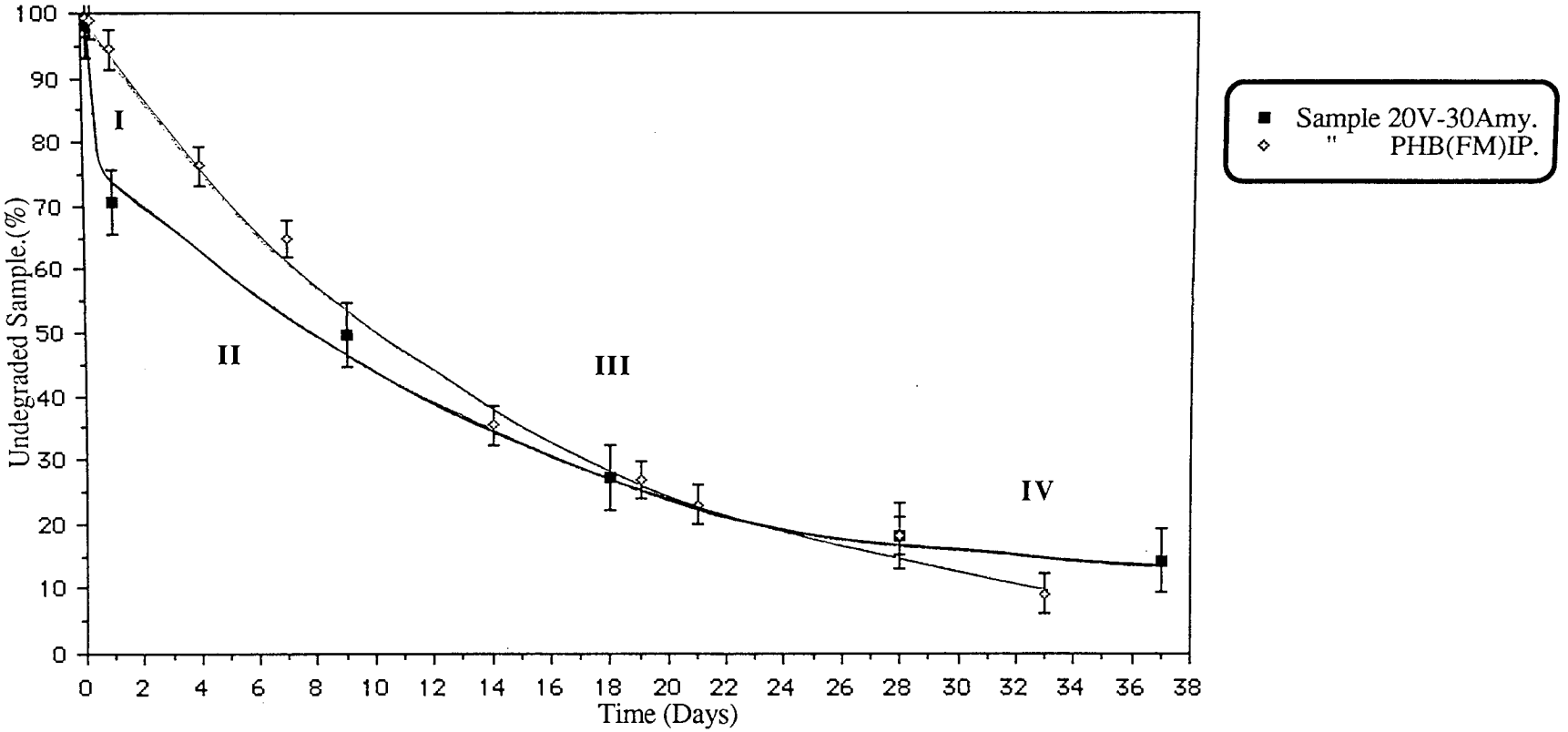


**Graph 7.6.**

**Degradation Profile For Sample 20V-30Amy. In The Accelerated Degradation Model. Determined By Dry Weight Loss Analysis. Compared To PHB(FM)IP.**

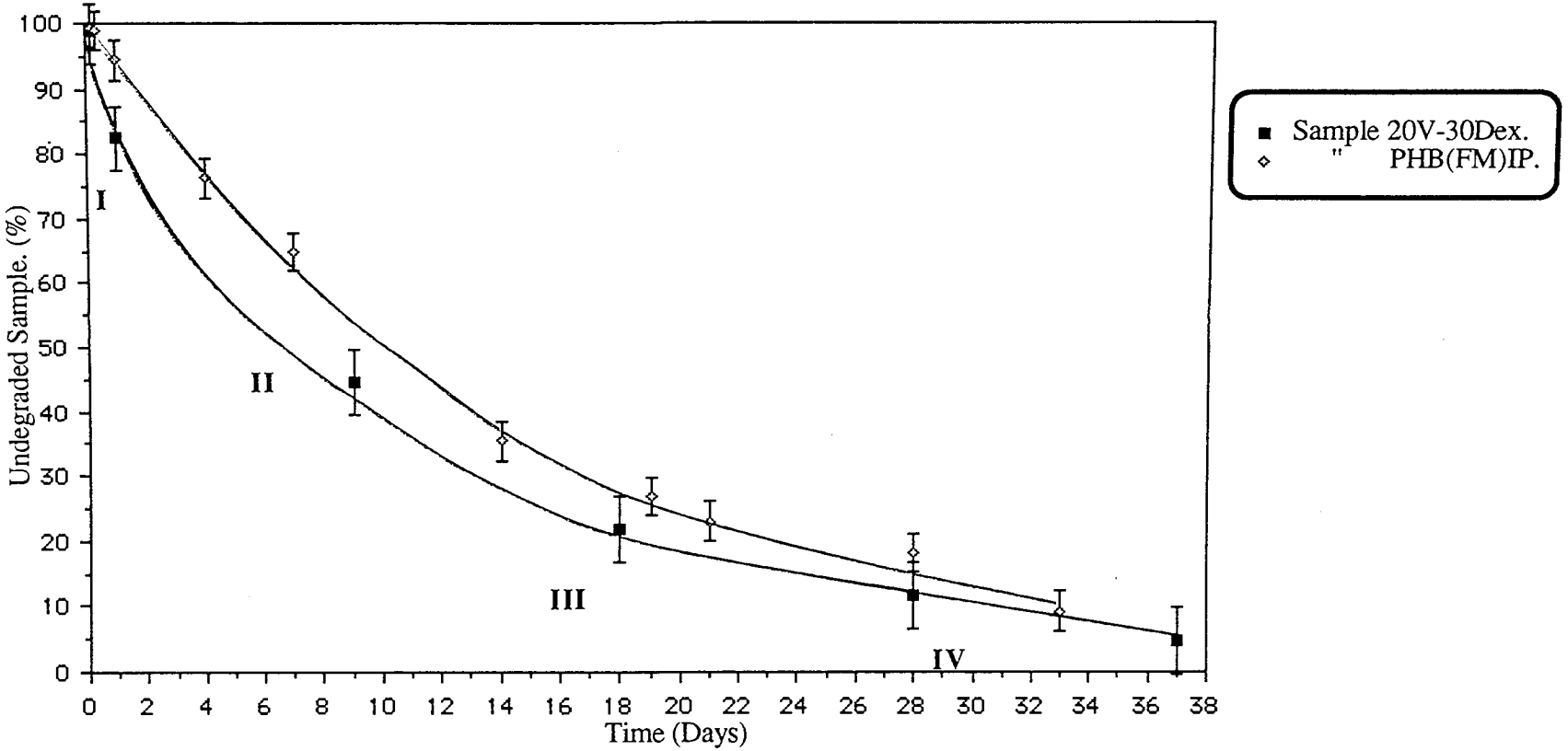


**Graph 7.7.**

**Degradation Profile For Sample 20V-30Dex. In The Accelerated Degradation Model. Determined By Dry Weight Loss Analysis. Compared To PHB(FM)IP.**

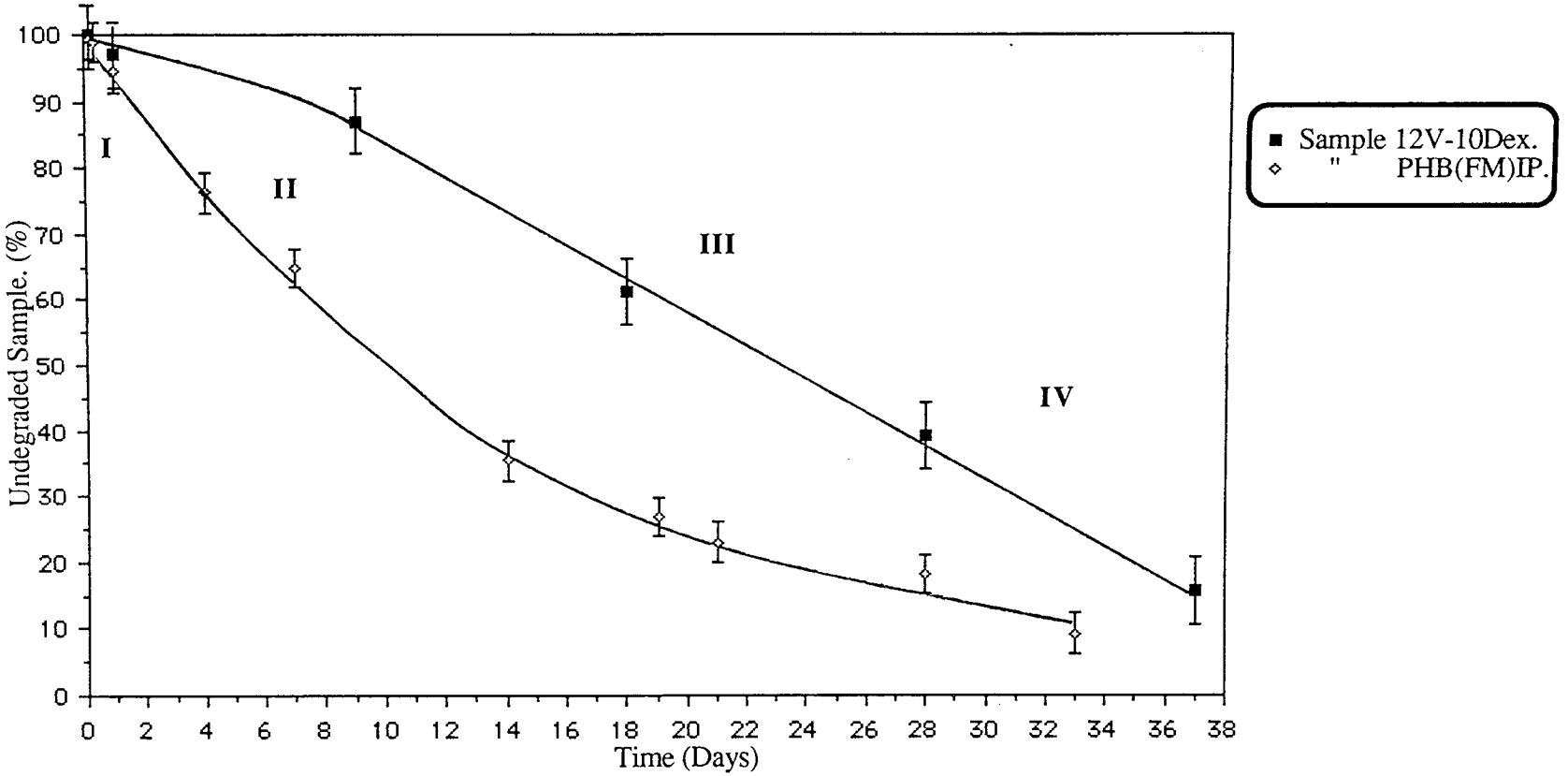


**Graph 7.8.**

**Degradation Profile For Sample 12V-10Dex. In The Accelerated Degradation Model, Determined By Dry Weight Loss Analysis, Compared To PHB(FM)IP.**

resistant material, whilst for the IP sample it was the particulate matter settlement and compaction. Therefore, the potential for further degradation was greater for the IP sample than for 20V-30Amy., as the slight agitation at day 33 confirmed, (Graph 7.6).

The buffer penetration into sample 20V-30Dex. was more gradual than that for sample 20V-30Amy. due to the comparatively faster dissolution of the amylose compared to the dextran, (Graph 7.7). Consequently, the 20V-30Dex. collapse was more gradual and the degradation of the P(HB-HV) progressed to a comparatively greater extent and in a more continuous order than the separate stages observed for the 20V-30Amy. sample. At the termination of the experiment, 20V-30Amy. possessed approximately 29.5% undegraded sample, whilst its dextran counterpart had only 4.4%. This indicated a retention of the sample structure for a comparatively longer period in 20V-30Dex. and this was confirmed by visual observations, (Plates 7.2 & 7.3).

Graph 7.8 illustrates the degradation profile for the half circular disc sample 12V-10Dex. After an initial induction period until day 9, with approximately 12% degradation, the degradation rate gradually increased until a linear rate of 2.5%dy.$^{-1}$ was observed around day 15 and continued until day 37 where approximately 84.5% degradation was determined. The induction period was therefore concluded as being due to the buffer penetration into the sample and the gradual erosion of the dextran. Similar to sample 20V-30Dex., the dextran in 12V-10Dex. was evenly distributed within the sample. Consequently, the dextran in 12V-10Dex. was not as readily available to the degrading medium due to the proportionately greater biopol loading when compared to 20V-30Dex. and thus, the buffer penetration was slower. The erosion of the 12V-10Dex. dextran

gradually increased the surface area to volume ratio of the partially degraded sample and maintained this ratio longer than 12V-30Dex. which collapsed. Thus, the PHB degradation in 12V-10Dex. was more gradual than in its 30% counterpart.

The IP sample degraded much quicker than 12V-10Dex. with no induction period but a gradual degradation until day 19, when matter compaction and the terminal step stage IV began. At day 19 the overall degradation rates assuming linearity were 3.3 and 2.2%$dy.^{-1}$ for the IP and 12V-10Dex. samples respectively.

Graph 7.9 illustrates the degradation of all the melt processed samples monitored by gravimetry (dry weight loss). As can be observed, the final degradations at day 37 varied comparatively slightly with only a maximum of 11.2% difference, (Table 7.1). However, the degradation profiles varied more substantially. A comparison between these profiles and that of the fibrous matrix degradation is discussed using the times for 10 and 50% degradation; $t_{10}$ and $t_{50}$ respectively, and by the percentage degradation and the overall linear degradation rates at day 19; the beginning of the step stage IV for the PHB(FM)IP sample. These values are illustrated in table 7.2.

The degradation of all the melt processed samples studied in this chapter was characterized by the initial dissolution of the blending agent into the buffer solution, this then increased the surface area to volume ratio of the remaining sample and facilitated in its degradation. For those samples with a comparatively large loading there was a rapid initial dissolution. The rate of this dissolution was dependent upon the carbohydrate nature; the dextran in 20V-30Dex. was slower to degrade than the amylose in its counterpart 20V-30Amy, and

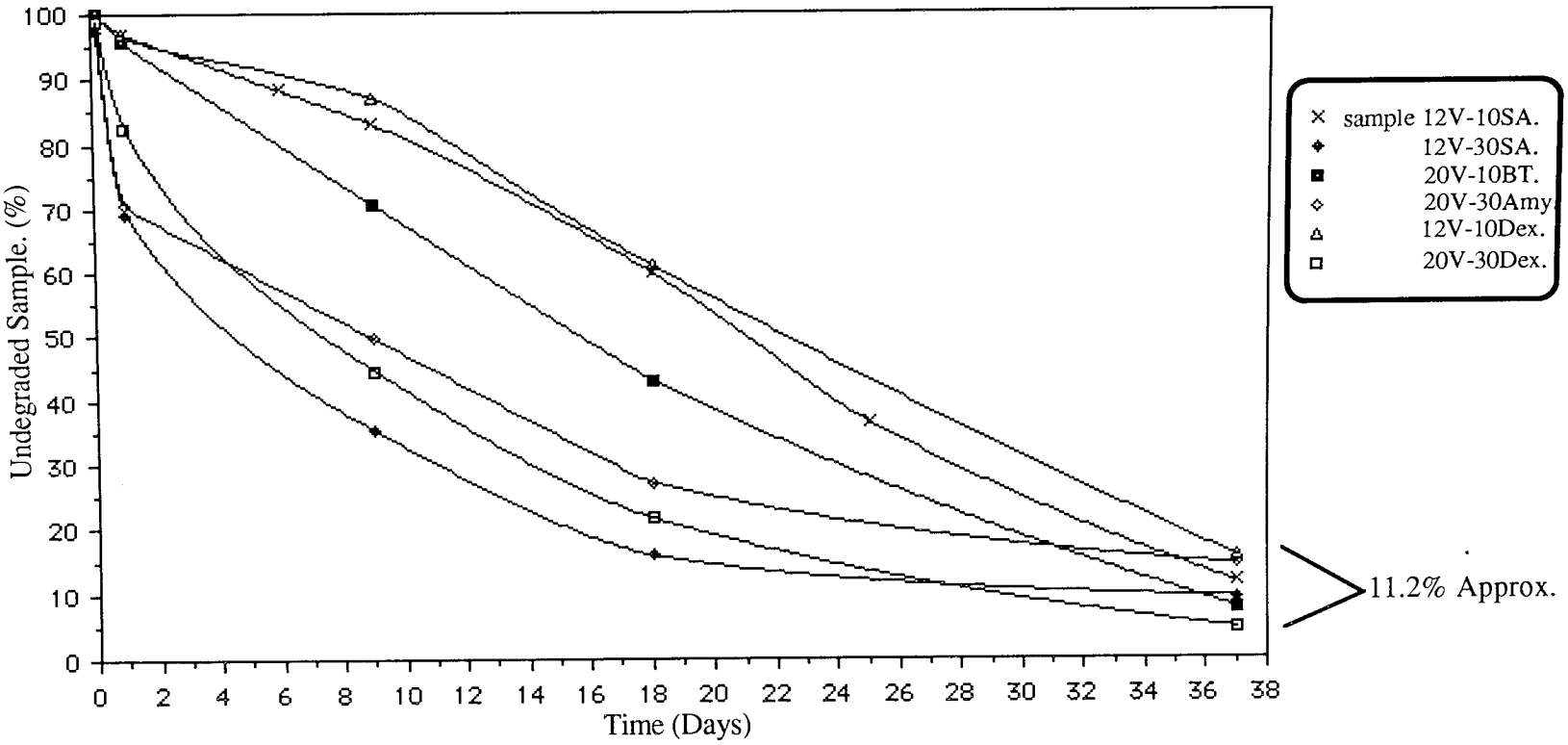


**Graph 7.9.**

**Degradation Profiles Of Melt Processed Samples In The Accelerated Degradation Model Determined By Dry Weight Analysis.**

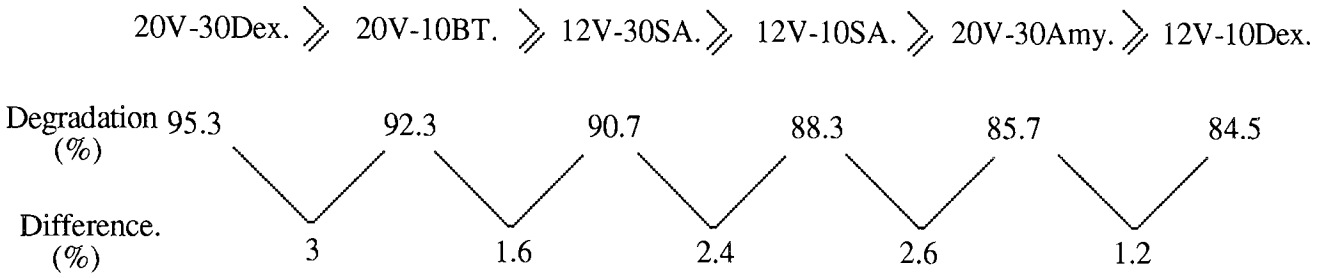


**Table 7.1.**

**Sample Degradation Order At Termination Day 37.**

| Sample: | $t_{10}$ (Days) | $t_{50}$ (Days) | % Degradation At Day 19. | Overall Linear Degradation Rate (%/dy.) |
|---|---|---|---|---|
| 20V-30Dex. | 1 | 6.5 Days | 78 % | 4.1%/dy. |
| PHB(FM)IP. | 2 | 11 | 73 | 3.8 |
| 12V-30SA. | 0.5 | 4.5 | 72 | 3.8 |
| 20V-30Amy. | 0.5 | 8.5 | 70 | 3.7 |
| 20V-10BT. | 3 | 16 | 59 | 3.1 |
| 20V-10Dex. | 5 | 23 | 39 | 2.1 |
| 12V-10SA. | 5.5 | 21.5 | 31 | 1.6 |

**Table 7.2.**

**Comparison Of Degradation Values For The Melt Processed And Fibrous Matrix Samples.**

thus it possessed a larger $t_{10}$. However, the $t_{50}$ for 20V-30Dex. was smaller than that of 20V-30Amy., this was due to the dextran sample maintaining a comparatively larger surface area to volume ratio for a longer time period. Therefore, the nature of the carbohydrate was concluded as being a factor in determining the degradation of a sample.

The carbohydrate dissolution was slower for those samples with a lower percentage loading eg: 12V-10SA., this was due to their distribution within the sample and their reduced availability to the degrading medium compared to those samples possessing larger percentage loadings eg: 12V-30SA. Consequently, the $t_{10}$ for these lower loaded samples was greater than for the larger loaded ones. Similarly, after dissolution the surface area to volume ratio of those samples with a low carbohydrate loading was comparatively smaller than those with the larger loading, consequently, the $t_{50}$ of these lower loaded samples was also greater. Thus, it was concluded that the percentage loading of the carbohydrate was a factor effecting the degradation of a sample.

It was observed that sample 12V-30SA. exhibited a smaller $t_{50}$ than either 20V-30Dex. or 20V-30Amy.; the other comparatively larger loaded samples. Although the carbohydrate dissolution rate and its subsequent effects on the sample surface area to volume ratio has been concluded as a factor, in this instance the initial sample shape could also have had an affect, 12V-30Dex. was a stepped plaque with an initially greater surface area to volume ratio than the half circular discs of 20V-30Dex. and 20V-30Amy. Similarly, the lower PHV loading may also have played a role. In the larger loaded samples the carbohydrate dissolution greatly increased the surface area to volume ratio, so that the initial sample shape and its surface area to volume ratio were less influential on the sample degradation

than in those samples with comparatively lower carbohydrate loadings. Sample 20V-10BT. had a noticeably smaller $t_{10}$ and $t_{50}$ than 12V-10Dex. and 12V-10SA., this was due to its initial stepped plaque shape compared to the half circular discs of 12V-10Dex. and 12V-10SA. Therefore, the initial sample shape was also concluded as being an influencing factor.

The stepped plaque shape of 20V-10BT. also helps to explain its lack of an induction period, as were observed in the other lower loaded samples 12V-10Dex. and 12V-10SA. Similarly, these lower loaded samples maintained their surface area to volume ratio for a comparatively longer period than the larger loaded samples, which exhibited the stage IV 'plateauing' effects to varying extents, (Graph 7.9).

Those samples possessing a comparatively small carbohydrate loading; 12V-10SA., 20V-10BT. and 20V-10Dex., exhibited larger $t_{10}$ and $t_{50}$s than the PHB(FM)IP and considerably smaller degradations at day 19, 31, 59 and 39% respectively, compared to 73% degradation for the PHB(FM)IP. Samples 12V-30SA., 20V-30Amy. and 20V-30Dex. possessed degradation values of 72, 70 and 78% at day 19 and these were more similar to that determined for the fibrous matrix sample. However, the $t_{10}$ and $t_{50}$ for the PHB(FM)IP, 2 and 11 days respectively, were slightly greater than those for the larger carbohydrate loaded melt processed samples. It was concluded from chapter 4 that the initial PHB weight of a sample effected its degradation in the accelerated degradation model, with the smaller weights exhibiting the faster degradations. It is important to remember, therefore, that the melt processed samples possessed an initially lower PHB weight than the PHB(FM)IP, when this is considered it becomes apparent that the fibrous

matrix degradation readily exceeded that of the melt processed samples. Since the PHB(FM)IP was unblended it was concluded that this comparative increase in the degradation was due to the sample structure, its comparatively larger surface area to volume ratio and process of degradation.

### 7.1.3. Conclusions.

The factors influencing the degradation of the melt processed samples in this chapter were concluded as being:

1) nature of the carbohydrate
2) loading and distribution of the carbohydrate
3) initial sample shape
4) PHV component loading.

These factors effected the sample degradation by reducing the initial PHB weight and by increasing the surface area to volume ratio of the partially degraded samples. Consequently, the main factor influencing the sample degradation was the surface area to volume ratio, which changed during the course of degradation. In those samples with a comparatively large carbohydrate loading there was an initial degradation followed by a stage IV 'plateauing' effect as the degradation kinetics, degradation resistant matter and matter compaction limiting factors influenced the degradation profiles. (See chapter 4). The comparatively lower carbohydrate loaded samples exhibited an induction stage before a more gradual degradation due to a sustained comparatively larger surface area to volume ratio. This induction stage was also dependent upon the initial sample shape and its fragmentation. Upon termination of the experiment at day 37, the degradation percentages

for all the melt processed samples were quite similar with a maximum difference of 11.2%. The fibrous matrix sample, by virtue of its comparatively large surface area to volume ratio, was concluded as degrading more rapidly than the melt processed samples.

## 7.2. The Degradation Of The Melt Processed Samples Compared To The PHB(FM)IP In The Physiological Degradation Model.

### 7.2.0 Introduction.

Samples 12V-10SA., 20V-10BT., 12V-10Dex. and 20V-30Dex. as described in section 7.1.0. were degraded in the physiological degradation model, (Chapters 2 & 3). Degradation was monitored by gravimetric analysis. The degradation profiles obtained were then compared to that determined for the PHB(FM)IP. Similarly, the profiles were also compared to the degradation profiles of the same samples determined by Yasin[99] in a similar physiological degradation model, with the same conditions of pH 7.4 and temperature 37.5°C.

The experiments in this section were performed in order to compare the degradation profiles of the melt processed samples and to get an indication as to their suitability as medical implantation devices. The comparison of these profiles to those obtained by Yasin, would then permit the comparison of the fibrous matrix samples to the wider range of injection moulded and melt processed samples investigated by Yasin, by utilizing these four samples as a reference.

### 7.2.1. The degradation Profiles For The Melt Processed Samples Compared To The PHB(FM)IP.

Graph 7.10 illustrates the degradation profiles for samples 12V-10SA. and PHB(FM)IP determined by dry and wet weight loss. The dry weight loss degradation profile of 12V-10SA. exhibited a similar trend to that obtained for the sample in the accelerated degradation model. There was a rapid degradation from 99.8% at day 1 to 93% at day 56 before the degradation rate decreased and a step stage was observed from approximately day 90 to day 225 with about 92% of the sample remaining. The initial degradation until day 56 was due to the penetration of the buffer into the sample and the dissolution of the sodium alginate, whilst the step stage between days 90 and 225 indicated that there was little degradation of the P(HB-HV). After day 225 the degradation of the P(HB-HV) progressed such that at termination of the experiment on day 450, 77.5% of the sample remained. In comparison, the IP sample exhibited an initial slow degradation period until approximately day 75 before the degradation rate gradually increased until day 125, when a linear degradation profile of approximately 0.11%dy.$^{-1}$ was determined.

As a result of the sodium alginate dissolution, the degradation of 12V-10SA. was initially greater than that of the IP sample. However, the fragmentation of the PHB(FM)IP increased the available surface area to volume ratio to a comparatively greater extent than the sodium alginate dissolution, so that the degradations of the two samples were equal at approximately day 152 with 92%. After day 152 the degradation progressed such that at day 324 there was approximately 73.2 and 85.5% sample remaining for the IP and 12V-10SA. samples respectively.

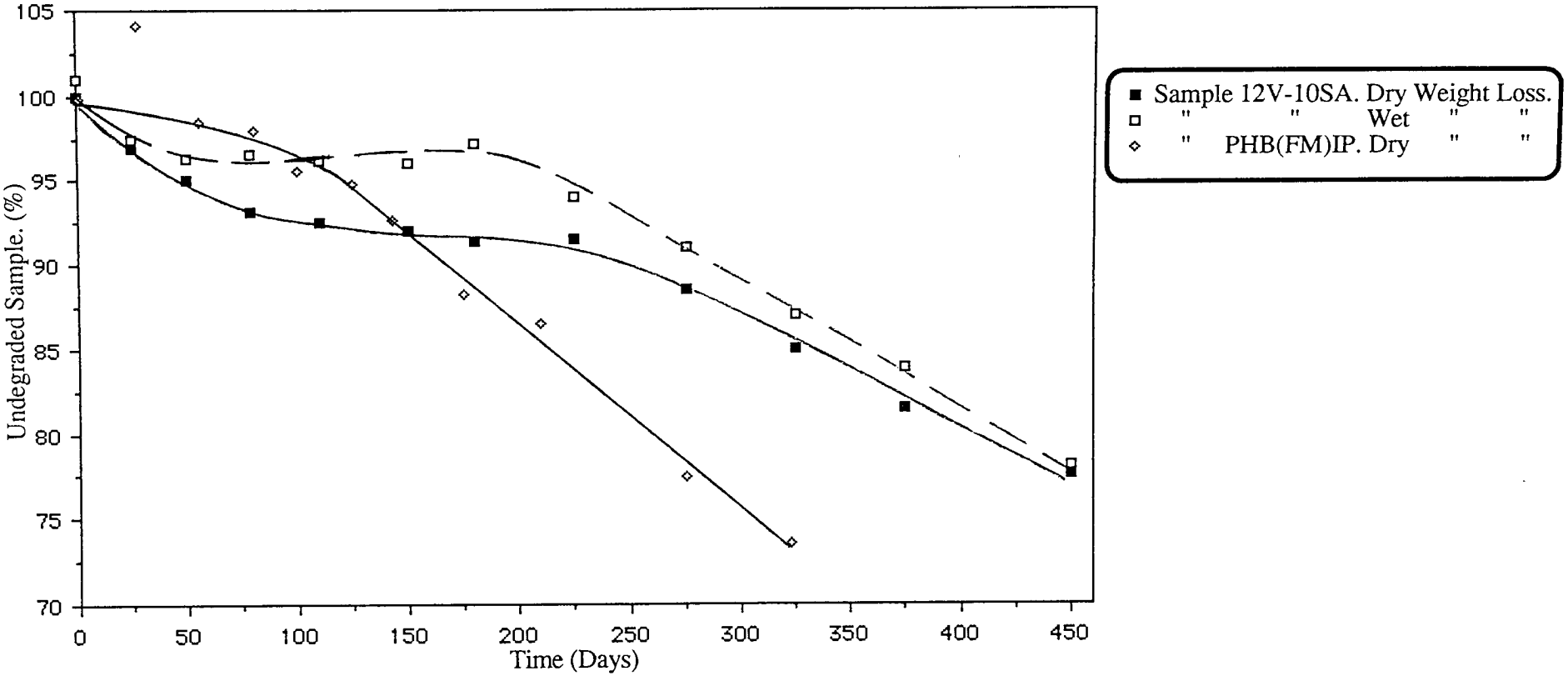


**Graph 7.10.**

**Degradation Profile For Sample 12V-10SA. In The Physiological Degradation Model. Determined By Gravimetric Analysis. Compared To PHB(FM)IP.**

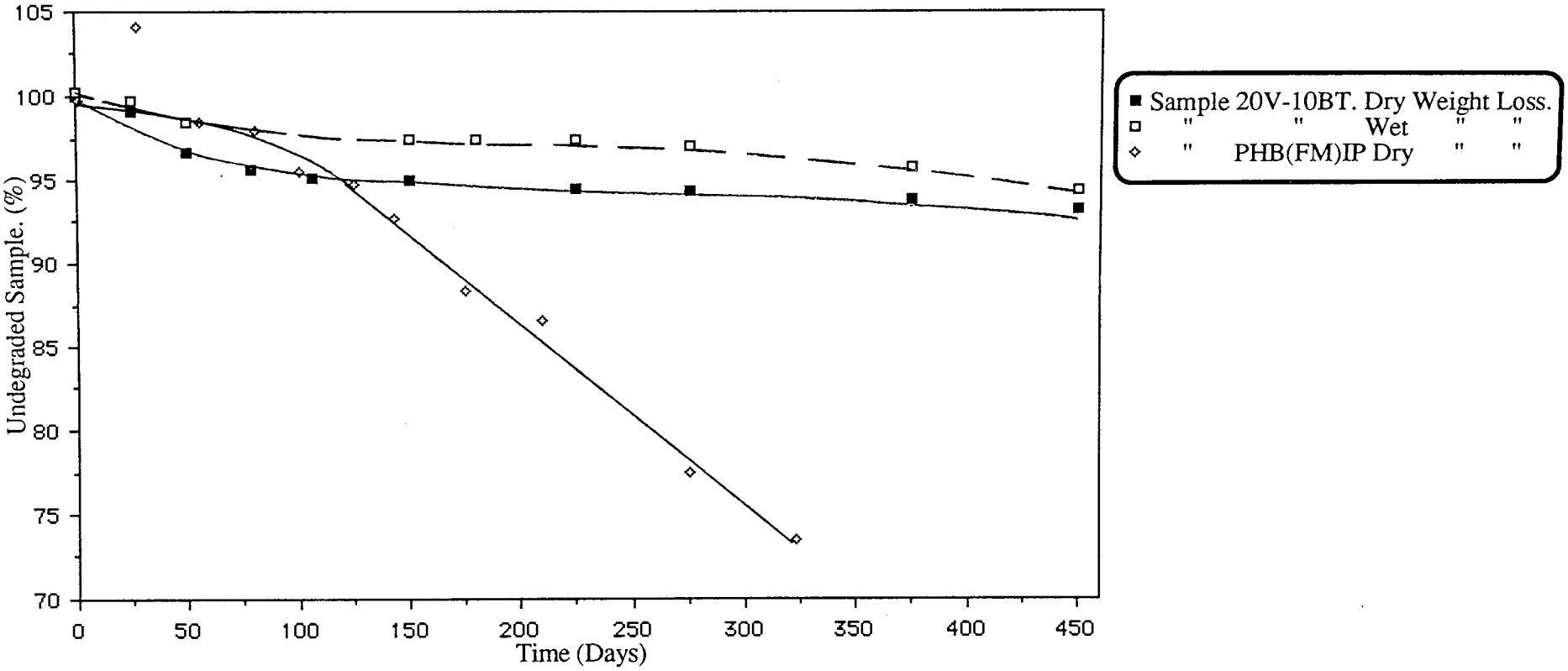


Graph 7.11.

Degradation Profile For Sample 20V-10BT. In The Physiological Degradation Model. Determined By Gravimetric Analysis. Compared To PHB(FM)IP.

There was little water adsorption into sample 12V-10SA. during the first 50 days of the experiment. However, as the sodium alginate dissolved, the penetration and absorption of water by the remaining sample increased to a maximum at around day 185, where approximately 6.5% of the initial sample weight was adsorbed. As the P(HB-HV) degraded after the step stage, the amount of adsorbed water proportionately decreased, such that at days 250 to 350 about 2% adsorption remained.

The degradation profile of sample 20V-10BT. possessed a similar initial induction period as 12V-10SA. but with a comparatively slower dissolution until day 90. After day 90 the degradation proceeded very slowly with a linear rate of approximately 0.007%dy.$^{-1}$. This was most likely a prolonged step stage. The 20V-10BT. degradation profile in the accelerated degradation model did not reveal such pronounced stages. Similar to the degradation of sample 12V-10SA., the blending agent dissolution ensured that 20V-10BT. exhibited an initially greater degradation than the IP sample until day 120, whilst at day 324 there was approximately 73.2 and 93.8% remaining for the IP and 20V-10BT. samples respectively, (Graph 7.11).

The wet weight loss profile mirrored the dry weight loss, with a trend similar to sample 12V-10SA. The initial induction period of 20V-10BT. retained a similar amount of water as the 12V-10SA. sample. The water absorption increased gradually to a maximum of 4.5% at day 250 and then gradually decreased to 1.3% at day 450. The initial dissolution of the 10% dextran loading in sample 12V-10Dex. was comparatively slower than the carbohydrates in samples 12V-10SA. and 20V-10BT. Little degradation was observed between days 1 and 56, after which the dextran gradually dissolved into the degrading

medium and a gradual increase in the degradation occurred until day 250, when a linear degradation rate of approximately 0.03%dy.$^{-1}$ was observed.

The degradation of 12V-10SA. was considerably greater than that for 12V-10Dex. despite both samples possessing the same sample shape and PHV/carbohydrate loading. Thus, the difference in degradation was due to the carbohydrate nature. Sodium alginate is a very hydrophilic polysaccharide with a weight average molecular weight of up to 240,000,[100] this blended readily with the P(HB-HV) and as a result of this, upon dissolution, it greatly increased the surface area to volume ratio and thus the subsequent sample degradation. In comparison dextran is a branched polymer with a comparatively larger molecular weight of 500,000.[101] Thus, the dissolution of the dextran was not as fast compared to the sodium alginate and this affected the subsequent P(HB-HV) degradation, (Graph 7.12). The comparatively slow dissolution of the dextran ensured that the degradation of 12V-10Dex. never exceeded that of the IP sample. At day 324, the termination of the IP experiment, 26.8% degradation had occurred, but only 5.5% for the 12V-10Dex. sample.

Increasing the dextran loading to 30% and the PHV content in the Biopol to 20% had a marked affect on the degradation profile. The relatively long induction period for 12V-10Dex. was absent from the degradation profile of 20V-30Dex. A rapid degradation occurred from day 1 to day 90 before the degradation rate gradually decreased, so that a slight step stage occurred. After day 225 the degradation rate then gradually increased and at day 425 approximately 60.5% undegraded sample remained, (Graph 7.13).

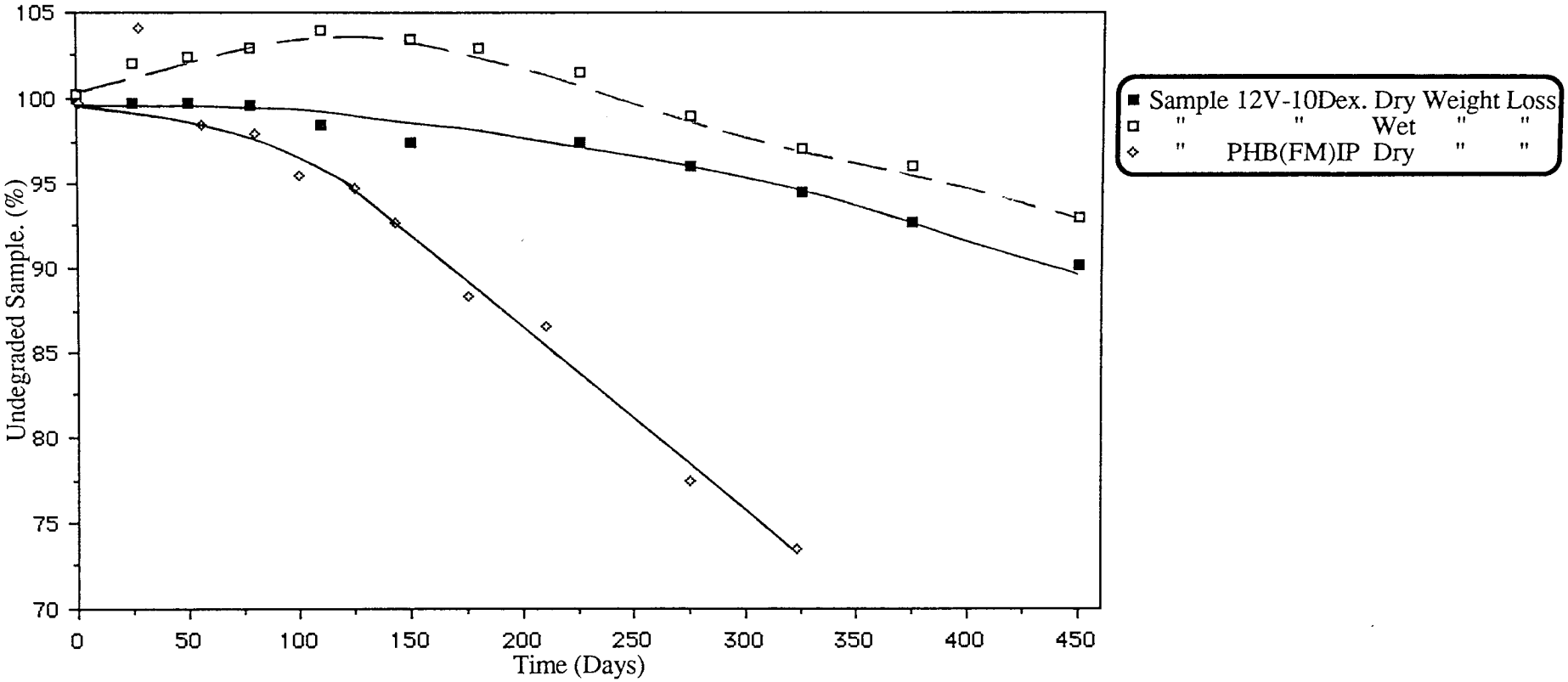


**Graph 7.12.**

**Degradation Profile For Sample 12V-10Dex. In The Physiological Degradation Model, Determined By Gravimetric Analysis, Compared To PHB(FM)IP.**

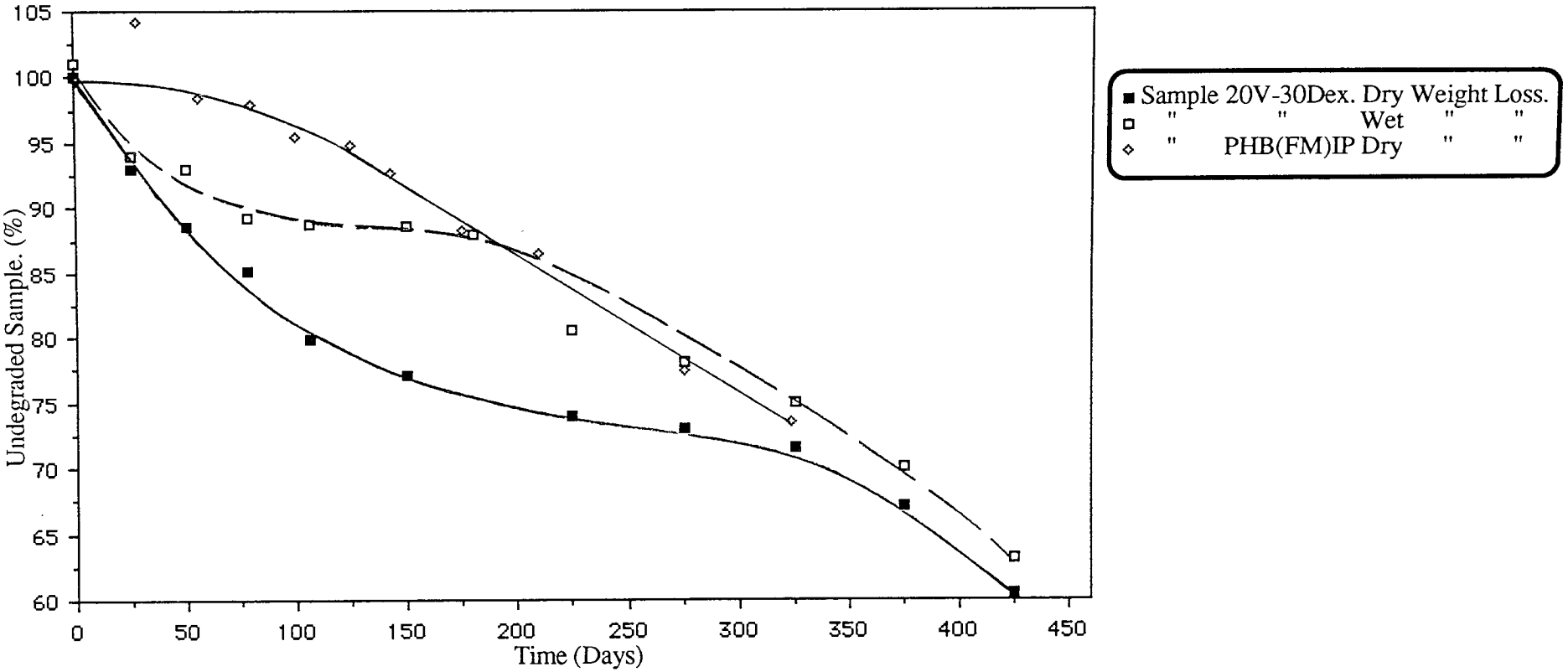


**Graph 7.13.**

**Degradation Profile For Sample 20V-30Dex. In The Physiological Degradation Model, Determined By Gravimetric Analysis, Compared To PHB(FM)IP.**

Similar to the 12V-10SA. and 20V-10BT. samples, the induction period for 20V-30Dex. ensured that a greater degradation than the IP sample was exhibited in the initial stages. However, this degradation was initially much greater when compared to the IP and other melt processed samples, but due to the step stage around day 323, the percentages of the IP and 20V-30Dex. samples remaining were approximately the same, 73.2 and 70.8% respectively.

The trends exhibited by the wet weight loss profiles for the dextran loaded samples were generally similar to those illustrated by the 12V-10SA. and 20V-10BT. samples. There was a gradual increase in the amount of water absorption for sample 12V-10Dex. until a maximum of 6% at day 150 was observed, before decreasing slightly to approximately 3% by day 450. There was comparatively little water absorption for sample 20V-30Dex. until day 26, after which the wet weight gradually increased to a maximum at day 180 (11%) and then decreased sharply to 7% at day 223. The water absorption then continued to gradually decrease to approximately 4% at day 450.

As discussed in section 7.1.3. and chapter 4, the initial PHB weight was reduced for the melt processed samples compared to the PHB(FM)IP and this serves to emphasize the somewhat greater degradation of the fibrous matrix sample when compared to the melt processed ones, as illustrated in graphs 7.10 to 7.13. Therefore, at day 325 the amount of degradation occurred in the following order:

20V-30Dex. $\gtrsim$ (IP) $>$ 12V-10SA. $>$ 20V-10BT. $\gtrsim$ 12V-10Dex.

29.2% 26.8% 15% 6% 5.5%

### 7.2.2. Comparison Of The Degradation Profiles From Different Degradation Models.

Graphs 7.14 to 7.17 illustrate the degradation profiles for the same melt processed samples from the physiological degradation model used in this thesis and that utilized by Yasin.[99] As can be observed there were differences in the degradation profiles from the two degradation models. In the degradation model utilized by Yasin, the stepped plaques and circular discs of varying initial weights around 600 to 700mg. were degraded in sample bottles with 200mls. of pH 7.4 buffer at 37.5°C. This model possessed a considerably larger buffer volume and sample weight than the model utilized in this thesis. Similarly, no definition of degradation pertaining to the model was stipulated by Yasin. Therefore, as discussed in chapter 4, the degradation profiles reported by Yasin were anticipated to differ from the ones determined here, mainly affected by the comparative increase in buffer volume and container size, whilst other changes would also occur due to differences in the classification of degraded and/or undegraded matter and the subsequent gravimetric analysis.

In the circular disc samples 12V-10SA., 12V-10Dex. and 20V-30Dex. and the stepped plaque sample 20V-10BT. the profiles determined by Yasin exhibited a comparatively greater degradation, as was anticipated. However, in all instances these differences reached a maximum of approximately 7.5% (20V-30Dex.) and in most cases remained below 5%, which was within a reasonable error range during the experimental time period of 425 to 450 days, (Graphs 7.14-7.17)

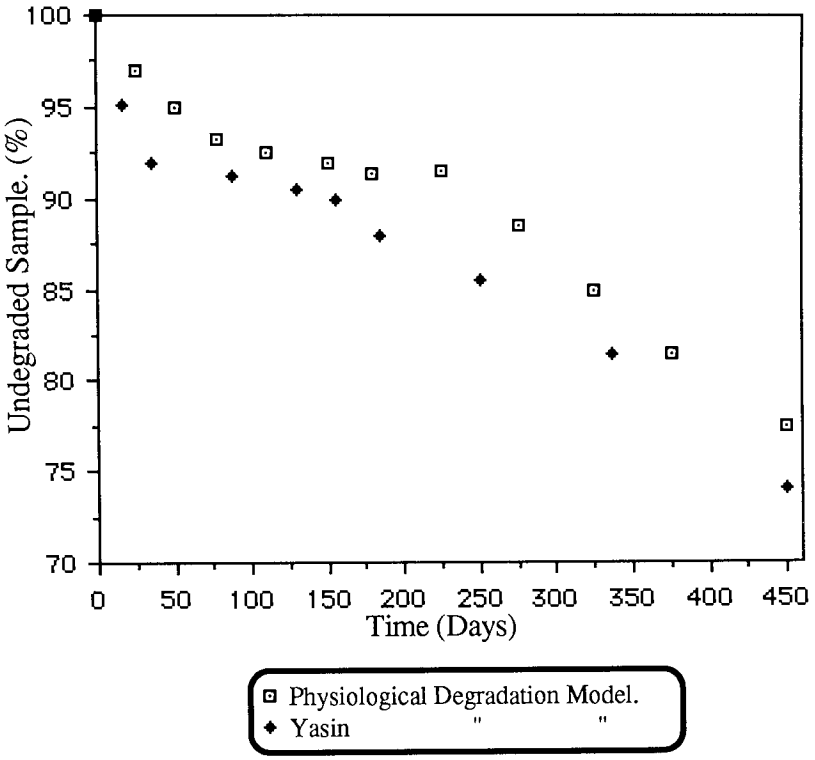


**Graph 7.14.**

**Comparison Of Degradation Profiles From Different Degradation Models For 12V-10SA.**

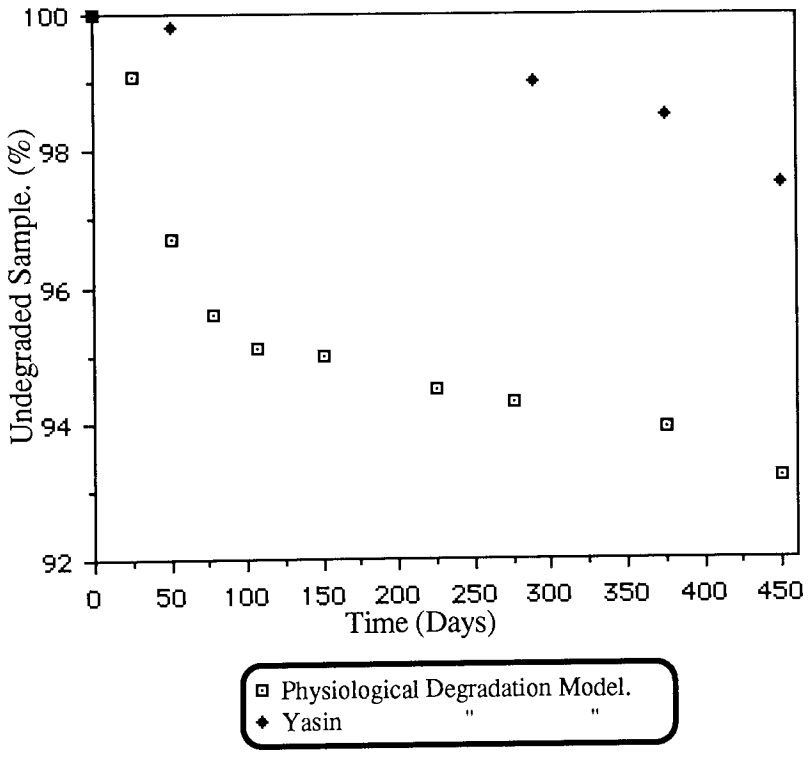


**Graph 7.15.**

**Comparison Of Degradation Profiles From Different Degradation Models For Sample 20V-10BT.**

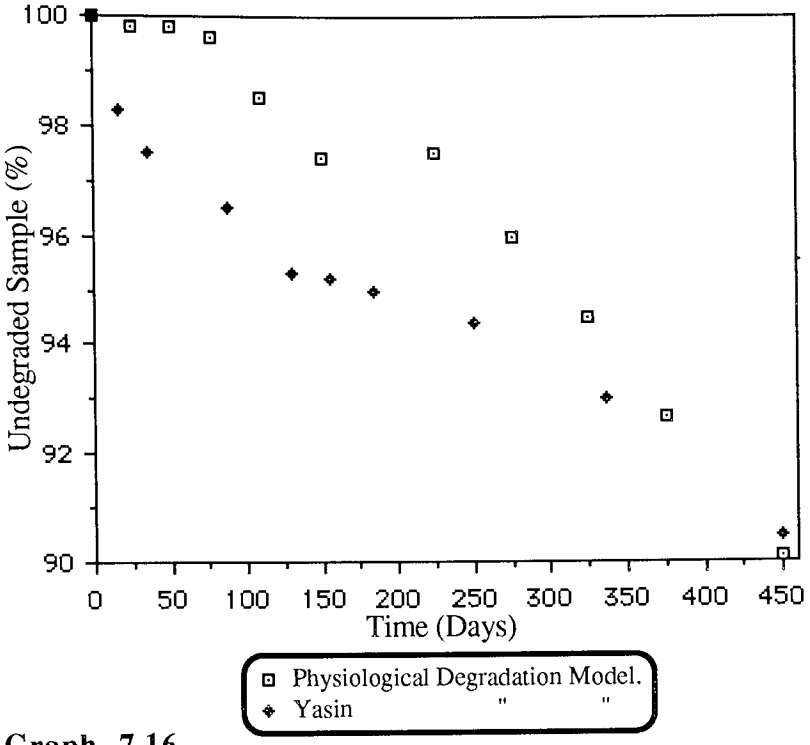


**Graph 7.16.**

**Comparison Of Degradation Profiles From Different Degradation Models For 12V-10Dex.**

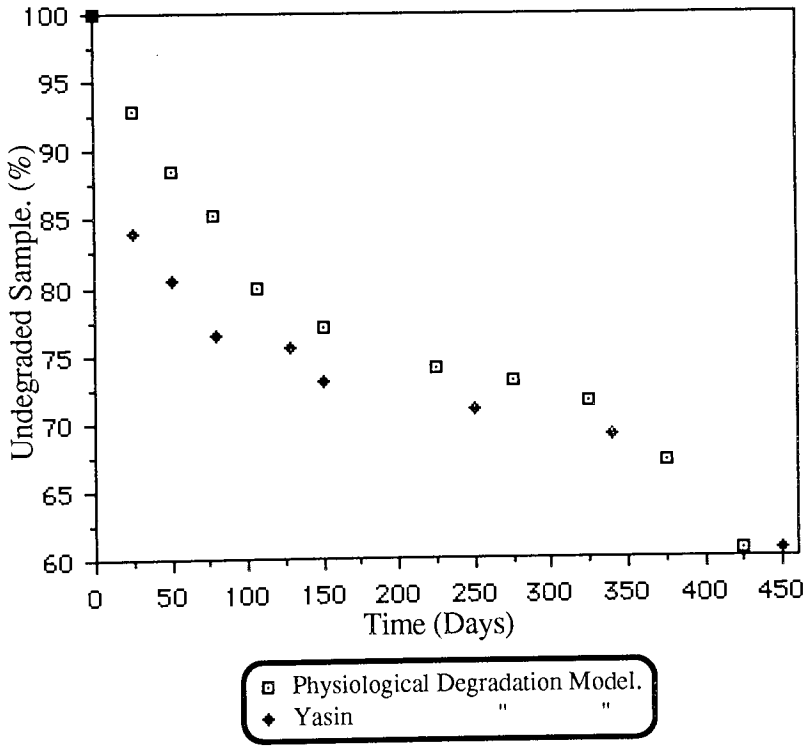


**Graph 7.17.**

**Comparison Of Degradation Profiles From Different Degradation Models For Sample 20V-30Dex.**

### 7.2.3. Conclusions.

It was concluded therefore, that the difference between the physiological degradation profiles for the melt processed samples, determined in this thesis and those determined by Yasin, were within a 5% error range. Despite the fact that these melt processed samples possessed less PHB initially than the PHB(FM)IP, the matrix sample degraded considerably faster than the melt processed samples. Thus, the comparatively large surface area to volume ratio of the PHB(FM)IP sample had a comparatively greater influence on the degradation than blending in these melt processed samples.

Utilizing the degradation profiles for samples 12V-10SA., 20V-10BT., 12V-10Dex. and 20V-30Dex. from the accelerated degradation model, the physiological degradation profiles could be extrapolated to estimate possible $t_{50}$ times, (Graph 7.18 & table 7.3). As can be observed from table 7.3, sample 20V-30Dex. exhibited a $t_{10}$ of only 45 days, whilst all the other melt processed samples had $t_{10}$ values significantly greater than that of the PHB(FM)IP at approximately 175 days. However, after the dissolution of the carbohydrates from each sample the degradations were such that the estimated $t_{50}$s for the PHB(FM)IP and the 20V-30Dex. were similar around 575 days, whilst the other melt processed samples had considerably greater $t_{50}$s.

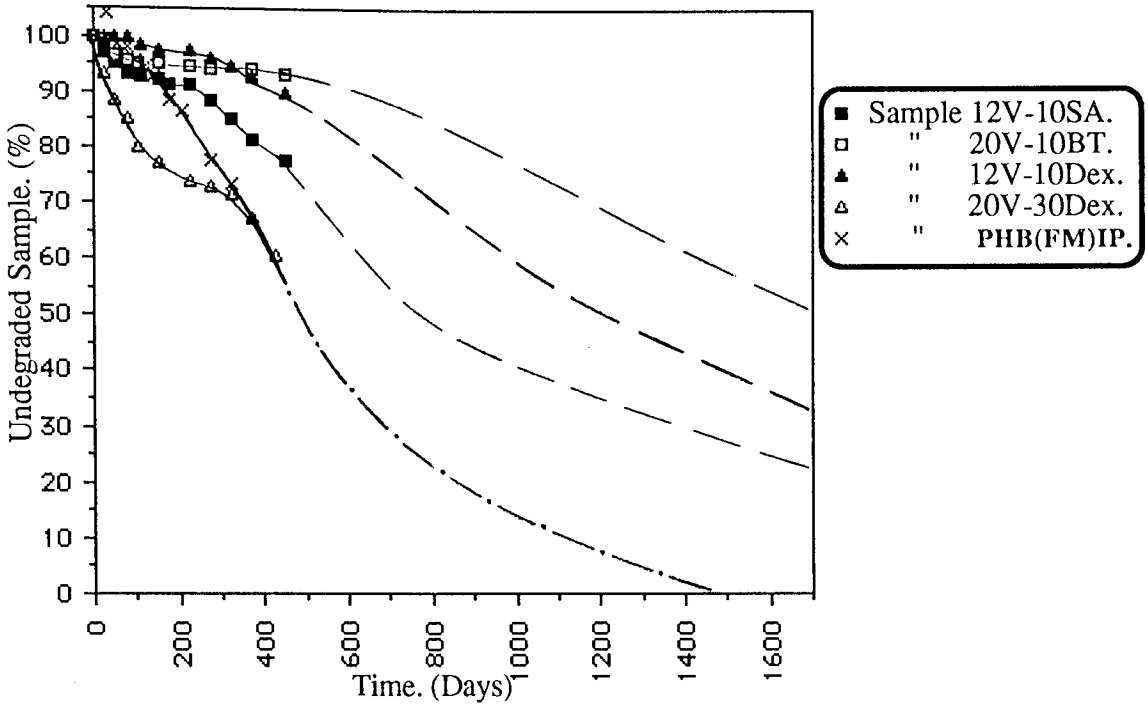


**Graph 7.18.**

**Extrapolation Of Degradation Profiles Of Melt Processed And Fibrous Matrix Samples In The Physiological Degradation Model**

| Sample | $t_{10}$ | $t_{50}$ |
|---|---|---|
| 20V-30Dex. | 45 Days. | [570] Days. |
| PHB(FM)IP. | 175 | [580] |
| 12V-10SA. | 255 | [750] |
| 12V-10Dex. | 255 | [1200] |
| 20V-10BT. | [775] | [1630] |

[ ] Estimated From Graph 7.18.

**Table 7.3.**

**Measured And Estimasted Times For 10 And 50% Degradation Of The Melt Processed And Fibrous Matrix Samples In The Physiological Degradation Model.**

## 7.3. General Conclusions.

This chapter has investigated the degradation of a number of melt processed samples in the accelerated and physiological degradation models and compared them to the degradation profiles determined for the PHB(FM)IP. There was a good correlation between the undegraded and degraded fractions of sample 12V-10SA. and once again, this confirmed the experimental accuracy of using monomer analysis.

The degradation profiles determined for those samples with a comparatively large carbohydrate loading were characterized by an initial rapid degradation followed by a stage IV 'plateauing effect', this was due to the limiting factors of degradation kinetics, degradation resistant matter and settlement/compaction as discussed in chapter 4. In contrast, the low carbohydrate loaded samples exhibited an induction stage due to the penetration of the buffer into the sample and the dissolution of the carbohydrate, this was then followed by a more gradual degradation. The extent of this induction stage was dependent upon the initial sample shape and its fragmentation.

The degradation profiles determined from the physiological degradation model were consistent with those determined from the accelerated. The degradation of PHB(FM)IP exceeded those of the melt processed samples, except in the initial stages and this was due to the carbohydrate dissolution, only sample 20V-30Dex. exhibited a similar degree of degradation.

It was concluded that the nature, distribution and loading of the carbohydrates and PHV

component within the melt processed samples and the initial sample shape affected the sample degradation. These effects were mainly upon the surface area to volume ratio of the sample and the initial PHB weight. It was concluded therefore, that the surface area to volume ratio was of paramount consideration in the alteration of the degradation profile of a sample. The fibrous matrix sample, by virtue of its comparatively larger surface area to volume ratio, exhibited an overall faster degradation than that of the melt processed samples. This was highlighted in the degradation of the samples in the physiological degradation model. Finally, it was determined that the degradation of the fibrous matrix sample in the physiological degradation model could be compared to the greater variety of melt processed samples as investigated by Yasin.[99]

Thus, the structure, degradation, and factors affecting the degradation of the various fibrous matrix and melt processed samples have been investigated in this thesis from chapters 3 to 7. In chapter 8 there is a general discussion of the conclusions from these chapters and suggestions for further work.

# Chapter Eight.

## Concluding Discussion And Suggestions For Further Work.

## 8.1. Concluding Discussion.

### 8.1.0. Introduction.

The aim of this work was to investigate the *in vitro* degradation of a new and novel gel-spun, fibrous form of PHB, and to alter its degradation times to those considered more favourable for its intended use as a wound scaffolding device. The work in this thesis involved three aspects:

(1) The investigation of the novel fibrous form, its structure and physical properties and the effects on these of altering the production process, blending with various polysaccharides and copolymerizing with poly(β-hydroxyvalerate), PHV. These investigations were neccessary in that, *a)* This was the first study of the novel fibrous form, later named PHB fibrous matrix, PHB(FM) as a result of these investigations. No other investigations had previously been carried out. *b)* The results would provide an indication as to the suitability and potential of the PHB(FM) for a role as a wound scaffolding device. *c)* The results were to be used as a baseline for the comparison with the partially degraded PHB(FM) samples.

(2) The development of an accelerated and physiological degradation model. The investigations of the gel-spun PHB(FM) revealed its relatively complex structure compared to other more convential PHB based samples, eg; melt processed discs and plaques. As a result of its rather unique and complex structure which combined a large volume with low mass and readily altered during, and as part of, the degradation process, the accurate quantitative degradation of the PHB(FM) was difficult to monitor. The

degradation monitoring techniques previously utilized for the more convential PHB based forms were unsatisfactory for this novel form. Therefore, a new method of monitoring the degradation had to be developed. This involved the determination of the monomer (HBA) concentration during degradation and using this to monitor both the degraded and undegraded fractions of the sample during degradation and the monitoring of both the sample and the PHB degradation.

(3) Utilizing the initial studies of the PHB(FM) from (1) as a baseline for comparison and the developed degradation models from (2), the degradation of the PHB(FM) was investigated. The changes in the degradation rates of this novel form due to blending and copolymerizing the sample and by altering its processing were investigated utilizing the accelerated degradation model. The results obtained were then compared to those determined for the samples in a physiological degradation model. Thus, providing a more accurate indication as to the potential biodegradation of the samples as implantation devices.

The results of these three aspects are discussed in detail in sections 8.1.1 to 8.1.3.

### 8.1.1. The Structure And Physical Properties Of The PHB(FM).

The PHB(FM) produced from technical grade polymer, PHB(FM)TG, consisted of hollow and porous fibres of varying, non-uniform diameters which agglutinated and branched to form a complex fibrous mass. Terminal bulbous regions were also observed at some fibre ends. The fibres possessed a main distribution of diameters (60%) between 0 and 5 microns with the majority at two peaks of 1-2 and 4-5um., whilst a small

percentage of those fibres counted had diameters greater than 15 microns and up to a maximum of approximately 72um.

It was determined that increasing the PHB purity, PHB(FM)IP, had apparently little effect on the matrix structure and only slightly increased the crystallinity and the various parameters calculated from the differential scanning calorimetry investigations; melting points, fusion enthalpies and glass transition temperatures. Altering the production solvent had a more noticeable effect on the matrix structure with a proportion of the fibres produced from methylene chloride extraction exhibiting a more heavily pitted and porous nature compared to those from the chloroform extraction, whilst those fibres produced from a 50/50 solvent mixture were comparatively smooth.

Blending the PHB(FM)IP with various polysaccharides produced noticeable differences in the fibre diameter distributions and physical properties when compared to the homopolymer matrix. The extent of these changes were dependent upon the nature and loading of the polysaccharide, generally, increasing the loading increased the diameters, however, the reverse effect was noticed for those samples blended with sodium alginate (SA-7. and SA-30.). Increasing the loading of low molecular weight pectin increased the number of large fibres with diameters greater than 15 microns, whilst the remaining diameter range was also shifted to the larger diameters. Blending was determined to be inefficient, with sample L.Pec.25.S. apparently possessing a lower load of pectin of a comparatively greater molecular weight than its counterpart L.Pec.25.E. Blending the PHB(FM)IP with high molecular weight pectin, H.Pec.10., produced a shift in the fibre diameter distribution towards the smaller diameters. The melting points, fusion enthalpies,

glass transition temperatures and crystallinities of the co-blends were generally lower than that of the homopolymer sample. Copolymerizing with 5% poly(β-hydroxyvalerate), PHV, produced similar effects to the blending. It was also observed that blending and copolymerizing apparently reduced the initial matrix strength.

The unusual, complex structure of the PHB fibrous matrix possessed a large surface area to volume ratio and this facilitated its degradation. Changes in the porosity and fibre diameter distributions due to blending, copolymerizing and alterations in the production process affected the surface area to volume ratio of the matrices and thus, their degradation.

### 8.1.2. The Development Of The Accelerated And Physiological Degradation Models.

Preliminary studies concluded that the degradation of the PHB(FM) favoured increasing temperature and pH, this was anticipated from published studies.[49-51] Similarly, the degradation of PHB under physiological conditions of pH 7.4 and temperature 37.5°C. is known to take a relatively long time,[47-49] thus, an accelerated degradation model of pH 10.6 and temperature of 70°C. was utilized in conjunction with the physiological in order to provide a clearer indication of the samples biodegradation within the body system.

An experimental procedure that takes into account the intrinsic problems presented by the novel structure of the PHB(FM) was devised and is summarised in figure 2.1. This experimental pathway was then implemented for all the samples investigated. The use of monomer measurement as a means of monitoring the PHB degradation was concluded as being accurate in the accelerated degradation model for a period of 14 days. However, the

method was found to be unsuitable in the physiological degradation model.

The effects of initial sample weight and agitation in the model were also investigated and from these experiments it was concluded that the degradation models should incorporate the following factors:

a) 20mls of buffer.

b) An initial sample weight of 305mg. ±1.6%.

c) Minimum agitation of the samples.

It was also concluded from these experiments that the degradation model affected the sample degradation in that it altered the available surface area to volume ratio of the samples during degradation. Therefore, the degradation profiles determined were a function of the sample degradation within the degradation model.

The degradation profiles confirmed that the experimental accuracy of measuring the undegraded (gravimetry) and degraded fractions (monomer + degraded particulate analysis) of the matrix during its degradation was within ±2%.

### 8.1.3. Degradation Of The PHB Fibrous Matrix, PHB(FM).

The monomer analysis degradation profile of the technical grade polymer, PHB(FM)TG, in the accelerated degradation model was characterized by a number of stages; there was an initial induction phase, stage 0, until approximately 6 hours with little degradation observed. This was due to the collapse to particulate matter of a proportion of the structurally weaker fibres in the diameter range 0-1um., the particulate matter continued to

fragment and this led to the stage I degradation which occurred until around day 7 degradation. Between days 7 and 9 there was a 'step' stage (II) with little degradation observed, this was due to fragmentation of the remaining matrix to fibre fragments and particulate matter and was not observed in the gravimetric analysis profile. Degradation to monomer progressed in stage III between days 9 and 18, after 18 days degradation the 'terminal step' stage IV began with little or no further degradation exhibited. The sample degradation, particularly at stage IV, was determined as being affected by the following 'limiting factors':

a) The kinetics of the experiment.

b) Matter settlement and compaction (a reduction in the surface area to volume ratio).

c) Degradation resistant matter (impurities and highly crystalline PHB).

A number of small and large 'unstable' fibres were observed in the approximate diameter ranges 0-2 and 15+um. respectively, their structural weaknesses were due to handling and manufacturing stresses and as a result of production, mainly bacterial impurities. Degradation occurred by hydrolytic action which randomly cleaved the ester linkages, initially weakening the fibres and eventually leading to their physical collapse to fibre fragments and progressively to the monomer. (See Figs. 4.1, 4.7 & 4.8).

The matrix degradation was characterized by a gradual decrease in the melting point with little change during the stage IV time period, whilst the fusion enthalpy and crystallinity increased to a peak after approximately 7 days degradation and then decreased. Thus, there was an initial degradation of the mainly amorphous regions followed by the crystalline. These trends were generally consistent to those observed for the increased

purity polymer sample PHB(FM)IP. However, in this case the melting point changes were not as great initially, with a more gradual decrease, whilst the enthalpy/crystallinity peak occurred earlier after 4 days degradation.

Purifying the PHB removed some of the impurities, solvent residue and amorphous regions of the PHB(FM)IP. This increased the matrix stability when compared to the technical grade matrix; PHB(FM)TG, so that no step stage II was observed and a gradual collapse and degradation of the PHB(FM)IP was observed. This then ensured a greater overall degradation when compared to the PHB(FM)TG. The affects of altering the production solvent on the PHB(FM)IP degradation was also investigated. Degradation was facilitated by the heavily porous nature of those fibres extracted from the methylene chloride solvent, such that the degradation exceeded that of the PHB(FM) from the chloroform. However, the degradation of those fibres extracted from the 50/50 solvent mixture exceeded that of both the other matrices.

It was concluded that the degradation profile of PHB(FM)IP could be altered by blending the matrix with various polysaccharides, the subsequent profiles were dependent upon the polysaccharide nature and loading. Generally, the co-blend degradation exhibited a noticeable step stage II, whilst increasing the polysaccharide loading facilitated the matrix collapse so that the terminal step stage IV was influenced by the settlement/compaction limiting factor to a comparatively greater extent than in the lower loaded samples and, as a result of this, the stage IV was more sudden. Similar to the homopolymer degradation, there was a good correlation between the profiles of the degraded and undegraded fractions, confirming the experimental accuracy.

Blending the PHB(FM)IP with pectin facilitated the matrix and PHB degradation. The blending was non-homogenous. The pectin degraded within the first day in the accelerated degradation model causing the formation of readily noticeable 'pectin cavities'. These cavities increased the surface area to volume ratio and decreased the stability of the remaining PHB matrix, so that the characteristic two step degradation profile was observed.

Increasing the pectin loading facilitated the matrix collapse by the introduction of mechanical stresses after the pectin degradation. The blending efficiency was reduced in the higher pectin loadings, so that the sample from the start of the manufacturing run was blended with a lower loading of comparatively higher molecular weight pectin than the sample from the end of the run (L.Pec.25.S. & L.Pec.25.E.). Pectin was also lost in the production process. The blending weakened the small and large diameter fibres (<6 & >15um.), whilst increasing the pectin loading increased the number of large diameter fibres and shifted the diameter distribution towards the larger diameter ranges. As a result of this, in samples L.Pec.9. and L.Pec.15. there was an initial fragmentation of the small and large diameter fibres, in L.Pec.25.S. a proportion of the medium sized fibres initially fragmented prior to the small and large, whilst for the L.Pec.25.E. sample a comparatively greater proportion of the medium diameter fibres fragmented more readily, closely followed by the larger ones.

The increase in the PHB degradation for the co-blends compared to the PHB(FM)IP was greater than could be justified by the reductions in the initial PHB weights and favoured the lower loaded sample L.Pec.9.

The changes in melting point of sample L.Pec.9. during degradation were characterized by an initial decrease and a 'step' stage around days 1 to 3, which was due to a reduction in the pectin component. After 3 days degradation the melting point decreased considerably before levelling off around day 14. This trend was also exhibited by the other pectin co-blends, but with less noticeable step stages. Similarly, the fusion enthalpy changes exhibited a characteristic double peak. The primary peak occurred within the first day and was due to the pectin dissolution, the secondary peak was due to the PHB degradation, (See Graph 5.59). The position of this secondary peak varied according to the extent of the PHB degradation and was at days 4/5 for samples L.Pec.9., L.Pec.15. and L.Pec.25.S. and days 7/8 for sample L.Pec.25.E. In all cases there was a gradual decrease in the glass transition temperatures, which were readily noticeable compared to the homopolymer matrix.

The higher molecular weight pectin blended more homogeneously with the PHB (H.Pec.10.) and this increased the long term matrix stability whilst maintaining a comparatively high surface area to volume ratio, this stability subsequently reduced the effects of compaction so that the sample and PHB degradation was greater than its low molecular weight counterpart. The melting point change for sample H.Pec.10. was similar to that observed for L.Pec.9. with a noticeable step stage, however, the H.Pec.10. fusion enthalpy change exhibited an initial sharp rise within the first day followed by a gradual linear increase. This initial rise was most likely due to the degradation of those readily available amorphous regions (primary amorphous regions) which probably comprised a considerable proportion of pectin.

Copolymerizing the PHB with 5% PHV also affected the parameters calculated from the DSC, there was an initial sharp decrease in the glass transition temperature and then a more gradual change, whilst the fusion enthalpy change exhibited a single peak. The DSC traces illustrated the gradual formation of a broad peak covering a comparatively large temperature range, indicating that the degradation was not uniform for the whole sample.

The copolymerized sample PHB/5V exhibited a similar PHB degradation profile to the co-blends, but with a reduced stage III degradation, this was due to the comparatively degradation resistant PHV. Similarly, the surface area to volume ratio of the fibres was reduced when compared to the co-blend fibres which possessed 'pectin cavities'. As a result of this, the PHB/5V sample degraded less than the co-blended and the homopolymer samples.

Therefore, it was concluded that the matrix and PHB degradation could be altered by blending and copolymerizing, the former of which increased the matrix and PHB degradation due to the changes in the surface area to volume ratio and stability which also affected the ratio during degradation, whilst the copolymerizing reduced the degradation due to a reduction in the ratio. Thus, the degradation of the PHB(FM) could be adjusted to provide various degradation profiles as may be suited for a particular medical implantation device or wound location.

**Regions:**

1

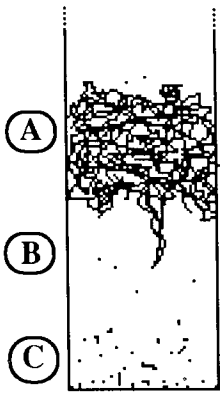


1

The 'floating' matrix at the beginning of the experiment. Buoyancy was due to trapped air in the matrix and the bubbles in with the hollow fibres and cavities. Some fibre fragments and particulate matter were present due to manufacture and handling.

There was penetration of the buffer medium into the fibres.

**This was the degradation stage 0.**

2

During the initial stage I on the monomer profile, there was a number of fibres which readily collapsed into fibre fragments and particulate matter, the rate of degradation of these was limited according to their situation:

(a) A proportion was trapped by the remaining matrix at region **A**, due to support by the matrix and possible bubbles contained within the fibre fragment.

(b) Fibre fragments/particulate matter degraded whilst falling to the base of the phial at region **B**.

(c) The matter collapsed at region **C** and degradation was reduced due to a comparative reduction in the surface area to volume ratio as a result of compaction.

2

Degradation occurred from the remaining matrix and proportionately more so from the fibre fragments and particulate matter.

**This was the degradation stage I.**

**Figure 8.1A.**
**Diagrammatic Representation Of Matrix Degradation.**

3

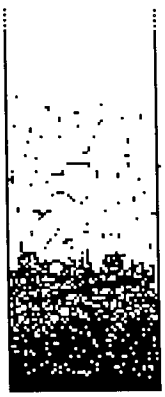

There was degradation to monomer of most of the particulate matter from the initial 'unstable' fibres at stage I, so that at stage II little degradation to monomer was monitored.

There was fragmentation at the structural weaknesses due to stresses and erosion of the secondary amorphous regions, accompanied by the release of the bubbles, this facilitated the collapse of the remaining matrix at region **B/C**. The more readily collapsed fibre fragments and some of the large particulate matter formed a comparatively dense layer at the phial base **C**.

This collapse increased the surface area to volume ratio and released relatively large quantities of particulate and degraded particulate matter. Fragmentation and fracturing continued throughout the matrix.

**This was The degradation step stage II**

The comparatively large amounts of fibre fragments and particulate matter from stage II continued to degrade and this led to the relatively large degradation rates monitored at stage III. The continued collapse increased the dense layer at C due to matter settlement.

**This was the degradation stage III.**

4

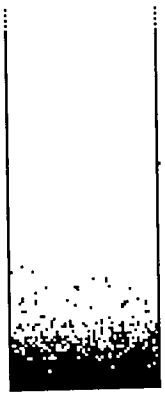

Compaction of the particulate matter with the remaining fibre fragments formed a relatively dense layer at region **C**, this reduced the surface area to volume ratio. The ratio decrease in combination with the degradation kinetics and the presence of degradation resistant material also reduced the degradation rate. Agitation of the sample increased this rate.

**This was the terminal step stage IV.**

**Figure 8.1B.**

**Diagrammatic Representation Of Matrix Degradation.**

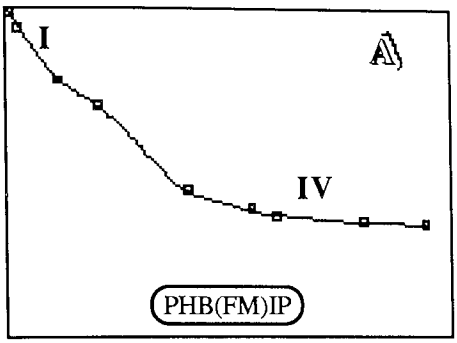


## A The Degradation Of PHB(FM)IP.

The degradation of the PHB(FM)IP generally followed the diagrammatic representation in figure 8.1. No stage II or III was observed. The stage IV 'plateauing' effect was due to limiting factors. The matrix collapsed gradually throughout the course of the degradation.

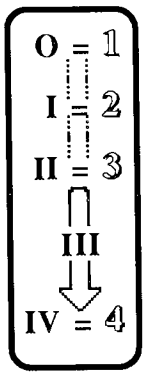


**Relation Of Degradation Stages To Diagrammatic Representation Of Matrix Collapse.**

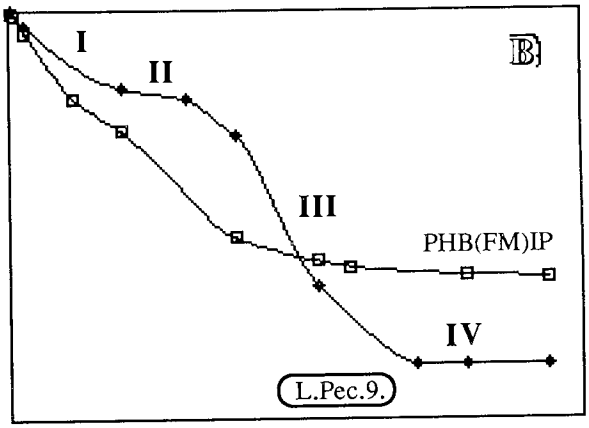


## B The Degradation Of The Co-blended Samples.

The degradation proceeded as illustrated by the diagrammatic representation in figure 8.1.

Blending of the PHB(FM)IP reduced the initial weight of PHB present and increased the initial stability of the matrix at the degradation stage I so that the degradation rate was less than that of the PHB(FM)IP.

The gradual erosion of the co-blend cavities increased the surface area to volume ratio and caused structural weaknesses within the fibres, this then facilitated the comparatively sudden collapse of the matrix with the release of particulate matter. This was observed as the noticeable step stage II. The continued degradation of the particulate matter and the semi-fibrous pieces produced the stage III.

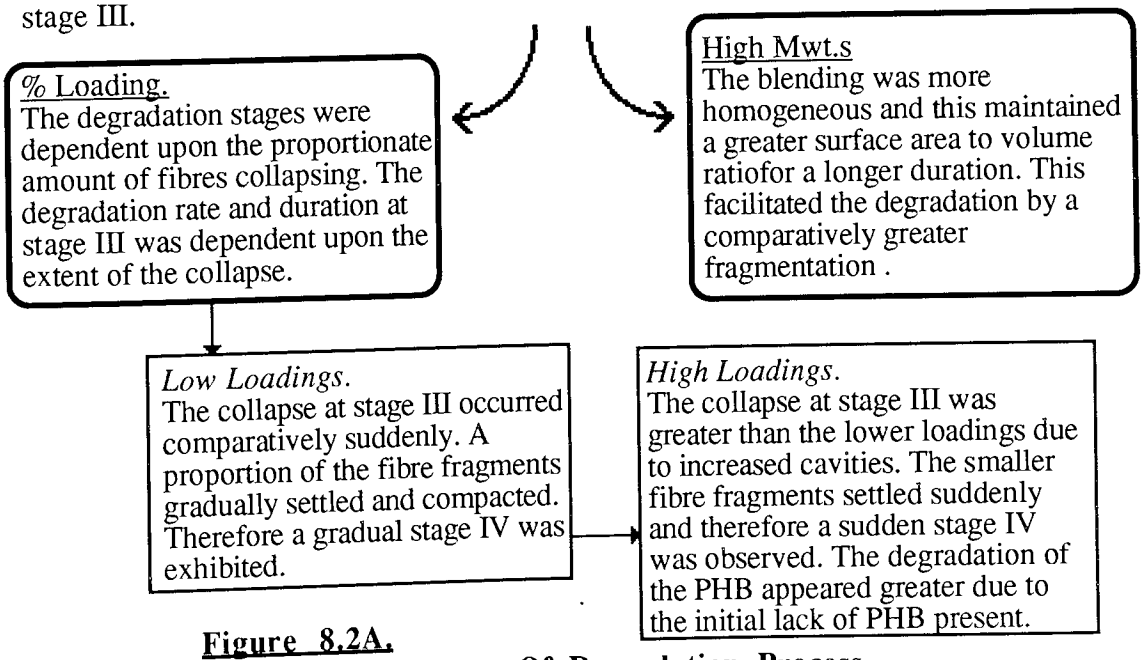


**Figure 8.2A.**
**Summary Of Degradation Process.**

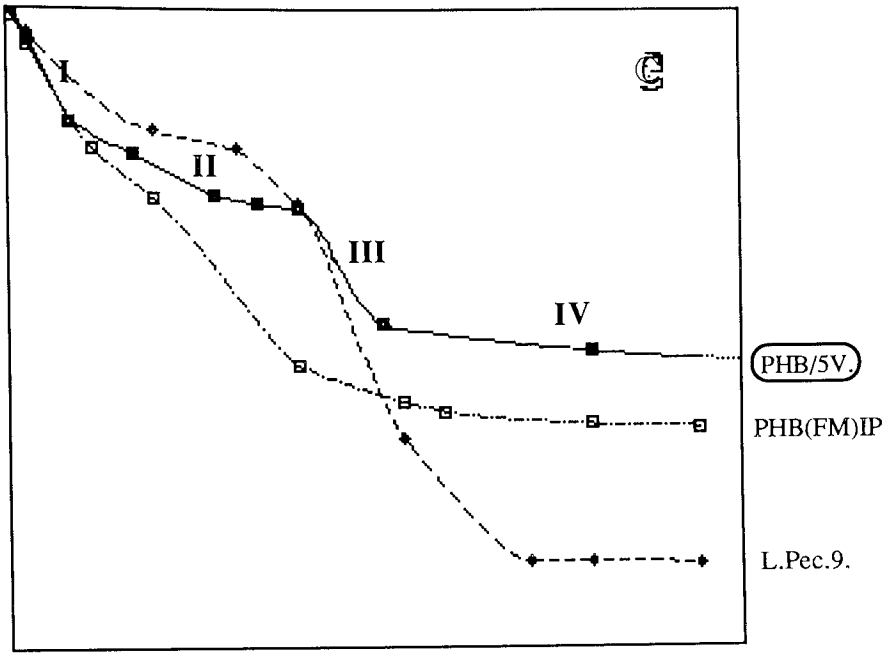


## C The Degradation Of The Copolymerized Sample.

Stage I degradation was similar to the PHB(FM)IP. The collapse of a proportion of the fibres was not as great as the PHB(FM)IP sample and thus, a gradual degradation between stage I and the step stage II occurred.

Stage II was similar to the co-blended samples with a greater stability due to the copolymer presence. The degradation of the PHB caused the gradual weakening of the fibres.

The fibres fragmented at the structurally weak points and the matrix subsequently collapsed. Relatively small amounts of particulate matter were produced compared to the co-blended samples. Fragmentation occurred to a greater extent than in the PHB(FM)IP such that smaller fibre fragments compared to the homopolymer were present. These then facilitated the compaction of the collapsed mass and subsequently reduced the surface area to volume ratio.

As a result of the compaction a short stage III degradation rate occurred and was primarly due to the degradation of the particulate matter.

Fragmentation and compaction was not as great as for the larger co-blend loadings but greater than the PHB(FM)IP, therefore, a less gradual stage IV compared to the PHB(FM)IP occurred.

The copolymer was comparatively degradation resistant.

**Degradation of the PHB in the samples was therefore concluded to occur in the following order:**

**Co-blend > Homopolymer > Copolymerized Samples.**

**Figure 8.2B.**
**Summary Of Degradation Process.**

The degradation of the PHB(FM)IP and the effects of blending and copolymerizing are briefly summarized in figures 8.1 and 8.2. The degradation of the co-blended and copolymerized samples in the accelerated degradation model were then related to the degradation of the same samples in the physiological degradation model.

The degradation of the blended and unblended PHB(FM)IP in the physiological degradation model was similar to the degradation in the accelerated model, however, the degradation stages were more prolonged and pronounced. There was a noticeable induction stage 0 lasting until around days 50 to 60 for the PHB(FM)IP degradation, during this time the buffer gradually penetrated the fibres and began to degrade the primary amorphous regions, this then led to the collapse of the weakened fibres; stage I. At stage I there was a gradual increase in the degradation rate until around day 125 where a linear rate of approximately 0.11%dy.$^{-1}$ was calculated. Similarly, the stage I in the accelerated degradation model exhibited a linear degradation rate of approximately 0.65%dy.$^{-1}$. Thus, the degradation profiles were comparable, (See Fig. 6.1). The degradation profiles for the co-blends were similar to that determined for the homopolymer. However, in these cases, initial weight losses followed by less noticeable induction stages were observed, this was due to the gradual degradation of the pectin.

The relatively more noticeable stages in the physiological degradation profiles helped to clarify the nature of the PHB(FM) degradation. The limiting factor of settlement and compaction apparently exhibited more influence on the sample degradation in the accelerated degradation model than the physiological and these were reflected in the degradation profiles obtained.

The phase contrast and scanning electron microscopy observations were consistent with the degradation process as determined from the accelerated degradation model and from the conclusions drawn from the physiological degradation profiles in chapter 6. Similarly, the fibre diameter distributions also confirmed those conclusions from the accelerated degradation studies, with fragmentation first occurring in the small diameter fibres followed by the large sized ones, and the diameter distribution gradually shifting to the larger diameter ranges.

There was little change in the melting points of the partially degraded samples during an induction period lasting until around days 50 to 75. After 75 days degradation, a gradual decrease was observed, so that at day 324, when the experiment was terminated, the PHB(FM)IP exhibited an overall decrease of approximately 6 ±2°C., compared to a decrease of around 12 ±2°C. In contrast to the fusion enthalpy change profiles determined from the accelerated degradation model, the fusion enthalpy changes for samples from the physiological degradation model showed no induction stage but gradually increased to a single peak which was attained more quickly for those samples with comparatively low pectin loadings, L.Pec.9. and L.Pec.25.S. Thus, the amorphous regions of the sample were initially degraded.

Table 8.1 compares the degradation of the samples from the accelerated and physiological degradation models by illustrating the times for 10 and 50% degradation, $t_{10}$ and $t_{50}$ respectively. However, this does not provide as complete a picture as the degradation profiles discussed in chapters 3 to 7.

| Sample: | | $t_{10}$ (Days) | $t_{50}$ | [ ] Estimated From Extrapolation Of Degradation Profiles. |
|---|---|---|---|---|
| **Fibrous Matrix Samples.** | | | | |
| PHB(FM)TG | | 0.6 (14 hours) | 8 | Accelerated Degradation Model. |
| PHB(FM)IP | | 2 | 11 | |
| Glu-42. | (PHB Component) | 2 | 16 | |
| Suc-42. | | 0.3 (7 hours) | [53] | |
| SCC-9. | | 1 | 14 | |
| SA-30. | | 2 | 19 | |
| SA-7. | | 2 | 14 | |
| L.Pec.9. | | 2 | 17 | |
| L.Pec.15. | | 3 | 15.5 | |
| L.Pec.25.S. | | 3 | 15 | |
| L.Pec.25.E. | | 3.5 | 16 | |
| H.Pec.10. | | 3 | 16 | |
| L.Pec.9. | (Sample) | 0.3 (8 hours) | 12.5 | |
| L.Pec.15. | | 0.1 (2 hours) | [10] | |
| L.Pec.25.S. | | 1 | [10] | |
| L.Pec.25.E. | | 0.1 (2 hours) | [8] | |
| H.Pec.10. | | 0.3 (7 hours) | [10] | |
| PHB(FM)IP | | 175 | [580] | Physiological Degradation Model. |
| L.Pec.9. | | 83 | 334 | |
| L.Pec.15. | | 30 | 325 | |
| L.Pec.25.S. | | 215 | [357] | |
| L.Pec.25.E. | | 11 | 307 | |
| **Melt Processed Samples.** | | | | |
| 12V-10SA. | | 1 | 6.5 | Accelerated Degradation Model. |
| 12V-30SA. | | 0.5 | 4.5 | |
| 20V-10BT. | | 0.5 | 8.5 | |
| 20V-30Amy. | | 3 | 16 | |
| 12V-10Dex. | | 5 | 23 | |
| 20V-30Dex. | | 5.5 | 21.5 | |
| 20V-30Dex. | | 45 | [570] | Physiological Degradation Model. |
| 12V-10SA. | | 255 | [750] | |
| 12V-10Dex. | | 255 | [1200] | |
| 20V-10BT. | | [775] | [1630] | |

**Table 8.1.**
**Times For 10 And 50% Degradation Of Samples Studied In This Thesis.**

Therefore, it was concluded that the degradation of the fibrous matrix samples in the accelerated degradation model provided an accurate indication as to the degradation of the same samples in the physiological degradation model and thus, a clearer picture as to their potential for biodegradation within the body system.

The degradation profiles of the PHB(FM)IP obtained from the accelerated and physiological degradation models were compared to the degradation profiles of a number of melt processed PHB based samples from the same models. This was done to confirm the importance of the surface area to volume ratio of the sample in determining its degradation. The comparison of these profiles also gave an indication as to the suitability of these melt processed samples as medical implantation devices.

Degradation profiles of the copolymerized melt processed samples blended with various carbohydrates were determined from the physiological degradation model and these were consistent with those determined from the accelerated degradation model. The degradation of PHB(FM)IP exceeded those of the melt processed samples, except in the initial stages and this was due to the carbohydrate dissolution, only sample 20V-30Dex. exhibited a similar degree of degradation. Table 8.1 compares the $t_{10}$ and $t_{50}$'s of these samples. It was concluded that the nature, distribution and loading of the carbohydrates and PHV component within the melt processed samples and the initial sample shape affected the sample degradation. These effects were mainly upon the surface area to volume ratio of the sample and the initial PHB component.

It was concluded therefore, that the surface area to volume ratio was a paramount

consideration in the alteration of a degradation profile of a sample. The fibrous matrix sample, by virtue of its comparatively larger surface area to volume ratio, exhibited an overall faster degradation than that of the melt processed samples. This was highlighted in the degradation of the samples in the physiological degradation model. It was determined that the degradation of the fibrous matrix sample in the physiological degradation model could be compared to the greater variety of melt processed samples as investigated by Yasin.[99]

The point of classification of degraded and undegraded material in this thesis was taken at the size of 3um. Thus, any partially degraded material above 3um. in size was considered as undegraded or partially degraded, whilst matter below this size was measured as degraded. This classification between the degraded and undegraded material in this thesis is neglected in a wide majority of papers and this complicates their comparisons, since no such point is stipulated. Similarly, as investigated and discussed in this thesis, the degradation model plays an important role in affecting a samples degradation and thus, such differences also complicate comparisons.

Consequently, such a definition of degradation, stipulating the point of which degradation is monitored would go some way to clarifying other degradation results and pave the way towards some form of standardization (possibly as suggested by Swift[102] and Mayer *et al.*[103]), which is desperately needed to expand the knowledge of biodegradation without confusion.

Originally work by Miller and Williams[47] claimed that little degradation of PHB occurred

under *in vitro* conditions of pH 7.2 and temperature 37°C. Subsequent work by Holland *et al.*[49,51] proved that PHB did indeed degrade under such physiological conditions. The work in this thesis has confirmed this and proved that the material factors such as processing, sample size and shape affect the degradation of the PHB, with a major factor being the surface area to volume ratio of a sample, both initially and during its degradation.

The work in this thesis has investigated the structure and physical properties of a previously unstudied novel gel-spun fibrous form of PHB. A unique accelerated degradation model which incorporates monomer analysis, was developed to monitor the undegraded and degraded fractions of the PHB(FM) and this model was utilized to investigate the degradation of various PHB fibrous matrix samples. Further information was obtained by the degradation of the matrices under physiological conditions and the comparisons with the melt processed samples.

Thus, it is envisaged that the work in this thesis will eventually lead to the production of biodegradable, biocompatible PHB fibrous matrix wound scaffolding devices, individually 'tailored' to suit a variety of wound types and to fulfill a neglected niche in the medical field.

## 8.2. Suggestions For Further Work.

As already stated, the work in this thesis involves the first study of this new and novel fibrous form of poly(β-hydroxybutyrate) fibrous matrix, PHB(FM). During these investigations work by Davies,[80] also of the Speciality Materials Research Group, has briefly studied cellular attachments to the undegraded homopolymer matrix samples. This work should continue to include co-blended and copolymerized samples and partially degraded samples.

The limiting factors of matter settlement/compaction was a function of the degradation model, removing this factor by agitating the samples was responsible for a further 11% degradation of the PHB(FM)IP sample in the accelerated degradation model. This limiting factor has already been concluded as playing an important role in determining a samples degradation, the effects of this factor should therefore be removed in subsequent degradation experiments by the use of an agitating waterbath.

Studies in this thesis have also shown that alterations to the processing can substantially facilitate the PHB and sample degradation. Further research into the effects of processing modification, such as temperature and spinning speeds, and pre-degradation treatments, such as autoclaving/sterilization and irradiation, on the degradation should also be carried out.

The PHB(FM)IP blended with 10% high molecular weight pectin, H.Pec.10., was determined to degrade more substantially than its low molecular weight counterpart, this was due to the greater homogeneity in the blending. Investigations of samples blended

with various loadings of high molecular weight pectin and other such polysaccharides etc. should also continue.

Although the use of accelerated and physiological degradation models to monitor a samples degradation *in vitro* gives an indication to its biodegradation within the body system, it is no substitution for *in vivo* studies. 'Promising' samples from future *in vitro* studies of the fibrous matrix should be selected for qualitative and quantitative *in vivo* degradation studies. The use of radiolabelled carbon in the production of PHB(FM) utilized in these *in vivo* studies may also provide further information regarding the samples biodegradation and fate within the body system.

# References.

1. Majno G. The Healing Hand: Man And Wound In The Ancient World. Harvard University Press, Cambridge, Mass. USA. **1975**.

2 Goldenberg I.S. Catgut, Silk And Silver: The Story Of Surgical Sutures. *Surgery*, 46 **1959** 908-912.

3 Halsted W.S. Ligature And Suture Material: The Employment Of Fine Silk In Preference To Catgut. *J. American Med. Assoc.* 60 **1913** 1119-11126.

4 Schmitt E.E. & Polistina R.A. Surgical Sutures.U.S. patent 3,297,033 10th. Jan. **1967**.

5 Bonfeld W., Grynpas M.D., Tully A.E., Bowman J. & Abram J. *Biomaterials*, 2 **1981** 185-186.

6 Baptist J.N. (W.R. Grace & Co.) U.S. Patent 3111496 **1966**.

7 Miller N.D. & Williams D.F. The Biodegradation Of Poly(β-hydroxybutyrate) (PHB) And PHB-Hydroxyvalerate Copolymers.6 Taylor L. Degradable Plastics: Solution or illusion. *Chem. Tech.* Sept. **1979** 542-548.

8 Korsatko W., Wabnegg B., Braunegg G., Lafferty R.M. & Strumpfl F. *Pharm. Ind.* Poly(hydroxybutyric acid) (PHBA) A Biodegradable Carrier For Long Term Medication Dosage I: Development Of Parental Tablets For Long TermApplication To Pharmaceuticals. 45(5) **1983** 525-527.

9 Korsatko W., Wabnegg B., Tillian H.M., Braunegg G. & Lafferty R.M. Poly(hydroxybutyric acid) (PHBA) A Biodegradable Carrier For Long Term Medication Dosage II: The Biodegradation In Animal Organism And *In Vitro, In Vivo* Correlation Of The Liberation Of The Liberation Of Pharmaceuticals From Parental Matrix Retard Tablets. *Pharm. Ind.* 45(10) **1983** 1004-1007.

10 Korsatko W., Wabnegg B., Tillian H.M., Egger G., Pfranger R. & Walser V. Poly(hydroxybutyric acid) (PHBA) A Biodegradable Carrier For Long Term Medication Dosage III: Studies On Compatability Of Poly(hydroxybutyric Acid) Implantation Tablets In Tissue Culture And Animals. D*Pharm. Ind.* 46 **1984** 952-954.

11 Trathnigg B., Weidmann V., Lafferty R.M., Korsatko B. & Korsatko W. Poly(hydroxybutyrate) Of Low Molecular Weight - Synthesis And Applications. *Angew. Makromol. Chem.* 161 **1988** 1-8.

12 Juni K. & Nakano M. Poly(hydroxy Acids) In Drug Delivery. CRC Critical Reviews In Therapeutic Drug Carrier Systems. 3(3) **1987** 209-232.

13 Kubota M., Nakano M. & Juni K. Mechanism Of Enhancement Of The Release Rate Of Aclarabicin From Poly(hydroxybutyrate) Microspheres By Fatty Acid Esters. *Chem. Pharm. Bull.* 36 **1988** 333-337.

14 Holland S.J., Tighe B.J. & Gould P.L. Polymers For Biodegradible Medical Devices I: The Potential Of Polyesters As Controlled Macromolecular Release Systems. *J. Controlled Release.* 4(3) **1986** 155-180.

15 Taylor L. Degradable Plastics: Solution Or Illusion. *Chem. Tech.* Sept. **1979** 542-548.

16 Potts J.E. Biodegradation, Aspects Of Degradation And Stabalization Of Polymers. H.H.G. Jellinek. (Ed.) Elsevier Scientific Publishing Co. Amsterdam. **1978** 617-657.

17 Williams D.F. Biodegradation Of Surgical Polymers. *J. Mater. Sci.* 17 **1982** 1233-1246.

18 Griffin G.J.L. Synthetic Polymers And The Living Environment. *Pure Appl. Chem.* 52 **1980** 399-407.

19 Kopet J. & Ulbrich K. Biodegradation Of Biomedical Polymers. *Pro. Polym. Sci.* 9 **1983** 1-58.

20 Pitt C.G., Marks T.A. & Schindler A. Biodegradable Drug Delivery Systems Based On Aliphatic Polyesters: Application To Contraceptives And Narcotic Antagonists. R.E. Willette & G. Barnett (Eds.) Naltrexone: Reasearch Monograph 28 **1980** National Institute Of Drug Abuse **1981** 232-253.

21 Gilbert R.D., Stannett V., Pitt C.G. & Schindler A. The Design Of Biodegradable Polymers, Two Approaches N. Grasse (Ed.) Developments In Polymer Degradation. 4 Applied Science Publishers. London **1982** 259-293. *Biomaterials*, 8 **1987** 129-137.

22 Doi Y. Microbial Polyesters. VCH Publishers. USA **1990** 135.

23 Gilding D.K. Biodegradable Polymers. *Biocompat. Clin. Implant. Mater.* 2 **1981** 209-232.

24 Zaikov G.E. Quantitative Aspects Of Polymer Degradation In The Living Body. *J. Macromol. Sci. Rev. Macromol. Chem. Phys.* C25 (4) **1985** 551-597.

25 Langer R.S. & Peppas N. Present And Future Applications Of Biomaterials In Controlled Drug Delivery Systems. *Biomaterials* 2 **1981** 201-214.

26 Heller J. Synthesis Of Biodegradable Polymers For Biomedical Utilization. *Acs. Symp. Ser.* 212 **1983** 373-392.

27 Drobnik J. & Rypacek F. Soluble Synthetic Polymers In Biological Systems. *Adv. Polym. Sci.* 57 **1984** 5-50.

28 Langer R. & Peppas N. Chemical And Physical Structure Of Polymers As Carriers For Controlled Release Of Bioactive Agents: A review. *J. Macromol. Sci. Rev., Macromol. Chem. Phys.* 23(1) **1984** 61-126.

29 Vert M., Christel P., Chabot F & Leray J. Bioresorbable Plastic Materials For Use In Bone Surgery. Hastings G.W. & Ducheyne P. (Eds.) *Macro. Biom.* CRC. Press, Boca Raton, Florida. **1984** ch:6 119-142.

30 Wise D.L. Polyesters From Krebs Cycle Monomers As Vehicles For Sustained Release.Wise D.L. (Ed.) Biopolymeric Controlled Release Systems. CRC. Press, Boca Raton, Florida. **1984** ch:12 187-205.

31 Vert M. Polyvalent Polymeric Drug Carriers. CRC. Initial Reviews In Therapeutic Drug Carrier Systems. 2 (3) **1986** 291-327.

32 Chowdhury A.A. *Arch. Microbiol.* 47 **1963** 167-200.

33 Delafield F.P., Dourdoroff M., Palleroni N.J., Lusty C.J. & Contopoulos R. *J. Bacteriol.* 90 **1965** 1455-1466.

34 Lusty C.J. & Doudoroff M. Poly(b-hydroxybutyrate) Depolymerases of *Pseudomonas lemoignei. Proc. Natl. Acad. Sci. USA.* 56 **1966** 960-965.

35 Gilding D.K. Biodegradable Polymers. *Biocompat. Clin. Implant. Mater.* 2 **1981** pg. 275.

36 Barham P.J. Physical Properties Of Poly(hydroxybutyrate) And Poly(Hydroxybutyrate-hydroxyvalerate) Dawes E.A. (Ed.) Novel Biodegradible Microbial Polymers. Kluwer Academic Publ. **1990** 81-96.

37 Kunioka M., Tamaki A. & Doi Y. Crystalline And Thermal Properties Of Bacterial Copolyesters: Poly(3-hydroxybutyrate-co-3-hydroxyvalerate) And Poly(3-hydroxybutyrate-co-4-hydroxybutyrate). *Macromolecules.* 22 **1989** 694-697.

38 Bonfield W., Doyle C. & Tanner K.S. *In Vivo* Evaluation Of Hydroxyapatite Reinforced Polyethylene Composites. Cristel P., Meunier A. & Lee A.J.C. (Eds.) Biological And Biomechanical Performances Of Biomaterials. Elsevier **1986** 153-158.

39 Doyle C., Tanner E.T. & Bonfield W. *In Vitro* And *In Vivo* Evaluation Of Poly(hydroxybutyrate) And PHB Reinforced With Hydroxyapatite. *Biomaterials.* 12 Nov. **1991** 841-847.

40 Pouton C.W., Kennedy J.E., Notarianni L.J. & Gould P.L. Biocompatibility Of Poly(hydroxybutyrate) And Related Copolymers. *Proceed. Intern. Symp. Control. Rel. Bioact. Mater.* 15 **1988** 179-180.

41 Kennedy J.E., Notarianni L.J. & Pouton C.W. Biocompatibility Of A Biodegradable Polyester In Rats. British Pharm.Conf. Science Sessions. Sept. **1987.**

42 Saito T., Tomita K., Juni K. & Ooba K. In Vivo And In Vitro Degradation Of Poly(hydroxybutyrate) In Rat. *Biomaterials.* 12 April **1991** 309-312.

43 Kronenthal N.L. Biodegradable Polymers In Medicine And Surgery. Polymers In Medicine And Surgery. Kronenthal, User & Martin. (Eds.) Plenum Press, New York. **1974** 126.

44 Kanke M., Simmons G.H., Weiss D.L., Bivins B.A. & DeLuca P.P. Clearance Of $^{141}$Ce-labelled Microspheres From Blood Distribution In Specific Organs Following Intravenous And Intra-arterial Administration In Beagle Dogs. *J. Pharm. Sci.* 69 **1980** 755-762.

45 Chen J. Effects Of Poly(β-hydroxybutyrate) Implant Matrix On Granulation Tissue Formation. Confidential Personal Communication Convatec Wound Healing Research Institue. June **1989.**

46 Hammond T. Personal Communication. ICI Biopolymers Ltd. **1990.**

47 Williams D.F. & Miller N.D. Degradation Of Poly(Hydroxybutyrate) (PHB). *Advances In Biomaterials.* 7 **1987** 471-476.

48 Kanesawa Y. & Doi Y. Hydrolytic Degradation Of Microbial Poly(hydroxybutyrate-hydroxyvalerate) Fibers. *Makromol. Chem. Rapid Commun.* 11 **1990** 679-682.

49 Holland S.J., Jolly A.M., Yasin M. & Tighe B.J. Polymers For Biodegradable Medical Devices II: Hydroxybutyrate-hydroxyvalerate Copolymers: Hydrolytic Degradation Studies. *Biomaterials.* 8 July **1987** 289-296.

50 Gould P.L., Holland .J. & Tighe B.J. Polymers For Biodegradable Medical Devices IV: Hydroxybutyrate-hydroxyvalerate Copolymers As Non-disintergrating Matrices For Controlled Release Oral Dosage Forms. *Int. J. Pharm.* 38 **1987** 231-237.

51 Yasin M., Holland S.J. & Tighe B.J. Polymers For Biodegradable Medical Devices V: Hydroxybutyrate-hydroxyvalerate Copolymers: Effects Of Polymer Processing On Hydrolytic Degradation. *Biomaterials.* 11 **1990** 451-545.

52 Yasin M., Holland S.J., Jolly A.M. & Tighe B.J. Polymers For Biodegradable Medical Devices VI: Hydroxybutyrate-hydroxyvalerate Copolymers: Accelerated Degradation Of Blends With Polysaccharides. *Biomaterials*. 10 **1989** 400-412.

53 Holland S.J., Yasin M. & Tighe B.J. Polymers For Biodegradable Medical Devices VII: Hydroxybutyrate-hydroxyvalerate Copolymers: Degradation Of Copolymers And Their Blends With Polysaccharides Under *In Vitro* Physiological Conditions. *Biomaterials* 11 **1990** 206-215.

54 Yasin M. & Tighe B.J. Polymers For Biodegradable Medical Devices VIII: Hydroxybutyrate-hydroxyvalerate Copolymers: Physical And Degradative Properties Of Blends With Polycaprolactone. *Biomaterials* 13(1) **1992** 9-16.

55 Pouton C.W., Majid M.I.A. & Notarianni L.J. Degradation Of Poly(hydroxybutyrate) And Related Coplymers. *Proceed. Intern. Symp. Control. Rel. Bioact. Mater.* 15 **1988** 181-182.

56 Doi Y., Kanesawa Y., Kawaguchi Y. & Kuntoka M. Hydrolytic Degradation Of Microbial Poly(hydroxyalkanoates). *Makromol. Chem. Rapid Commun.* 10 **1989** 227-230.

57 Knowles J.C. & Hastings G.W. *In Vitro* Degradation Of A Poly(hydroxybutyrate-hydroxyvalerate) Copolymer And A New Technique For Monitoring Early Surface Changes. *Biomaterials*. 12 March **1991** 210-214.

58 Bissery M.C., Varelote F. & Thies C. *In Vitro* And *In Vivo* Evaluation Of CCNU-Loaded Micropheres Prepared From Poly(±-lactide) And Poly(β-hydroxybutyrate) Davies S.S., Illum L., Mc.Vie J.G. & Tomlinson E. (Eds.) Microspheres And Drug Therapy. Pharmaceutical And Medical Aspects. Elsevier Amsterdam. **1984** 217-227.

59 Kunioka M., Nakamura Y. & Doi Y. New Bacterial Copolyesters Produced In *Alcaligenes eutrophus* From Organic Acids. *Polymer Commun.* 29 **1988** 174-176.

60 Kunioka M., Kawaguchi Y. & Doi Y. Production Of Biodegradable Copolyesters Of Poly(3-Hydroxybutyrate-Co-4-Hydroxybutyrate) By *Alcaligenes eutrophus*. *Appl. Microbiol. Biotechnol.* 30(6) **1989** 569-573.

61 Saito T., Suzuki K., Yamamoto J., Fukiu T., Miwa K., Tomita K., Nakanishi S., Odani S., Suzuki J. & Ishikawa I. Cloning Nucleotide Sequence And Expression In *Escherichia coli* Of The Gene For Poly(3-hydroxybutyrate) Depolymerase From *Alcaligenes faecalis*. *J . Bacteriol.* 171 **1989** 184-189.

62 Doi Y., Kanesawa Y., Kunioka M. & Saito T. Biodegradation Of Microbial Polyesters Poly(3-hydroxybutyrate-co-3-hydroxyvalerate) And Poly(3-hydroxybutyrate-co-4-hydroxybutyrate). *Macromolecules.* 23 **1990** 26-31.

63 Grasse N., Murray E.J. & Holmes P.A. The Thermal Degradation Of Poly(-(D)-β-HydroxyButyric Acid) Part 1: Identification And Quantities Analysis Of Products. *Polymer Degradation And Stabalization.* 6 **1984** 47-61.

64 Minkowski O. Über das Vorkommen von Oxybuttersäure im Harn bei Diabetes mellitus. *Arch. Exptl. Pathol. Pharmakol.* 18 **1884** 35-

65 Külz E. Über eine neue linksdrehende Säure (Pseudooxybuttersäure). *Z. Biol.* 20 **1884** 167-

66 Bondy P.K., Blom W.L., Whitner V.S. & Farrar B.W. Studies Of The Role Of The Liver In Human Carbohydrate Metabolism By Venous Cathetet Technic. II: Patients With Diabetic Ketosis, Before And After The Administration Of Insulin. *J. Clin. Invest.* 28 **1949** 1126-

67 Quantitative Enzymatic Determination Of β-Hydroxybutyrate In Serum Or Plasma At 310nm. Sigma Diagnostics Instruction Manual. Proced. 310-UV.

68 Lehninger A.L. Principles Of Biochemistry. Worth Publ. Inc. New York. USA. 2nd.Edn. **1982.**

69 Li P.K. β-HydroxyButyrate. *Clin. Chem. News.* 11 No.2:13 **1985.**

70 Dawes E.A. & Senior P.J. *Adv. Microb. Physiol.* 10 **1973** 135-266.

71 Stinson M.W. & Merrick J.M. Extracellular Enzyme Secretion By *Pseudomonas lemoignei. J. Bacter.* 119 **1974** 152-161.

72 Tanio T., Fukui T. Shirakura Y., Saito T., Tomita K. & Masamune S. An Extracellular Poly(3-hydroxybutyrate) Depolymerase From *Alcalignes faecalis. Eur. J. Biochem.* 124 **1982** 71-77.

73 Shirakura Y., Fukui T., Saito T., Okamoto Y., Narikawa T., Keide K., Tomita K., Tukemasa T. & Masemune S. Degradation Of Poly(3-hydroxybutyrate) By Poly(3-hydroxybutyrate) Depolymerase From *Alcaligenes faecalis* $T_1$ *Biochemica et Biophysica Acta.* 886 **1986** 46-53.

74 Merrick J.M. Studies On The Enzymatic Synthesis And Degradation Of Poly(hydroxybutyrate) Personnal Communication **1989.**

75 Senior P.J. & Dawes E.A. *J. Biochem.* 134 **1973** 225-238.

76 Nakada T., Fukui T., Saito T, Miki K., Oji C., Matsuda A., Ushijima A. & Tomita K. Purification And Properties Of D-β-hydroxybutyrate

Depolymerase From *Zoogloea ramifera.J. Biochem.* 89 **1981** 625-635.

77 Holmes P.A. Applications Of PHB, A Microbially Produced Biodegradable Thermoplastic. *Physics In Technology.* 16(1) **1985** 32-36.

78 Mitomo H., Barham P.J. & Keller A. Lamellar Tickening Behaviour Of Poly(β-hydroxybutyrate) And Its Copolymer On Annealing. *Sen'IL GavKaishi* 42(1) **1986** 589-596.

79 Scandola M., Cerrorulli G. & Pizzoli M. The Physical Aging Of Bacterial Poly(D-β-hydroxybutyrate). *Makromol. Chem. Rapid Commun.* 10 **1989** 47-50.

80 Davies S. Cellular Responses To Potential Biomaterials. PhD. Thesis Aston University **1991**.

81 Personal Communication. Wella Biopol Shampoo Bottles Release. ICI Biopolymers Ltd. May **1991**.

82 Bardkte D., Püchner P. & Mueller W.R. Investigation Of The Behaviour Of Biopol Bottles With Particular Reference To Lanfill Dumping And Composting In Domestic Refuse. Confidential Personal Communication, (1st. report.) Personnal Communication. Nov. **1990**.

83 Brandl H. & Püchner P. The Degradation Of Shampoo Bottles In A Lake. Dawes E.A. (Ed.) Novel Biodegradable Microbial Polyesters. Kluwer Academic Press 1990 421-422.

84 Jewell W. & Krupp L. *Environmental Science And Technology* 26 193. In: Most Biodegradable Plastics Are A 'Con'. Coghlan A. *New Scientist* 8 Feb. **1992** 27.

85 Narayan R. Recycling Back To Nature: Environmentally Degradable Plastics. International Symposium On Biodegradable Polymers, Proceedings And Abstacts.Japan. **1990** Oct. 35-44.

86 Fredericks R.J., Melveger A.J. & Dolegierity J. Morphological And Structural Changes In A Copolymer Of Glycolide And Lactide Occurring As A Result Of Hydrolysis. *J. Polym. Sci. Poly. Phys. Edn.* 22 **1984** 57-66.

87 Dawson R.M.C. Data For Biochemical Research. Oxford University Press. UK. **1969** 195-209.

88 Tabata Y. & Ikada Y. Macrophage Phagocytosis In Mice. *J. Biomed. Mat. Res.* 220 **1988** 837-858.

89 Custer E.M., Myers J.L., Poffenbarger P.L. & Schoen I. The Storage Stability Of 3-Hydroxybutyrate In Serum, Plasma And Whole Blood. *Amer. Soc. Clin. Path.* **1983** 375-380.

90 Moore J.J., Marcus M. & Sax S.M. Kinetic Assay Of β-Hydroxybutyrate In Plasma With A COBAS-BIO Centrifugal Analyzer. *Clin. Chem.* 28(4) **1982** 702-703.

91 Li P.K., Lee J.T., MacGillivray M.H., Schaefer P.A. & Sagel J.H. Direct, Fixed-Time Kinetic Assays For β-Hydroxybutyrate And Acetoacetate With A Centrifugal Analyzer Or A Computer-Backed Spectrophotometer. *Clin. Chem.* 26(12) **1980** 1713-1717.

92 Hansen J.L. & Freier E.F. Direct Assays Of Lactate, Pyruvate, β-Hydroxybutyrate And Acetoacetate With A Centrifugal Analyzer. *Clin. Chem.* 24(3) **1978** 475-479.

93 Chandrasekaran A., Glover R.J. & Lord P.S. A Spectrophotometric Micro-method For The Enzymatic Determination Of Beta-Hydroxybutyrate. *Clin. Chim. Acta.* 37 **1972** 371-380.

94 Antonis A., Clark M. & Pilkington T.R.E. A Semiautomated fluorimetric Method For The Enzymatic Determination Of Pyruvate, Lactate. Acetoacetate And β-Hydroxybutyrate Levels In Plasma. Enzymatic Analysis Of Metabolites *J. Lab. Clin. Med.* 68(2) **1966** 340-343.

95 Williamson D.H., Mellanby J. & Krebs H.A. Enzymatic Determination Of D(-)-β-Hydroxybutyric Acid And Acetoacetic Acid In Blood. *J. Biochem.* 82 **1962** 90-97.

96 Williams D.H. & Fleming I. Spectroscopic Methods In Organic Chemistry. McGraw-Hill Book Company UK. 3rd. Edn. **1980**.

97 Nicolet Technical Services. Personnal Communication. **1991**.

98 Pearce A.G.E. Histochemistry, Theoretical And Applied, Vol.2 Analytical Technology. 4th. edn. Churchill Livingstone **1985**.

99 Yasin M. Melt Processable Biomaterials For Degradable Surgical Fixation Devices. PhD. Thesis. Aston University. **1988**.

100 Whistler R.L. & Smart C.L. Polysaccharide Chemistry. Academic Press, New York. USA. **1953**.

101 Borey F.A. Enzymatic Polymerization 1: Molecular Weight And Branching During The Formation Of Dextran. *J. Polym. Sci.* 35 **1959** 167-182.

102 Swift G. Biodegradation Tests And The Need For Standardization. International Symposium On Biodegradable Polymers. Programme And Abstracts. Japan **1990** Oct. 167-182.

103 Mayer J.M., Greenberger M., Kaplan D.L., Gross R. & McCarthy S. Development Of Standard Methods For Accelerated Degradation Studies Of Polymer Films. Personnal Communication. **1989**.